6 Geological result

The geological maps shown in this section are the first version of the GSG-model. We expect that there will be updates of the GSG-model in the future, resulting in a new version. Caveats and future work are described in the quality control chapter, section 5.4.

6.1 Surface to NAP-50 m depth range

6.1.1 Groningen gas field

Using the workflow described in chapter 4, a map of geological areas was derived for the entire Groningen gas field including the 5 km buffer. This includes surface waters, such as lakes and part of the Wadden Sea. As discussed in section 5.3.2, the polygons originally containing both land and Wadden Sea have been split into land and sea parts. Figure 6.1 shows the map with geological areas from version 1 of the GSG-model. The legend is provided in Figure 6.2. The map is included on A3 size in Appendix N. The Formations that are present in the area of interest (Groningen gas field +5 km buffer) are described in Appendix H. The consistency and quality checks performed for this map are described in section 5.3.

The map shows distinct differences in detail from north to south. In the north, the polygons are generally larger and suggest a more homogeneous composition of the subsurface. In the south, the polygons have much more detailed shapes. This level of detail suggests clearly defined boundaries. The reason for this difference lies in the geomorphological expression of the sequences in the mapping. The Pleistocene paleo-land surface in the north is covered by peat and tidal flat and channel deposits, but in the south the Pleistocene reaches the current surface (Figure 2.4). When this is the case, topographical depressions are filled in with peat and brook deposits which form the relevant geological sequence for site effect modelling. Hence, in the south the relevant geological sequences have a typical topographical expression on which the subdivision of the geological areas is based. In the northern part, the topographical expression is much less pronounced. The distribution of geological sequences in the northern part is interpreted from borehole information. This leads to much less detail in the definition of geological areas in the northern part.

Figure 6.3 to Figure 6.5 show the overlays of several relevant Formations with the geological areas. From these overlays, it is clear that the boundaries of the geological areas in the northern part are primarily based on the extent of the different Formations.

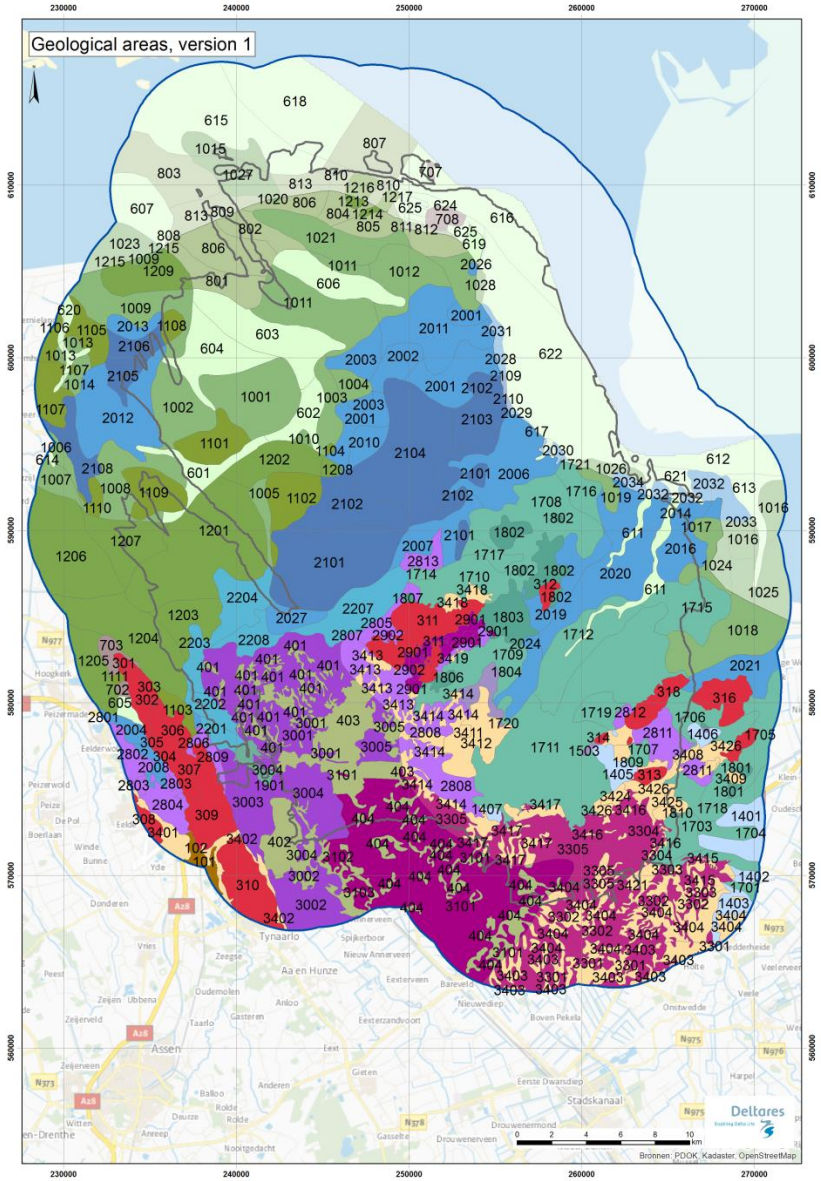

Figure 6.1 Map of geological areas for the surface to NAP-50 m depth range for the Groningen gas field and 5 km buffer (version 1). Identical colours indicate similar geological build-up. The first 1-2 digits denote the profile type (for legend, see Figure 6.2), the last 2 digits represents a serial number. The map is provided on A3 scale with a legend in Appendix N.

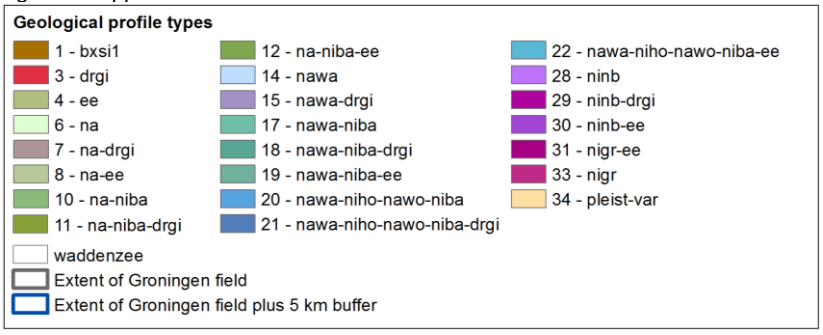

Figure 6.2 Legend to the map of geological areas for the surface to NAP-50 m depth range for the Groningen gas field and 5 km buffer.

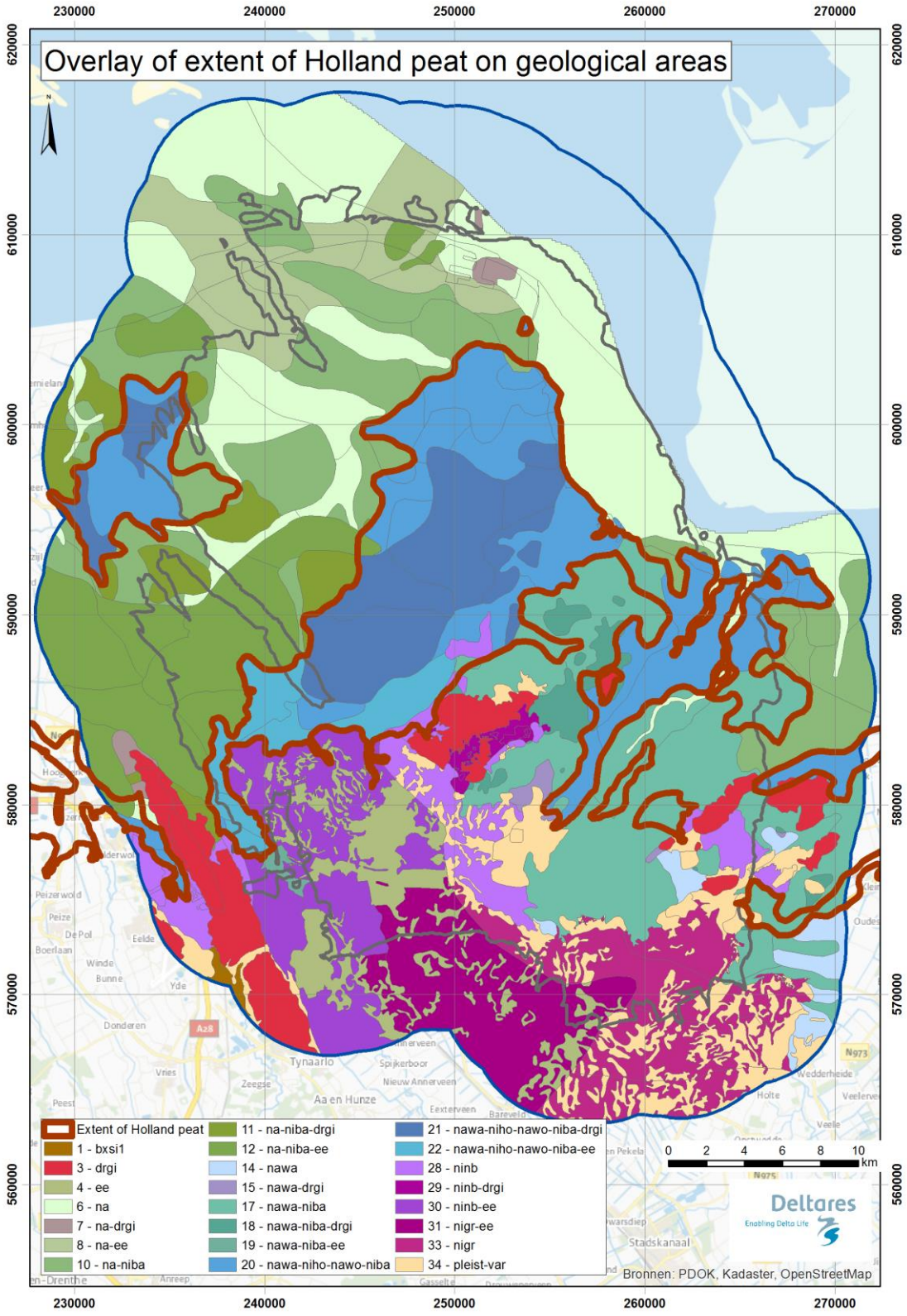

Figure 6.3 Overlay of extent of Holland peat, represented by the brown line (Figure 2.6) and the geological areas (Figure 6.1).

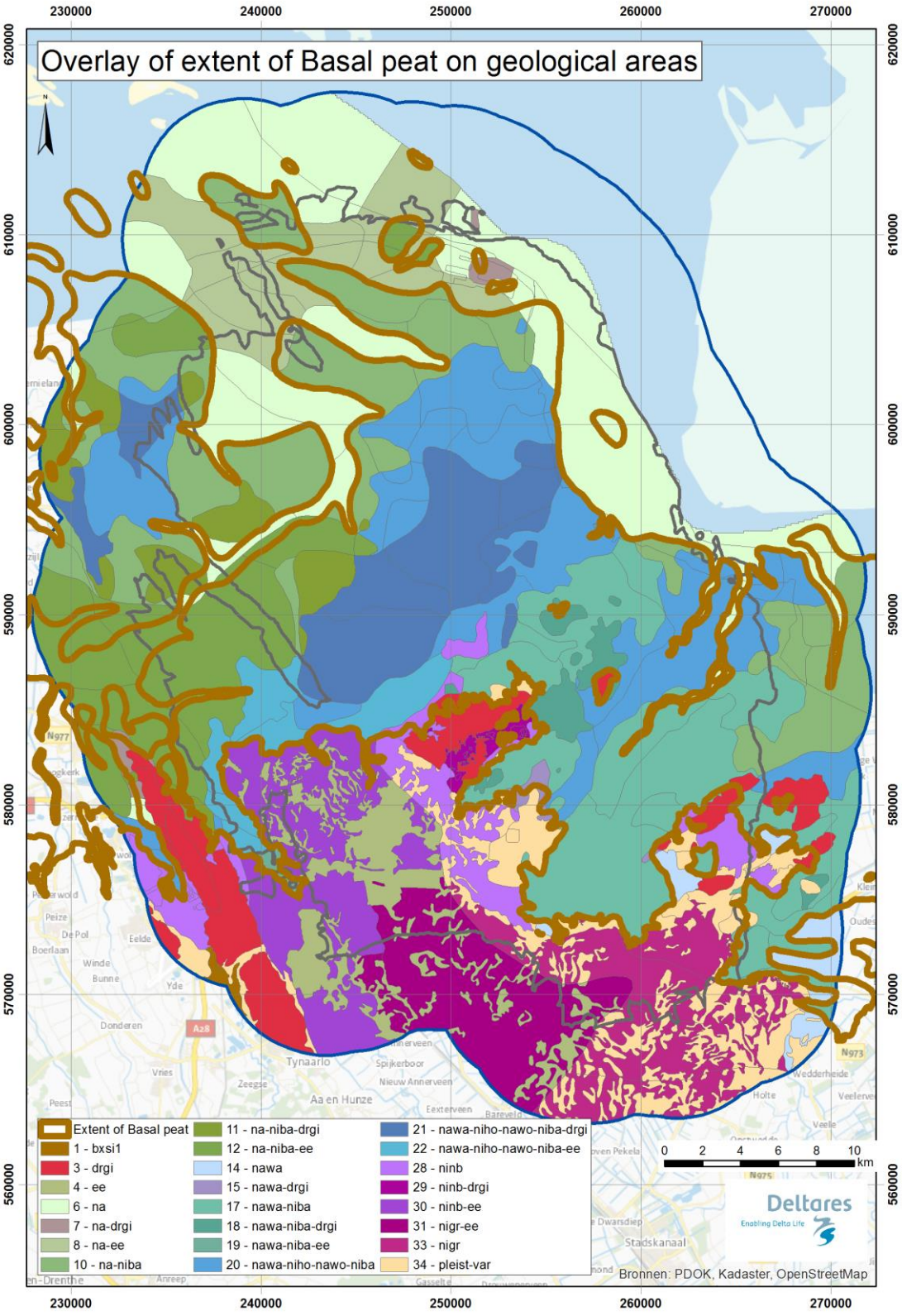

Figure 6.4 Overlay of extent of Basal peat, represented by the brown line (Figure 2.6) and the geological areas (Figure 6.1).

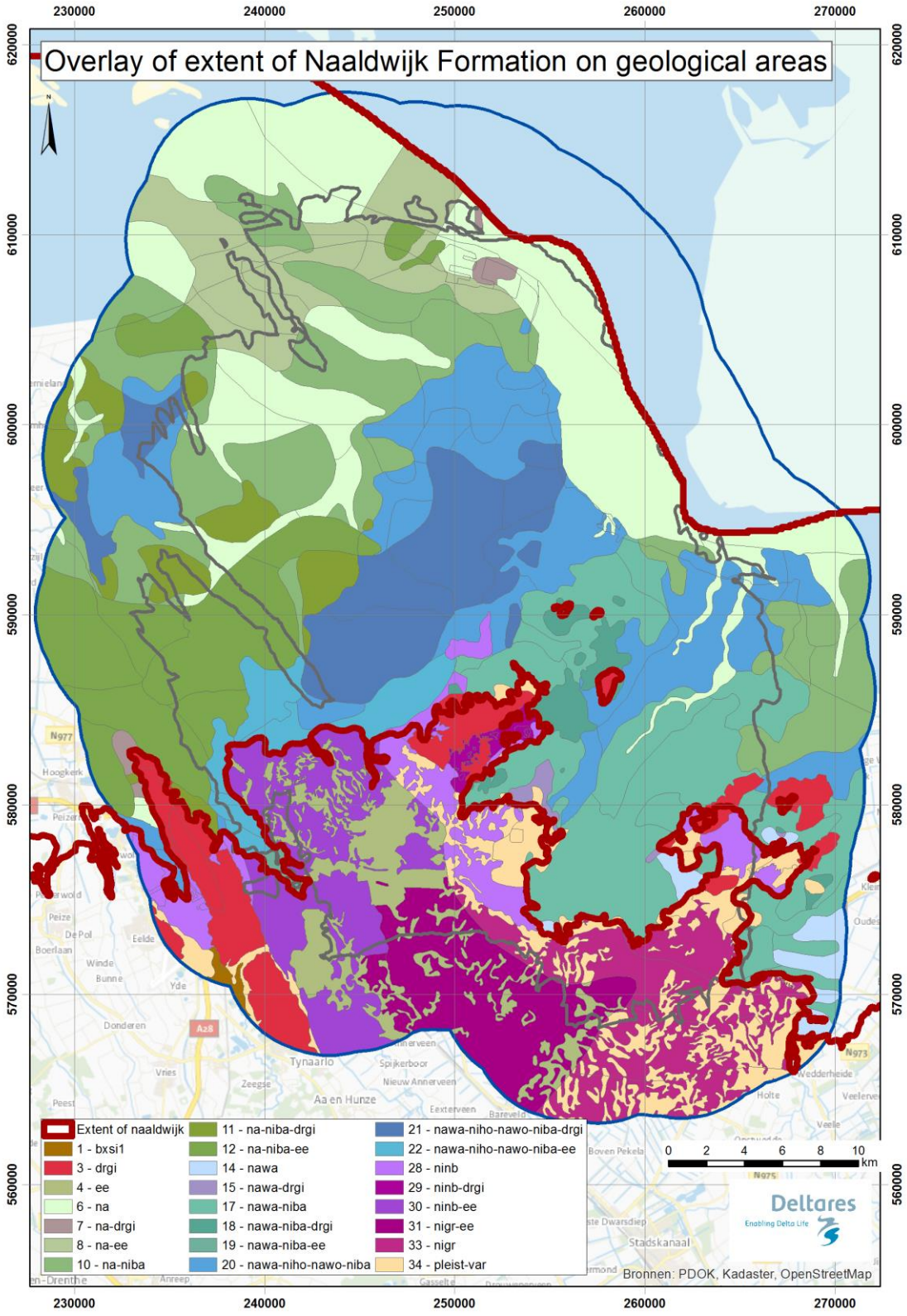

Figure 6.5 Overlay of extent of Naaldwijk Formation, between the burgundy lines (Figure 2.6) and the geological areas (Figure 6.1).

6.1.2 Municipality of Loppersum pilot

For the municipality of Loppersum pilot (Loppersum pilot for short), the map with version 1 of the GSG-model geological areas is shown in Figure 6.6. Since geology is not related to municipality boundaries, the geological areas extend beyond the boundaries. The quality check preformed for the Loppersum pilot was described in section 5.2.

The map shows that the entire municipality is underlain by tidal deposits of the Naaldwijk Formation. The division in geological areas is mainly based on the presence of Holland peat and basal peat and differences in depth or thickness. In addition, a channel with deposits of the Eem Formation protrudes the area in the southwest (polygons 1201, 1202 and 1208). Around this channel, patches of glacial till (Drenthe Formation, Gieten Member) which is present below the Holocene deposits determines the division of three polygons (1101, 1102 and 1104).

In order to prepare the Loppersum pilot for calculations of site response, the GeoTOP voxel stacks within the geological areas need to be resampled (method in section 4.4.3) and V_s values need to be assigned to the layers (method in section 4.6). The result of the resampling and V_s assignment is one file for each GeoTOP voxel stack, containing entries for location (RD coordinates), depth of layers, thickness of layers, stratigraphy (Formation), lithology, soil type and V_s. The combination of stratigraphy and lithology defines the soil type. From the V_s lookup table (Appendix J), the corresponding V_s value has been selected. The resampling procedure and resulting V_s profile is visualised for each voxel stack (e.g. Figure 4.6).

The geological areas within municipality Loppersum together with their extensions across the municipality boundary resulted in more than 30,000 files. These files serve as input for the calculations for site response using STRATA in the next stage of the project.

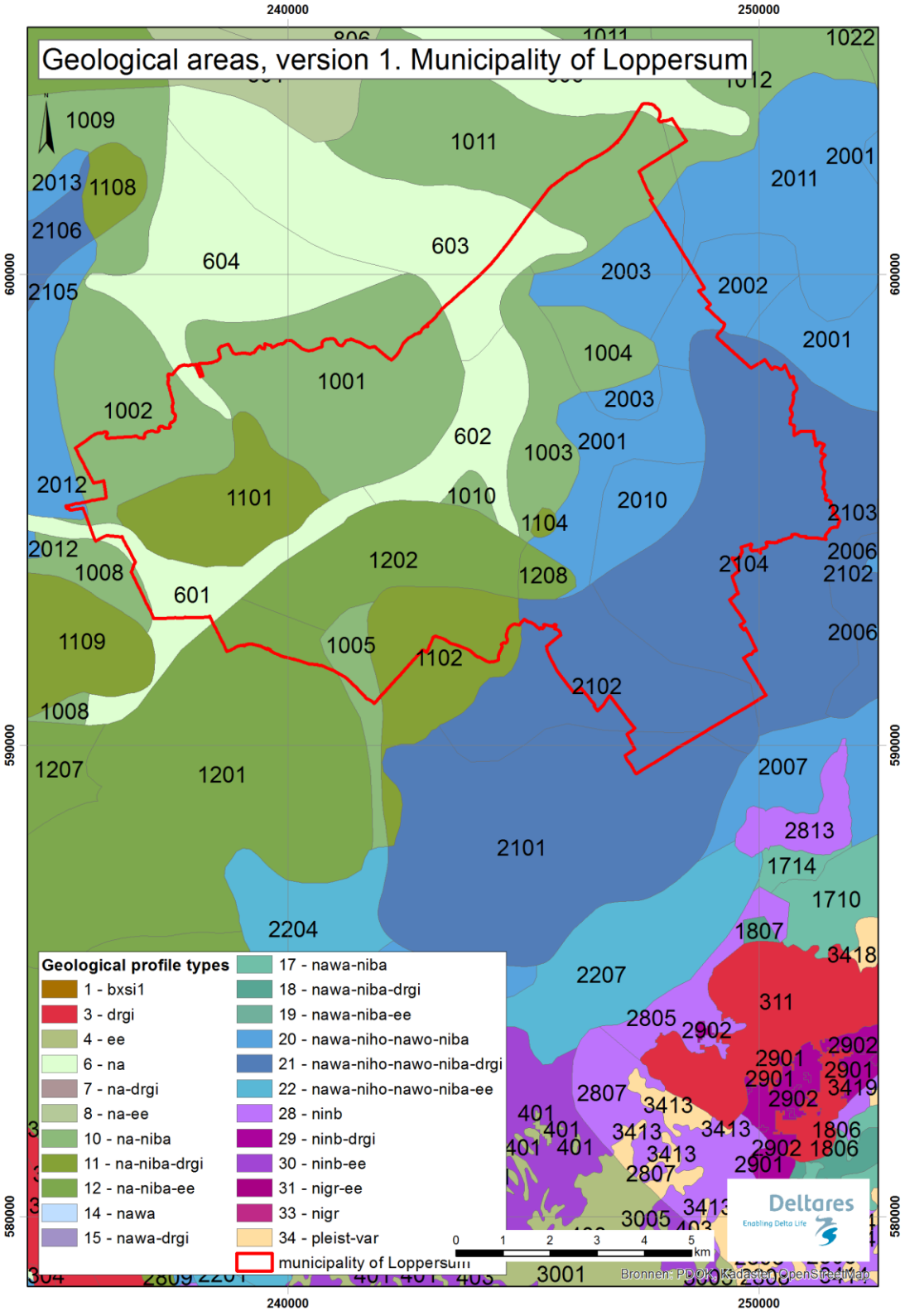

Figure 6.6 Map of geological areas for the surface to NAP-50 m depth range for the municipality of Loppersum pilot (version 1). Note that geological areas extend beyond the municipality boundary.

6.1.3 Municipality of Groningen pilot

For the municipality of Groningen pilot (Groningen pilot for short), the map with geological areas is shown in Figure 6.7. Since geology is not related to municipality boundaries, the geological areas extend beyond the boundaries. However, the municipality of Groningen extends beyond the area of interest (Groningen gas field +5 km buffer). Only the part of municipality of Groningen that falls within the area of interest has been schematised. At this stage of the project, no resampling of GeoTOP voxel stacks and V_s assignment has been performed for the Groningen pilot.

The division in geological areas is mainly based on the presence of the Eem Formation in the north (polygons 401, 1203, 1204, 1205, 1901, 2201-04 and 2208, 3001), often covered by Holocene tidal deposits (polygons 12xx, 19xx and 22xx). In the south-eastern area, the Eem Formation is overlain by Pleistocene cover sands and peat (Nieuwkoop Formation, Nijbeets Member). Since the cover sands were not used as a distinctive Formation in the profile types, these areas are incorporated in the geological profile type of “4. Ee” and “30. Ninb Ee”. From the south, the Hondsrug is penetrating into the municipality. This ridge is mainly composed of glacial till (polygons 301-304, 306, 307 and 309), and at the fringes overlain by basal peat and tidal deposits (702, 703, 1103 and 1111).

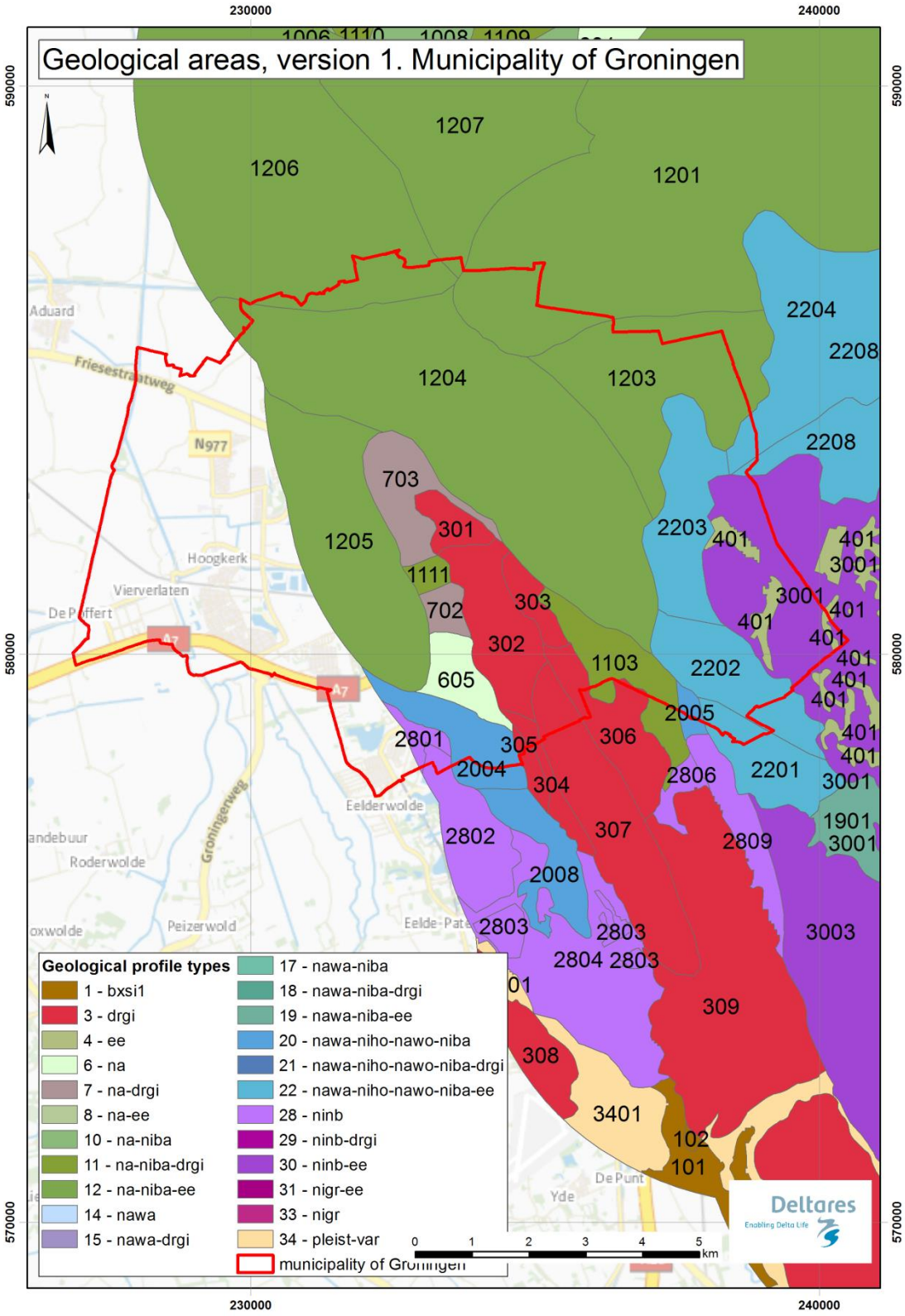

Figure 6.7 Map of geological areas for the surface to NAP-50 m depth range for municipality Groningen pilot (version 1). Note that geological areas extend beyond the municipality boundary and that the municipality Groningen extends beyond the area of interest.

6.2 NAP-50 m to NAP-200 m depth range

The schematisation of the deeper subsurface resulted in an ArcGIS polygons shapefile containing geological areas covering the area of interest. Since no GeoTOP voxel stacks are available for this depth range, the geological composition is registered using one or more scenarios per geological area in a spread sheet. Usually the schematisation extends down to NAP-200 m, often with the Oosterhout or Breda Formation as the deepest unit. In three areas the base of the Peelo Formation extends below NAP-200 m (geological areas 26, 30 and 32). In these cases the scenarios extend to the modelled base of the Peelo Formation, with a maximum depth of NAP-235 m.

The scenarios are accompanied by additional remarks, concerning the presence of thinner (<5 m thick) clay beds, local variations, combined lithostratigraphic units in one facies and the presence of salt domes. Special attention was paid to data density. Generally, there are a limited number of wells available. Some areas, however, are entirely without wells or only contain rather shallow wells. In these areas, the scenarios are defined using the DGM and REGIS models mainly. This is added in the remarks in the scenarios. The visual representation of the scenarios is included in Appendix O.

Figure 6.8 shows the area of interest with its geological area polygons. The elongated, cigar-like structures are a direct imprint of glacial tunnel valleys (Peelo Formation) incising into older geological units. The overlaying elongated ellipses represent the incision into progressively deeper units and corresponding stacked channel fills. In the eastern part of the area, a north-south oriented graben structure defines the outlines of the polygons (geological areas 12 and 17 west and geological areas 5 and 8 east of the fault). The lack of detailed subdivisions in the northern one-third of the area may partly be the result of low data density. Some geological features, such as filled channels, may not be represented, because very few wells in that area extend to a depth below NAP-50 m.

At this stage of the project, the two depth ranges (surface to NAP-50 m from GeoTOP and approx. 50 to NAP-200 m described in this section) remain two separate products. The reason for this is that the depth of the reference baserock horizon has not yet been defined.

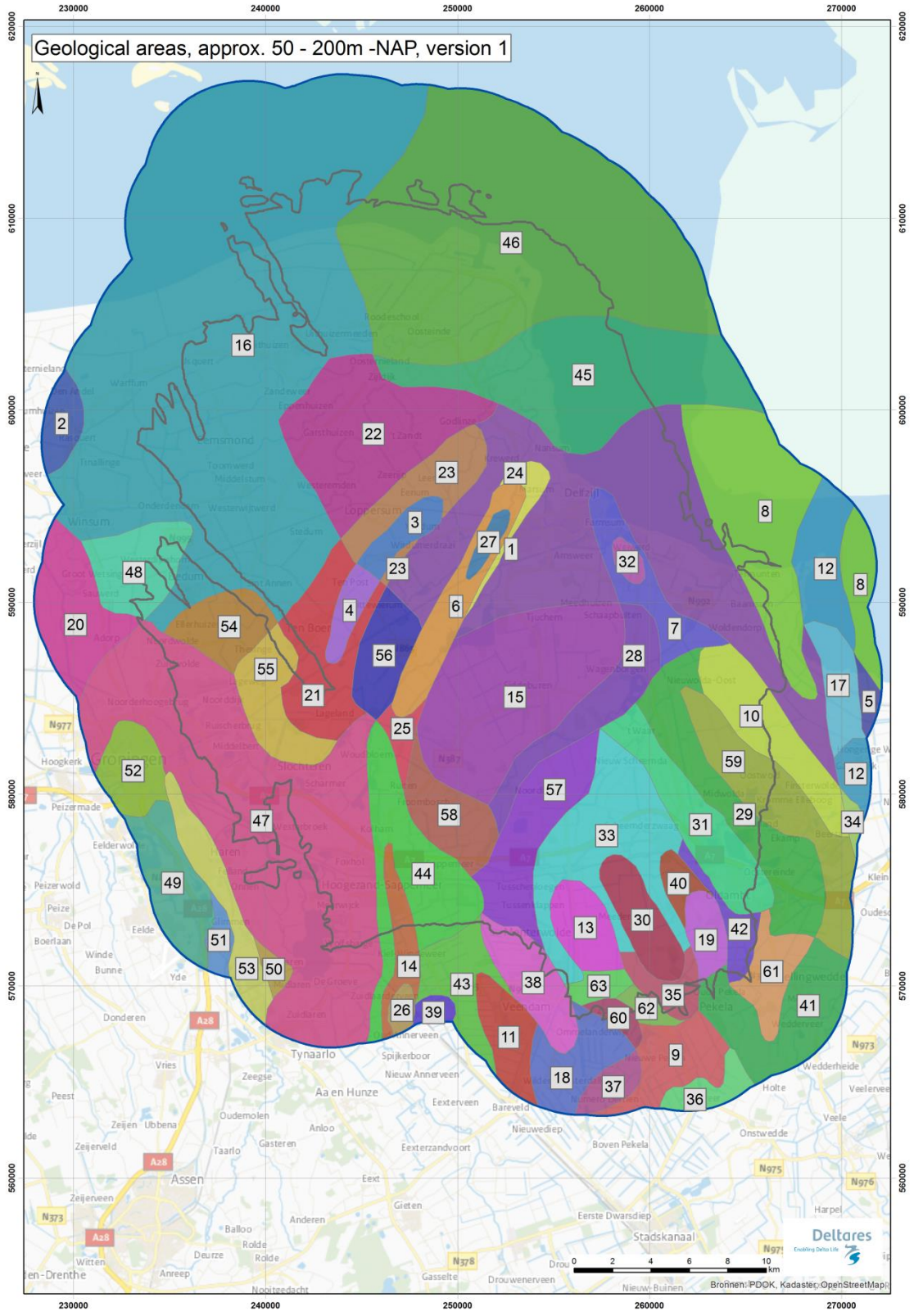

Figure 6.8 Version 1 map of geological areas for the deeper subsurface, approx. NAP-50m to NAP-200 m for the Groningen gas field and 5 km buffer. In this figure, the colours have no meaning. The geological areas of the two depth ranges (surface to NAP-50 m in Figure 6.1 and NAP-50 to -200 m in this figure) are not yet connected.

6.3 Reliability of the GSG-model

The GSG-model presented in sections 6.1 and 6.2 are based on a highly variable density of background information. This section provides some basic observations on reliability that should be kept in mind while using the GSG-model. The reliability of the GSG-model varies across the field as well. It is related to borehole/CPT density per unit area.

In order to visualize the borehole and CPT data density at various depths below the surface, maps showing data rich and data sparse areas within the area of interest were constructed. To do so, the amount of boreholes or amount of boreholes+CPTs were determined within a circle of 2.5 km^2 (corresponding radius = 892 m). This radius is of particular importance, since a large part of the hand-cored boreholes lay in a grid of ca. 1 by 1 km. This implies that every borehole of this grid accounts once within the density calculation. Iterative testing with different radius lengths proofed that shorter and longer radius lengths resulted in either too many separate single dots in the figures, or in one blurred, merged conglomerate of dots.

Figure 6.9 shows the variation of the borehole densities for various depths below the surface. The maps are included on A4 size (see Appendix P), showing both borehole density and the outline of the geological areas of the GSG-model.

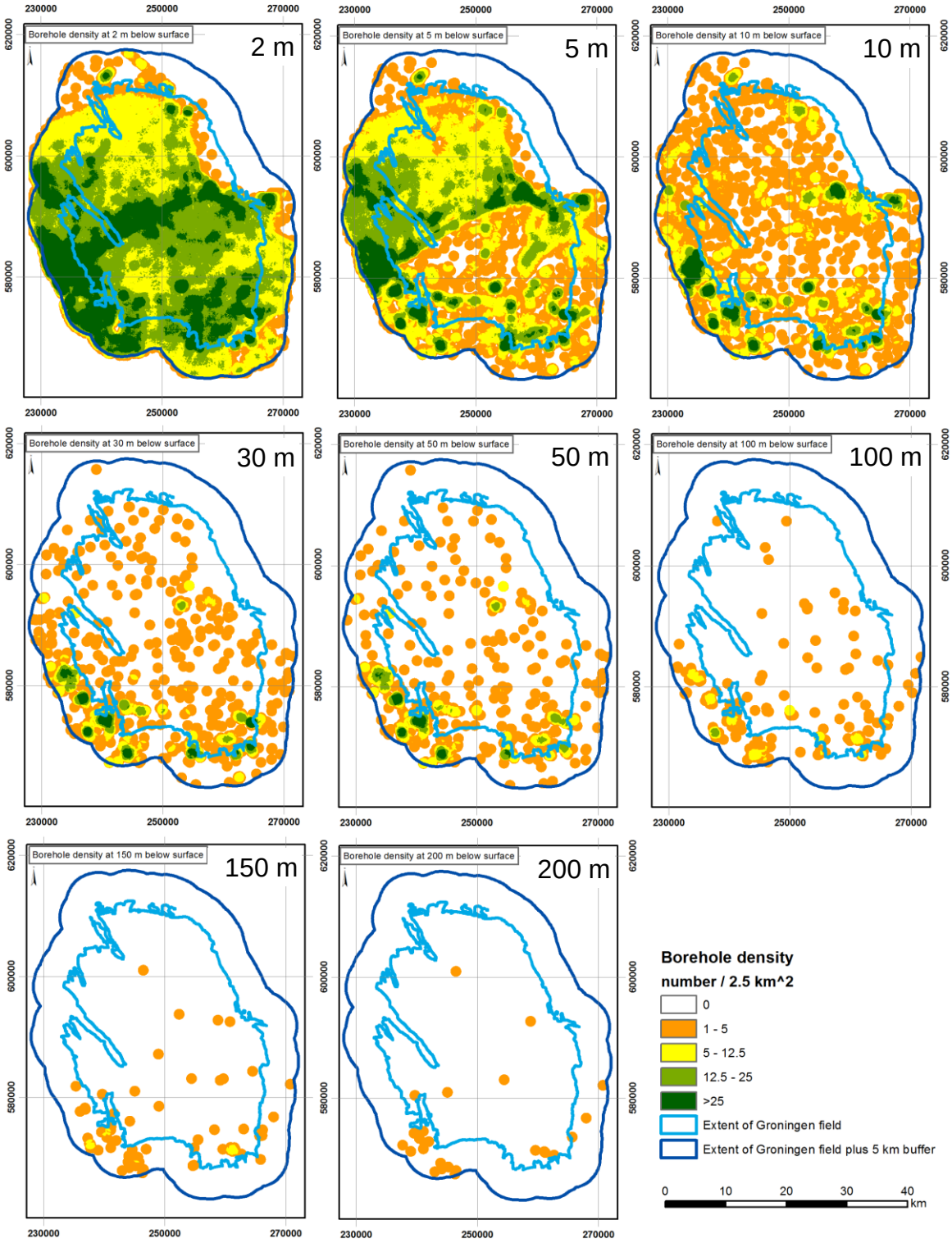

Figure 6.9 Densities of borehole records from DINO for various depths below the surface, expressed as number of borehole records per 2.5 km^2. The maps show data rich and data sparse areas within the area of interest. From top left to bottom right: borehole densities at 2 m, 5 m, 10 m, 30 m, 50 m, 100 m, 150 m and 200 m. The depths are indicated at the top right of each panel. The maps are provided on A4 format in Appendix P.

6.3.1 Surface to NAP-50 m depth range

The maps in Figure 6.9 and Figure P.1 to Figure P.5 in Appendix P show that coverage by borehole records is very good at very shallow depths (2 to 5 m below the surface). At 10 m below the surface, some gaps appear in the data coverage. For depths of 30 m and deeper, there are large areas with very limited numbers of borehole records or no data at all. This means that the models derived from borehole records, such as GeoTOP, are based on a limited amount of data in the depth region deeper than 10 m below the surface.

The division of the area of interest into geological areas was primarily based on distributions of Holocene sediments, up to approx. 10 m below the surface. This falls within the depth range with reasonable coverage by borehole records. This makes the boundaries of geological areas based on the distribution and thickness of Holocene sediments relatively robust.

In the case of definition of a geological area based on the distribution and thickness of Pleistocene sediments, from the range deeper than 10 m below the surface, the boundaries of the geological areas are less reliable.

The infill of the GeoTOP voxel stacks is based on borehole records and extents of geological formations. Due to the decrease in data density with depth, the infill of the voxels becomes less certain for larger depths. One of the consequences is the random assignment of clay or sand lithology to the deeper voxels, as can be observed in Figure K.1 in Appendix K. The impact of the less reliable infill of the voxels on the site response calculations could be investigated during sensitivity studies of site response using STRATA in a later stage of the project.

6.3.2 NAP-50 m to NAP-200 m depth range

The maps of the borehole density at 50, 100, 150 and 200 m (Figure 6.9 and Figure P.5 to Figure P.8 in Appendix P) are relevant for the deeper part of the GSG-model, from 50 to approx. NAP-200 m. This part of the model is based on the limited amount of borehole records as shown in the maps, supplemented by DGM, REGIS II, new borehole logs and expert geological knowledge. DGM has been constructed using boreholes as the primary data source, combined with faults, areal extent of the geological units and supplementary data (trend surfaces, so-called steering points for modelling pinching out, etc.) (Gunnink et al, 2013). The REGIS II model is primarily based on the sparse borehole records as well.

Relative to the surface to NAP-50 m depth range, the GSG-model of the NAP-50m to NAP-200 m depth range is less certain.

6.3.3 Addition of CPTs to fill the gaps

In the schematisation, information from CPTs has also been used in the division of the area into geological areas. However, CPTs are not included in GeoTOP. Figure 6.10 shows the density of borehole records and CPTS lumped together. This represents the maximum density dataset, including the CPTs delivered by Fugro and Wiertsema en Partners. The maps of Figure 6.10 are included on A4 format in Appendix Q.

The maps show that potential data coverage can be much improved for the depth range between 10 and 50 m below the surface, when CPTs are included in the subsurface models.

The addition of more CPT information for the robustness of the GSG-model is currently being tested.

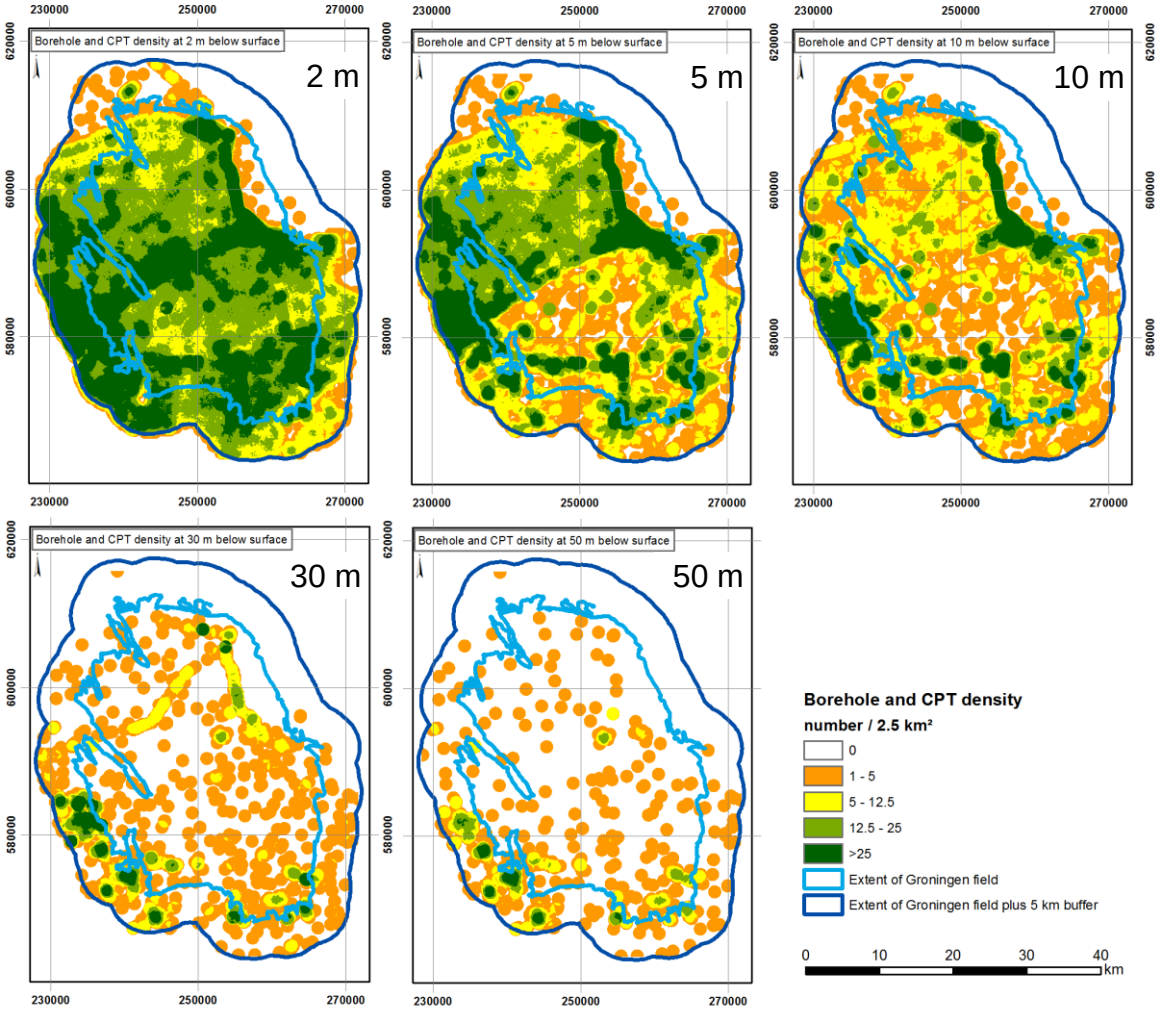

Figure 6.10 Borehole and CPT densities for various depths below the surface, showing data rich and data sparse areas within the area of interest. From top left to bottom right: borehole densities at 2 m, 5 m, 10 m, 30 m and 50 m. The depths are indicated at the top right of each panel. The maximum depth of CPT is 83 m. Therefore, maps of data densities at 100 m and deeper are identical to those shown in Figure 6.9. The maps are provided on A4 format in Appendix Q.

7 V_{s30} map for the Groningen field

7.1 V_{s30} map for Groningen field + 5 km buffer

V_s values determined using the method described in section 4.6.3 were assigned to the GeoTOP voxel stacks following to the procedure described in section 4.6.4. For each x,y coordinate of GeoTOP voxel at the surface, the corresponding V_{s30} value was calculated 100 times. This is a state-of-the-art approach that takes into account both the actual measured V_s values and the geology in the area of interest.

The average V_{s30} values for each geological area in the Groningen field + 5 km buffer are shown in Figure 7.1; the corresponding standard deviation for each geological area is shown in Figure 7.2. The Wadden Sea area has been excluded from the maps. The cut-off of the Wadden Sea geological areas is based on the sea defence dyke (Nationaal Basisbestand 2012 Dijkringgebieden, version 4.0) adjusted at Eemshaven and Delfzijl to include the harbours in the map.

The average values for V_{s30} for the geological areas range from 148 to 275 m/s. The standard deviations for the geological areas range from 8 to 51 m/s. The average V_{s30} calculated over all voxel stacks and all realisations is 210 ± 38 m/s.

7.2 Geological explanation of V_{s30} patterns

There is a distinct pattern in V_{s30}, showing lower V_{s30} values in the north and higher V_{s30} values in the south. This agrees with the general pattern found by Arup (Villani, and Neto, 2014). The more detailed patterns of higher and lower V_{s30} in the new V_{s30} map can be explained in terms of geology.

In the southern part, the high V_{s30} values reflect the presence of Pleistocene sediments at or near the surface. The Hondsrug is clearly recognisable as a high V_{s30} zone in the southwest, situated between the outline of the field and the 5 km buffer. East of the Hondsrug there is a channel infill with tidal deposits, resulting in a relatively low V_{s30} value. There is a sharp contrast in V_{s30} between the Hondsrug and the adjacent tidal deposits. This sharp contrast is expected, because of depositional environment of a tidal zone next to a ridge structure. One small Holocene channel infill can be recognised in the east (geological area 1718). One large channel, with clayey infill, giving rise to low V_{s30} values is present in the east (geological area 2020). In the north and west, two sandier channel infills (geological area 802 and 1107+2108+1110) can be discerned in a more clayey environment.

The northern part generally shows lower V_{s30} values relative to the south. The resulting V_{s30} value is an interplay between the lithological infill and thickness of the Naaldwijk Formation, and the presence or absence and the thickness of peat layers. Generally, the Naaldwijk Formation is expected to be more sandy and consisting of a thicker layer to the north. Both aspects have counteracting effects on V_{s30}. Local Pleistocene shallow occurrences also increase the V_{s30}.

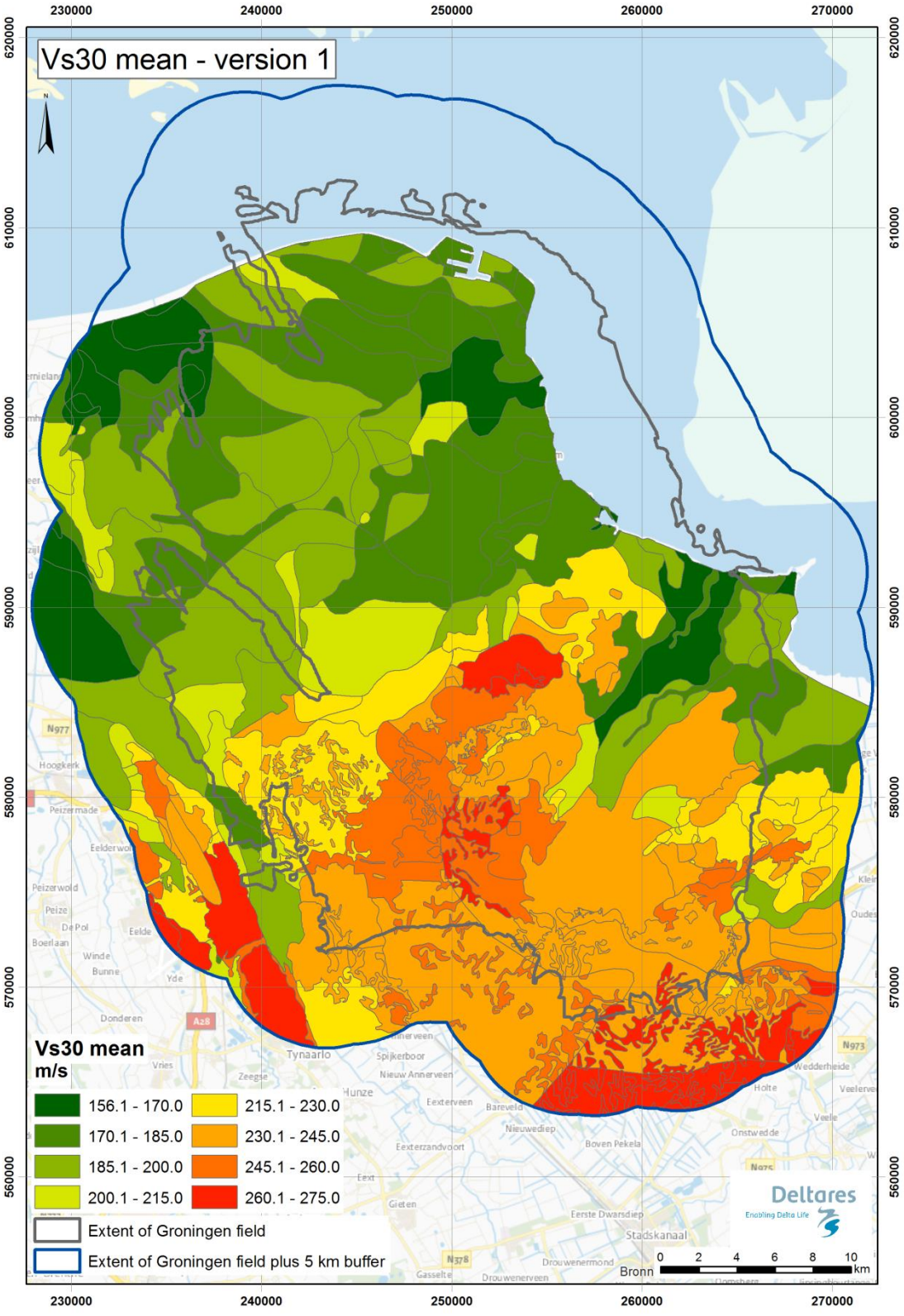

Figure 7.1 Average V_{s30} map (version 1) for the Groningen field + 5 km buffer (excluding the Wadden Sea) based on GSG-model version 1, assignment of V_s to GeoTOP voxels via the look-up table for V_s (method in section 4.6, table in Appendix J).

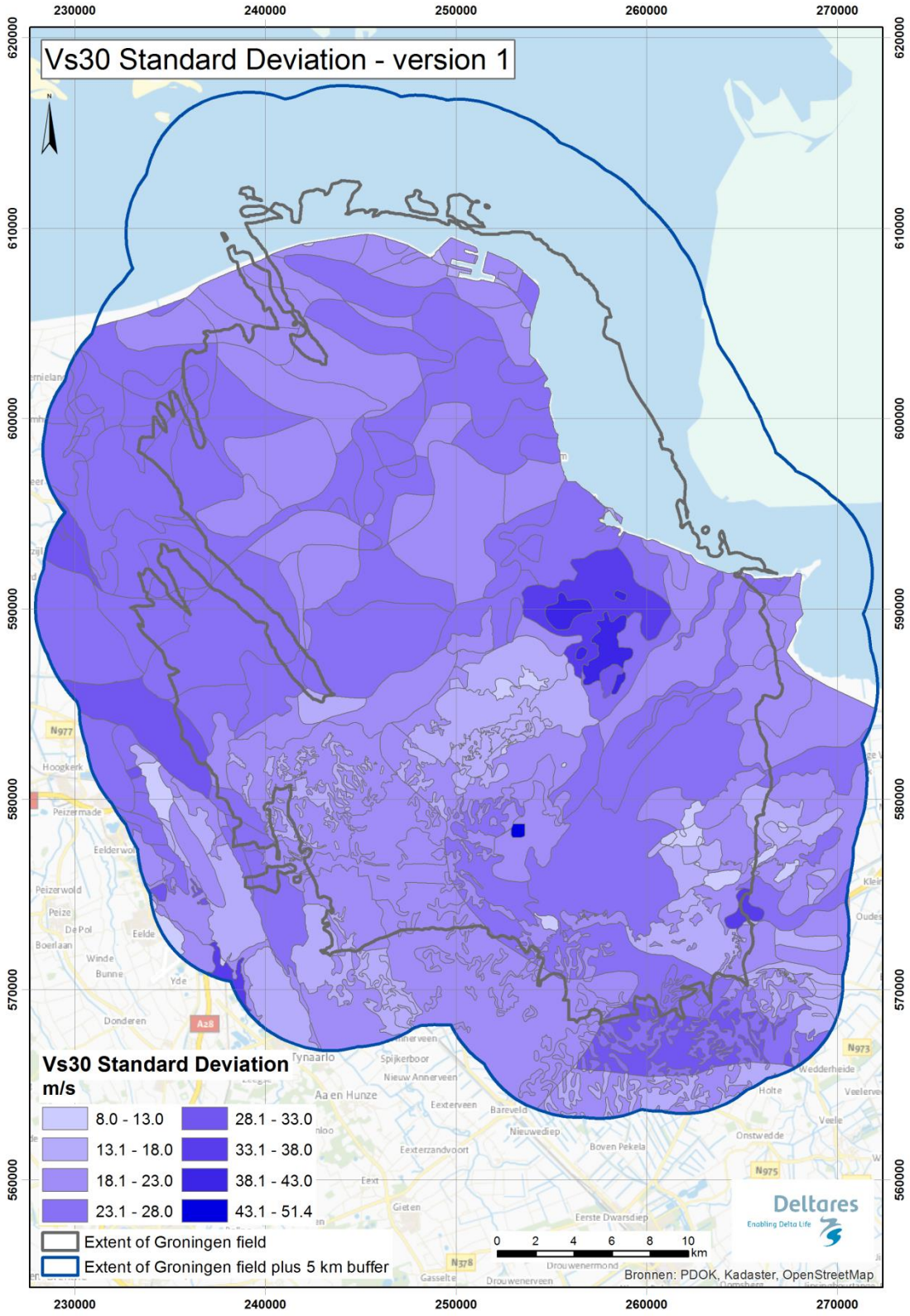

Figure 7.2 Standard deviation of V_{s30} map (version 1) for the Groningen field + 5 km buffer (excluding the Wadden Sea) based on GSG-model version 1, assignment of V_s to GeoTOP voxels via the look-up table for V_s (method in section 4.6, table in Appendix J).

In the very south of the area of interest, there are patches of the EE profile type (multipart polygons of geological area 404) embedded in an environment of profile type NIGR-EE (geological areas 3101, 3102, 3102). The NIGR-EE profile type contains peat, whereas the EE profile type does not. Therefore, it is expected that the patches of EE geological area 404 have higher V_{s30} values than the surrounding NIGR-EE geological areas 3101, 3102 and 3103. A similar pattern is distinguished more to the east: patches of variable Pleistocene at the surface (geological areas 3403 and 3404) show relatively high V_{s30} values. They are embedded in an environment of profile type NIGR (geological areas 3301, 3302 and 3303) containing peat and therefore show lower V_{s30} values.

The distinct pattern in average V_{s30} between north and south is also reflected in the standard deviations. The northern part consists of more heterogeneous tidal deposits of alternating peat and clay, giving rise to higher standard deviations of V_{s30}. The southern part, generally containing sandier deposits, shows lower standard deviations.

7.3 Effect of boundaries of geological areas

Because of the interplay between lithological infill and thickness in the northern part, the variations in V_{s30} are probably gradual. In the V_{s30} map, the values change abruptly across geological area boundaries. Adjacent geological areas do not only have distinct average V_{s30} values, but also associated standard deviations. The two distributions of adjacent areas might overlap in cases of gradual variations. An example of the gradual variations on V_{s30} of adjacent geological areas in the northern part (from southwest to northeast) is visualised in Figure 7.3. In this track, the variation of V_{s30} between the adjacent areas is much smaller than the standard deviation associated with the V_{s30} of the geological areas. This means that the V_{s30} distributions of the adjacent areas are overlapping.

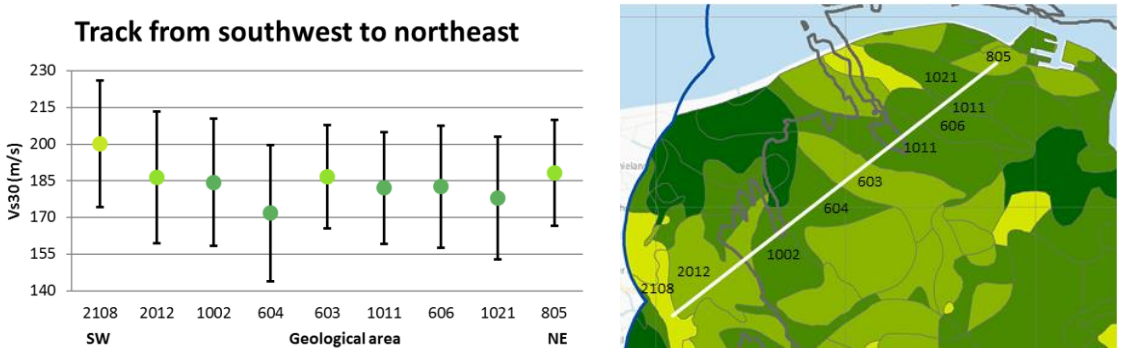

Figure 7.3 Left: Example of variability of V_{s30} across a track in the northern part of the Groningen field. Right: inset of Figure 7.1 showing the location of the track (white line). The numbers indicate the geological areas. For colour scale, see Figure 7.1.

7.4 Caveats and future work

Caveats regarding the V_s relation (look up table) that form the basis of the V_{s30} map are described in section 0. Specifically for the V_{s30} map of the Groningen field (+5 km buffer), we identified the following caveat:

- Error sources of V_s were included in the standard deviation of the V_{s30} maps. Uncertainties in lithology were accounted for by aggregation of all GeoTOP based V_{s30} values within one geological area. Uncertainties in V_s values of individual voxels were accounted for by drawing 100 V_s values for each voxel from the V_s distribution belonging to the combination of lithostratigraphy and lithological class for that voxel.
- Possible depth dependency of V_s has not been taken into account in this version of the V_{s30} map.

For the next version of the V_{s30} map for the Groningen field (+5 km buffer), we anticipate the following future developments:

- Improved V_s relations. The recommendations are included in section 0.
- Construction of an improved V_{s30} map based on the improved V_s relations.
- Study on the sharpness of the boundaries between the geological areas in terms of V_{s30}.
- In the future, the V_{s30} map as a proxy for site response can be replaced by a site amplification map based on STRATA calculations of site response.

8 Recommendations and future developments

Deltares has built a geological model for the Groningen field (+ 5 km buffer) for the purpose of the construction of V_{s30} maps and as input for the calculations of site amplification. These results will feed into the new GMPEs. The GSG-model is, among other data sources, based on the beta version of GeoTOP (a 3D geological model of the Netherlands), provided by TNO Geological Survey of the Netherlands. The GSG-model built by Deltares consists of a map defining geological areas and voxel stacks containing stratigraphy and lithological classes with depth. Additionally, a V_{s30} map was derived for the Groningen field + 5 km buffer, using Groningen-specific V_s values and the GSG-model

This report presents version 1 of the GSG-model and the derived V_{s30} map. It is a state-of-the art model, based on the current knowledge and the available data sources described in chapter 3. As new data becomes available continuously, updates of the GSG-model are planned for in the future.

The caveats and proposed future developments were described at the end of chapters 3, 4, 5 and 7. From these sections, the recommendations for future versions of the GSG-model and related work are summarised below. They are listed into 3 categories.

Category 1 - Recommendations regarding background data:

- Use the official version of GeoTOP for the calculation of the site response of the entire Groningen field (+5 km buffer). The final version of GeoTOP is expected to be available earliest in the second quarter of 2015.
- Include subsurface information from 70 vertical seismic arrays to 200 m depth (mainly composition) and other relevant information data from Shell, NAM and third parties.
- Collect Groningen-specific data on parameters, such as V_s from fieldwork campaigns (at accelerograph stations, at vertical seismic array locations and across the field to fill gaps).

Category 2 - Recommendations regarding updates of the GSG-model:

- Perform an update of the GSG-model upon release of the official version of GeoTOP.
- Assess the treatment of dwelling mounds and recently reclaimed areas in the GSG-model.
- Include relevant data that became available between17 November 2014 and the cut-off date of the next version of the GSG-model. Possible additional sources are mentioned in section 3.8.
- Couple the two depth ranges of the model and extend to the reference baserock horizon.
- Assess the need to adjust the GSG-model for inconsistencies in the use of AHN, inland surface water bodies and split Wadden Sea/land polygons after site response calculations are performed.
- Deactivate voxel stacks containing surface water.
- Improve V_s relations for Groningen. Methods are proposed in sections 0.
- Construction of an improved V_{s30} map based on the improved V_s relations.
- Study on the sharpness of the boundaries between the geological areas in terms of V_{s30}.
- In the future, the V_{s30} map as a proxy for site response can be replaced by a site amplification map based on STRATA calculations of site response.
- Construct a GSG-model dedicated for liquefaction purposes.

Category 3 - Recommendations related to site response calculations:

- Assess the impact of known GeoTOP issues, such as representation of peat and Peelo Formation in the GeoTOP voxels, on the resulting site response calculations.
- Perform a systematic sensitivity analysis of site amplification for depths to the reference baserock horizon (at least to 200 m).
- Investigate the boundaries between geological areas in terms of sharpness (wide or narrow transition zones), because of the gradual variations of depths and thickness of layers in the subsurface that are relevant for site response.
- Derive Groningen damping relations from local data, e.g. existing and new SCPT measurements and from analysis of earthquake signals at available vertical seismic arrays.
- Determine the shear degradation and damping relations for Groningen (especially peat) from additional laboratory tests.
- Site response: perform calculations based on beta version of GeoTOP for Loppersum pilot and link the results to the geology. In this way, the procedure of batch calculations and preparation steps in order to interpret the site response result can be optimised.

A References

Andrus, R. D., Mohanan, N. P., Piratheepan, P., Ellis, B. S. and Holzer, T. L. (2007). Predicting shear-wave velocity from cone penetration resistance. In: Proceedings of the 4th International Conference on Earthquake Geotechnical Engineering, Thessaloniki, Greece (p. 25-28).

Akkar, S., M. A. Sandıkkaya, and J. J. Bommer (2014). Empirical ground-motion models for point-and extended-source crustal earthquake scenarios in Europe and the Middle East. Bulletin of earthquake engineering, 12.1, p. 359-387.

Bommer, J.J. (2014). Groningen Field Seismic Hazard and Risk Assessment - White Paper on GMPE Development, version: 1 December 2014

Bosch, J.H.A. (2000). Standaard Boor Beschrijvingsmethode. Netherlands Institute of Applied Geosciences TNO, Report NITG 00-141-A (in Dutch). Available at: http://www2.dinoloket.nl/nl/about/dataTypes/bor/standards.html

Castellaro, S., F. Mulargia, P. Rossi (2008). Vs30: Proxy for site amplification?, Seism. Res. Lett., 79, p. 540-544.

Chilès, J.-P. and Delfiner, P. (2012). Geostatistics – Modeling Spatial Uncertainty. Wiley & Sons, Hoboken, New Jersey, 699 pp.

Cohen, K.M., Finney, S., Gibbard, P.L. (2013). International Chronostratigraphic Chart, International Commission on Stratigraphy. Available at: http://www.stratigraphy.org/ICSchart/ChronostratChart2013-01.pdf

Dambrink, R.M., Maljers, D. & Stafleu, J. (2014). Customised geological information derived from multi-purpose 3D voxel models (Abstract). 12th Nederlands Aardwetenschappelijk Congres (NAC12), April 8-9 2014, Veldhoven, The Netherlands. Available at: http://nac12.nl/conference-details/programme/poster/529

De Crook, Th. and Wassing, B. (2001). Voorspelling van de opslingering van trillingen bij aardbevingen. Geotechniek 2001, nr. 2, p 48-53 (in Dutch).

De Mulder et al. (Eds.) (2003). De ondergrond van Nederland. ISBN 90011605141; Wolters Noordhoff, 379 pp (in Dutch).

De Vries, F., de Groot, W.J.M., Hoogland, T., Denneboom, J. (2003). De Bodemkaart van Nederland digitaal; toelichting bij inhoud, actualiteit en methodiek en korte beschrijving van additionele informatie. Wageningen: Alterra (Alterra-rapport 811) - 45 pp (in Dutch).

De Vries, F., D.J. Brus, B. Kempen, F. Brouwer en A.H. Heidema (2013). Actualisatie bodemkaart veengebieden - Deelgebied 1 en 2 in Noord-Nederland. Wageningen: Alterra (Alterra-rapport 2556, in Dutch).

Douglas, J. B. and R. S. Olsen (1981). Soil Classification using Electric Cone Penetrometer. Symposium on Cone Penetration Testing and Experience, Geotechnical Engineering Division, ASCE, St. Louis, p. 209-227.

EPRI. (1993). Guidelines for Determining Design Ground Motions. EPRI TR-102293

Goovaerts, P. (1997). Geostatistics for Natural Resources Evaluation. Oxford University Press, New York, 483 pp.

Gunnink, J.L., Maljers, D., Van Gessel, S.F., Menkovic, A. & Hummelman, H.J. (2013). Digital Geological Model (DGM): a 3D raster model of the subsurface of the Netherlands. Netherlands Journal of Geosciences - Geologie en Mijnbouw 92 - 1, p. 33-46. Available at: https://www.dinoloket.nl/meer-weten-over-dgm

Hijma, M.P. and Kruse, G.A.M. (2014). WTI 2017: Stochastische Ondergrondschematisatie - WTI-SOS. Deltares report 1209432-000-GEO-0006 (draft version, in Dutch).

Hijma, M.P., Van der Meij, R. and Lam, K.S. (2015, in review). Grasping the heterogeneity of the subsurface: using buildup scenarios for assessing flood-protection safety. Conference paper for the fifth International Symposium on Geotechnical Safety and Risk 2015, Rotterdam, The Netherlands.

Idriss, I.M. (1990). Response of soft soil sites during earthquakes. Proceedings Memorial Symposium to honor Professor Harry Bolton Seed, California, Vol. II.

Koomen, A.J.M and Maas, G.J. (2004). Geomorfologische Kaart Nederland (GKN); Achtergronddocument bij het landsdekkende digitale bestand. Wageningen, Alterra-report 1039, 38 pp (in Dutch).

Kottke, A.R., Wang, X. & Rathje, E.M. (2013). Technical Manual for Strata. Geotechnical Engineering Center, Department of Civil, Architectural, and Environmental Engineering, University of Texas. Available at: https://nees.org/resources/7290/download/Strata_Manual-rev-399.pdf

NAM (2013). Technical Addendum to the Winningsplan Groningen 2013: Subsidence, Induced Earthquakes and Seismic Hazard Analysis in the Groningen Field. November 2013.

Robertson, P.K. (2009). Interpretation of cone penetration tests - a unified approach". Canadian Geotechnical Journal, Volume 46, p.1337-1355.

Roeleveld, W. (1974). "The Holocene evolution of the Groningen marine clay district". Berichten Rijksdienst Oudheidkundig Bodemonderzoek 24, supplement, p1-132 (in Dutch).

Schnabel, P.B., John Lysmer, H. Bolton Seed. Shake (1972). A computer program for earthquake response analysis of horizontally layered sites. Report EERC 72-12. College of Engineering, University of California, Berkeley California.

Soares, A. (1992). Geostatistical estimation of multi-phase structure. Mathematical Geology 24 (2), p.149-160.

Stafleu, J., Maljers, D., Gunnink, J.L., Menkovic, A. & Busschers, F.S. (2011). 3D modelling of the shallow subsurface of Zeeland, the Netherlands. Netherlands Journal of Geosciences - Geologie en Mijnbouw 90 - 4, p. 293-310. Available at: https://www.dinoloket.nl/meer-weten-over-GeoTOP.

Stafleu, J., Maljers, D., Busschers, F.S., Gunnink, J.L., Schokker, J., Dambrink, R.M., Hummelman, H.J., Schijf, M.L. (2012). GeoTOP modellering. TNO Report 2012 R10991, 216 pp. (in Dutch). Available at: https://www.dinoloket.nl/meer-weten-over-GeoTOP.

Steur, G.G.L. and W. Heijink (1991). Bodemkaart van Nederland, Schaal 1:50 000. Algemene begrippen en indelingen, 4e uitgebreide uitgave. Wageningen, DLO Staring Centrum (in Dutch).

Van Staalduinen, C.J. (red.) (1977). Geologisch onderzoek van het Nederlands Waddengebied. Rijks Geologische Dienst Haarlem, 77 p (in Dutch).

Vernes, R.W. and Van Doorn, Th. H. M. (2005). Van Gidslaag naar Hydrogeologische Eenheid – Toelichting op de totstandkoming van de dataset REGIS II. Netherlands Institute of Applied Geosciences TNO, Report 05-038-B, 105 pp (in Dutch). Available at: https://www.dinoloket.nl/meer-weten-over-regis-ii

Vernes, R.W., Bosch, J.H.A., Harting, R., Maljers, D. & Schokker, J. (2013). Data-inventarisatie, kartering en parametrisatie van keileem in het MIPWA-gebied (in Dutch). TNO Report 2013 R10107, 152 pp. Available upon request at info@dinoloket.nl

Villani, M., Neto, D. (2014). Groningen Preventive Structural Upgrading Ground Conditions in the Groningen Region. Arup report number REP/229746/SR009, date 27 May 2014, draft report rev. 0.02

Vos, P. C., Bazelmans, J., Weerts, H. J. T., & Van der Meulen, M. J. (2011). Atlas van Nederland in het Holoceen. Bakker, Amsterdam (in Dutch).

Vos, P.C. (2013). Lithostratigrafie van de Holocene kustafzettingen in Noord Nederland. Deltares report 1208302-000-BGS-0008 date 9 July 2013 (in Dutch).

Vos, P.C., E. Knol, S. de Vries, Groninger Museum (2014). Paleogeografische kaarten van het Waddengebied tussen Marsdiep en Weser, 500 v. Chr. – heden. Groninger Museum, 31 pp (in Dutch).

Vos, P.C. (2015, in preparation). Origin of the Dutch coastal landscape. Long-term landscape evolution of the Netherlands during the Holocene (Chapter 1, Introduction). PhD Thesis Utrecht University.

Vucetic, M., & R, Dobry. (1991). Effect of Soil Plasticity on Cyclic Response. Journal of the Geotechnical Engineering Division, 117(1), p. 89-107.

Wassing, B.B.T., Maljers, D., Westerhoff, R.S., Bosch, J.H.A. & Weerts, H.J.T. (2003). Seismisch hazard van geïnduceerde aardbevingen, Rapportage fase 1. Report nr. NITG-03-185-C-def (in Dutch).

Wassing, B.B.T. and Dost, B (2012). Seismisch hazard van geïnduceerde aardbevingen, Integratie van deelstudies. TNO/KNMI-report TNO 2012 R11139, 24 December 2012 (in Dutch).

Wehling, T. M., Boulanger, R. W., Arulnathan, R., Harder Jr, L. F., & Driller, M. W. (2003). Nonlinear dynamic properties of a fibrous organic soil. Journal of geotechnical and geoenvironmental engineering, 129(10), p. 929-939.

B Abbreviations and terminology

Table B.1 Abbreviations and expressions used in the report

Abbreviation / expression	Description
AHN	Actueel Hoogtebestand Nederland: digital terrain model of the Netherlands.
Baserock	Reference horizon defined (in this report) for the distinction between the elastic half-space below this horizon and soil layers sensitive to site amplification above this horizon.
Bedrock	Deposit of solid rock that is typically buried beneath soil and other broken or unconsolidated material.
Borehole records DINO	Database containing records (descriptions) from boreholes from the shallow subsurface (< 500 m depth). Both from manual as from mechanical borings.
Borehole logs	Logs of geophysical measurement performed in an open borehole. Possible parameters to be measured are temperature, gamma ray, short and long normal resistivity and seismic velocities.
CPT	Cone Penetration Test, measuring cone resistance and sleeve resistance upon pushing the probe into the soil.
DINOloket	Portal containing subsurface information, such as borehole records, CPTs and geological subsurface models. https://www.dinoloket.nl/
DGM	Digital Geological Model (of the shallow subsurface) is a layer model of geometry of geological Formations present in the Dutch Quaternary and Neogene. The geometry of each Formation is given as a top- and base surface and a thickness. The depth range of DGM is from the surface to approx. NAP-500 m.
Geological area	Area with distinct mappable geological build-up, expressed by one or several characteristic sequence(s) of deposits (“profile types”). The aim is to account for all potential sequences occurring within this area. Therefore, a geological area can either be homogeneous and contain one main profile type or heterogeneous containing several profile types. The mappability depends on the quality and distribution of subsurface information and associated uncertainties in actual composition.
GeoTOP	GeoTOP is a 3D model of the subsurface containing voxels (volume cells) of 100 m x 100 m and 0.5 m thickness. Each voxel contains geological (stratigraphical) unit, lithological class and (in the future) various physical and chemical properties as attribute. The depth range of GeoTOP is from the surface to maximum of 50 m- NAP. Currently, GeoTOP is constructed for the entire Netherlands.
GMPE	Ground Motion Prediction Equation
iMOD	Interactive MODeling. The package consists of a user-friendly interface initially built to support the use of (large-scale) groundwater flow models, based upon the concept of MODFLOW 1. Recent additions to the iMOD interface facilitate the visualization of different kinds of 3D subsurface data, such as borehole records, CPTs and subsurface models.

Table B.1, continued. Abbreviations and expressions used in the report

Abbreviation / expression	Description
Lithological class	A combination of lithology and sand grain-size classes.
Lithofacies	The rock record of any particular sedimentary environment, including both physical and organic characteristics.
Lithology	A description of the physical characteristics of rock, sediment or soil, such as colour, texture, grain size, or composition.
Lithostratigraphy	The element of stratigraphy that deals with the description and nomenclature of the rocks/sediments of the Earth based on their lithology and their stratigraphic relations.
MASW	Multichannel Analysis of Surface Waves. Geophysical technique to derive a vertical profile of shear wave velocities (V_s).
MIPWA	Methodiekontwikkeling Interactieve Planvorming ten behoeve van het Waterbeheer (translation: Development of a method for interactive strategy for Water Management).
NAP	Normaal Amsterdams Peil, Dutch Ordnance Datum
NL3D	Low resolution prequel of GeoTOP. NL3D is a 3D model of the subsurface containing voxels of 250 m x 250 m and 1 m depth. Each voxel contains lithological information only, but on a nation-wide scale. The depth range of NL3D is from the surface to NAP-50 m. NL3D is not available at DINOloket.
PGA	Peak Ground Acceleration. Expressed in m/s^2 (e.g. 1.0 m/s^2) or as portion of the gravitational acceleration (9.81 m/s^2, e.g. 0.10 g).
PSA	Spectral acceleration
Profile type	Characteristic sequence of deposits.
REGIS II	REgional Geohydrological Information System II is a hydrogeological addition to DGM. The subsurface is divided into sand and clay layers, corresponding to permeable and non-permeable layers. The model contains the geometry of these layers. In addition, for each unit the average hydrogeological parameters are given. The maximum depth of REGIS II is approx. NAP-500 m.
Scenario	Characteristic sequence of lithofacies, with information on depth, thickness and probability of occurrence for the different layers in the scenario.
SCPT	Seismic Cone Penetration Test or Seismic CPT, performed with a seismic source at the surface and a cone containing geophones. While pushing the cone into the soil, at each given depth a seismic measurement is taken. In this way, both CPT and a seismic velocity profile (usually V_s) are obtained.
Soil	There are several definitions of soil. For a physical geographer, soil refers to the mixture of minerals, organic matter, gases, liquids, and myriad organisms that together support plant life. For a geomechanical engineer, soil refers to for the unconsolidated sediments as opposed to bedrock. In this report, we adopt the geomechanical definition of soil.
STRATA	One-dimensional site response analysis with stochastic variation of site properties using either time series or random vibration theory. https://nees.org/resources/strata

Table B.1, continued. Abbreviations and expressions used in the report

Abbreviation / expression	Description
Voxel stack	Succession of vertically stacked voxels
Voxel	A voxel represents a value on a regular grid in three-dimensional space. Voxel is a combination of "volume" and "pixel" where pixel is a combination of "picture" and "element".
V_p	Velocity of the compressional wave (P-wave)
V_s	Velocity of the shear wave (S-wave)
V_{s30}	Time-averaged shear wave velocity over the depth interval between 0 and 30 m below the surface.

Table B.2 Abbreviations for lithofacies codes used in the schematisation

Lithofacies code	Sedimentary environment	General lithology	Period	Stratigraphic notes
Pfsf	Fluvial channel belt	Fine sand	Pleistocene	Various
Pfsm	Fluvial channel belt	Medium coarse sand	Various	Various
Pfsc	Fluvial channel belt	Coarse to very coarse sand	Various	Various
Pxlp	Various	Low permeability, clay/loam	Various	Various
Pasf	Cover sand	fine sand	Boxtel	BXWI
Pvsm	Streamlet	Medium to coarse sand	Boxtel	BX without clay/loam/peat
Pvbd	Streamlet	Fine sand, loam, clay & peat (very diverse)	Boxtel	BXSI with clay/loam/peat
Pgcs	Glacial Till	Loam, sandy clay, gravelly, occasional sand inclusions	Drente	Glacial (Drente/Peelo)
Pgsc	Fluvioglacial	Coarse gravelly sand, gravelbeds, boulders	Drente	Drente Schaarsbergen
Pgcc	Potclay, glaciolacustrine clays	Clay, compact, occasional fine sand beds	Peelo	Peelo Nieuwolda
Pgsf	Glacial outbreak	Fine sand	Peelo	Peelo
Ptsc	Channel	Sand (clayey or silty), usually fine	Eem	Tidal (Eemian)
Ptsm	Channel	Medium coarse sand	Eem	
Ptcc	Mudflat	Clay, some sand/silt beds	Eem	
Pxpp	Swamp/Marsh	Peat	Eem	
Tfcc	Mudflat	Clay	Holocene	Tidal/Marine
Tfcp	Supratidal	Organic clay and peat alternations	Holocene	
Tfsc	Mudflat channels	Clay and sand, alternating	Holocene	
Tfss	Sandflat	Sand (clayey)	Holocene	
Tcsf	Channel belt	fine sand (clayey)	Holocene	
Tcss	Channel belt	fine, medium sand	Holocene	
Tcsm	Estuarine channel belt	medium sand (clayey)	Holocene	
Tccs	Channel fill	Clay sandy	Holocene	
Shpp	Swamp/Marsh	Peat, amorphous to not-amorphous	Holocene	Holland Peat
Sbpp	Swamp/Marsh	Compacted peat	Holocene	Basal Peat
Aaop	Landfill	various (clay, loam, sand, peat, concrete, rubble, wood)	Holocene	Anthropogenic

For abbreviations of geological Formations, see Figure D.2 in Appendix D.

C Overview of information sources

Table C.1 Overview of sources of subsurface information used for schematisation, including source, other potential use and included in NAM database.

Dataset	Version	Source	Used for schematisation	Other potential use	Included in NAM database
AHN	1	AHN; http://www.ahn.nl/pagina/het-ahn/het-ahn.html	Yes		no
Borings DINO	2-Sep-2014	TNO Geological Survey of the Netherlands; https://www.dinoloket.nl/	Yes		yes
Borehole logs	6-Oct-2014	Deltares; raw data from 15 available on DATE from new vertical seismic array locations	Yes	Improvement of REGIS model TNO	no
DGM	2.2 (2014)	TNO Geological Survey of the Netherlands; https://www.dinoloket.nl/	Yes		no
GeoTOP	Beta version of 11-Sep-2014	TNO Geological Survey of the Netherlands; https://www.dinoloket.nl/	Yes		no, no official release
NL3D		TNO Geological Survey of the Netherlands	No		no
REGIS II	2.1 (2008)	TNO Geological Survey of the Netherlands; https://www.dinoloket.nl/	Yes		no
CPT Arup	11-Sep-14	Arup	Partly	1. V_S information for each CPT, derived from SCPT calibration 2. For liquefaction potential	yes
CPT DINO	8-Sep-2014	TNO Geological Survey of the Netherlands; https://www.dinoloket.nl/	Yes		yes
CPT FUGRO	6-Oct-2014 and 24-Oct-2014	Fugro	Partly		yes
CPT Deltares	13-Oct-2014	Deltares archive	Partly		no (confidential)
CPT Wiertsema en partners	17-Sep-2014 and 17-Nov-2014	Wiertsema en partners	Partly		yes

Table C.1 Continued. Overview of sources of subsurface information used for schematisation, including source, other potential use and included in NAM database.

Dataset	Version	Source	Used for schematisation	Other potential use	Included in NAM database
Seismic CPT	16-Oct-2014	Fugro, Deltares, Wiertsema	No	1. New relation Vs and CPT 2. Parameterisation of geological units	yes
Raw data from 200 m deep borehole logs at 15 locations for vertical seismic arrays	8-Oct-2014	Deltares	Yes	When interpreted and for all vertical seismic array stations this is a valuable source to improve the data density to 200 m depth.	no
Holocene paleogeographic maps	2.0 (2013)	Vos et al. (2011) and updates by Deltares	Yes		no
Fault maps	2.2 (part of DGM)	TNO Geological Survey of the Netherlands	Yes		no
Salt dome maps	2.2 (part of DGM)	TNO Geological Survey of the Netherlands	Yes		no
Buildings in Groningen field	2-Sep-2014	NAM	No		no
V_{s30} Arup	draft 27-May-2014	Arup report “Groningen Preventive Structural Upgrading Ground Conditions in the Groningen Region", report number REP/229746/SR009, date 27 May 2014, draft report rev. 0.02	No		no
V_{s30} KNMI	11-Nov-14	KNMI, personal communication Tijn Berends	No		no
V_p and V_s information from Shell	Not yet available	Shell	No	1. For parameterisation of GSG-model with respect to V_s. 2. To derive V_p-V_s relations	no
Geomorphological map of the Netherlands	2004	Koomen, A.J.M and Maas, G.J. (2004) Geomorfologische Kaart Nederland (GKN); Achtergronddocument bij het landsdekkende digitale bestand. Wageningen, Alterra-report 1039, 38 p.	No (but used for GeoTOP by TNO).		no

D GeoTOP Oostelijke Wadden

The description of GeoTOP Oostelijke Wadden is provided by TNO Geological Survey of the Netherlands.

1 Introduction

GeoTOP is the latest generation of 3D subsurface models produced at TNO – Geological Survey of the Netherlands. The model schematizes the shallow subsurface of the onshore part of the Netherlands in millions of voxels each measuring 100 by 100 by 0.5 m (x, y, z) up to a depth of 50 m below sea level (Stafleu et al., 2011, 2012). Each voxel in the model contains lithostratigraphical information, lithological class information (including grain-size classes for sand) and the probability of occurrence for each of the lithological classes.

The GeoTOP model is constructed in model areas that roughly correspond to the Dutch provinces. The model area that covers the Groningen gas field is called “Oostelijke Wadden” and is still under construction. Impressions of lithostratigraphic units and most likely lithological classes for GeoTOP Oostelijke Wadden are shown in Figure D.1 to Figure D.3.

The impact of using the beta version of GeoTOP Oostelijke Wadden is described in the main report in section 3.5.1. Specific issues of GeoTOP to the GSG-model are described in section 3.5.2. The findings of the first round of quality control by TNO are included in section 3.5.4.

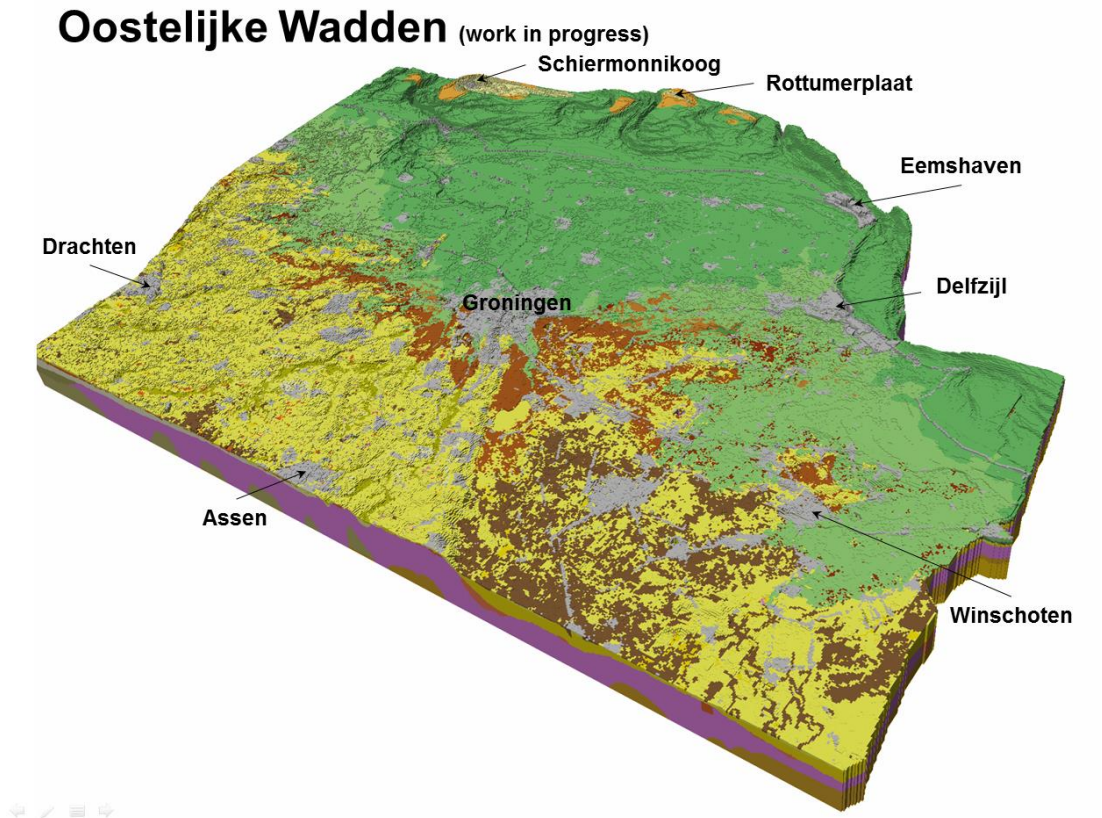

Figure D.1 Impression of the GeoTOP model “Oostelijke Wadden” colour-coded with the lithostratigraphical units. Legend in Figure D.2.

Anthropogenic deposits	
AAOP	Anthropogenic deposits
Naaldwijk Formation	
NASC	Naaldwijk Formation, Schoorl Member
NAZA	Naaldwijk Formation, Zandvoort Member
NA	Naaldwijk Formation, no differentiation between Wormer and Walcheren Members
NAWA	Naaldwijk Formation, Walcheren Member
NAWO	Naaldwijk Formation, Wormer Member
Nieuwkoop Formation	
NINB	Nieuwkoop Formation, Nij Beets Member
NIHO	Nieuwkoop Formation, Hollandveen Member
NIBA	Nieuwkoop Formation, Basal Peat Bed
Boxtel Formation	
BX	Boxtel Formation
BXKO	Boxtel Formation, Kootwijk Member
BXSI1	Boxtel Formation, Singraven Member, upper unit
BXWI	Boxtel Formation, Wierden Member
BXSI2	Boxtel Formation, Singraven Member, lower unit
Other units	
EE	Eem Formation
DR	Drente Formation
DRGI	Drente Formation, Gieten Member
DN	Drachten Formation
URTY	Urk Formation, Tynje Member
PE	Peelo Formation
UR	Urk Formation, Tynje Member
ST	Sterksel Formation
AP	Appelscha Formation
PZWA	Peize and Waalre Formations (Peize in this area)

Figure D.2 Legend for Figure D.1.

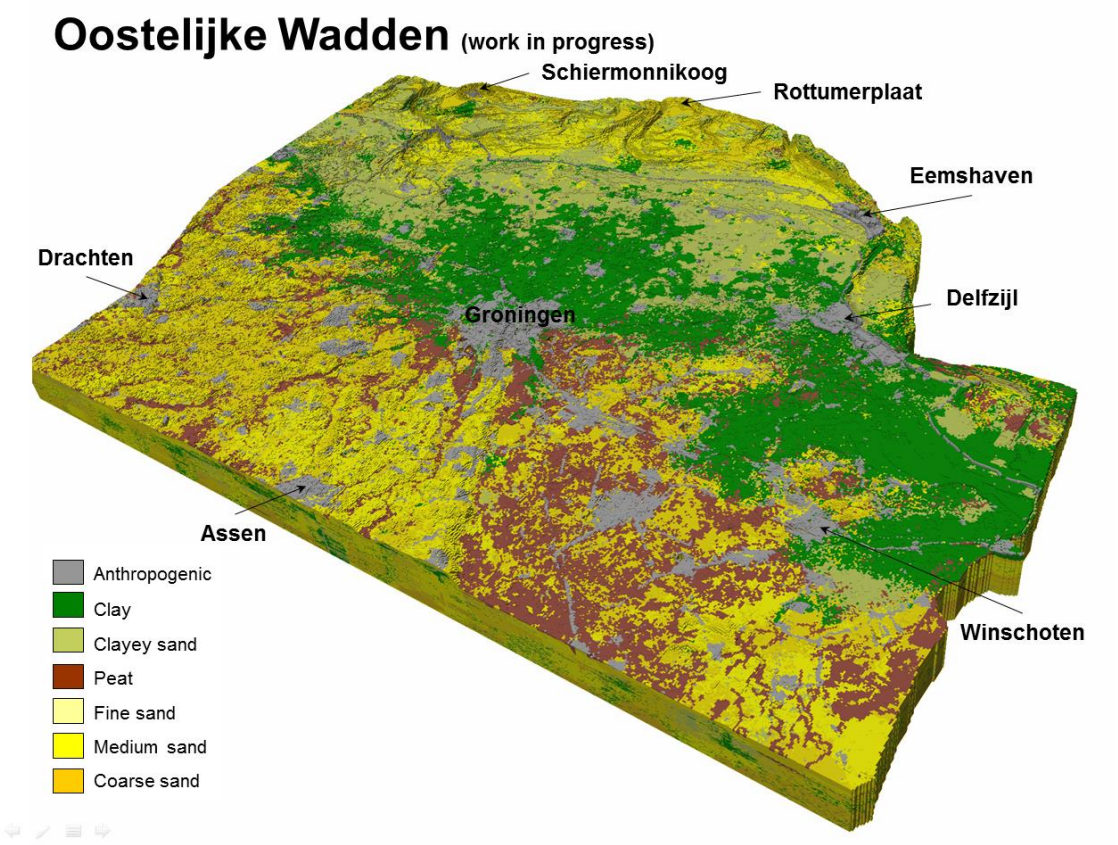

Figure D.3 Impression of the GeoTOP model "Oostelijke Wadden" colour-coded with the most likely lithological class.

2 Construction of the Oostelijke Wadden model

2.1 Model characteristics

GeoTOP Oostelijke Wadden schematises the shallow subsurface in ~42.6 million voxels each measuring 100 by 100 by 0.5 m (x, y, z). Each voxel in the model has a number of attributes. These are:

(1) The **lithostratigraphical unit** to which the voxel is assigned (Figure D.1);
(2) **100** statistically equally probable **realizations** of the lithological class that is representative for the entire voxel;
(3) The **probability of occurrence** of each lithological class, calculated as the number of times the lithological class occurs in the 100 realizations divided by 100.
(4) The **most likely lithological class** that is representative for the entire voxel (Figure D.3). This most likely lithological class is calculated using the averaging method for indicator datasets described by Soares (1992).

In the GSG-model for the Groningen field (+5 km buffer), attributes 1 (lithostratigraphical unit) and 4 (most likely lithological class) are used.

The model area is bounded in the east by the Dutch-German border, in the north by the North Sea, in the west by the GeoTOP model area “Westelijke Wadden” (for areal extent see www.dinoloket.nl) and in the south by an east-west boundary at RD Y-coordinate of 558,000 m. The total area is 4185.35 km^2 (418,535 grid cells of 100 by 100 m).

The top of the model is defined by a combination of land surface and water depth. Land surface heights range from about NAP-2 m in the Holocene man-made lowlands to NAP+12 m on the island of Schiermonnikoog and NAP+20 m on the Hondsrug-ridge. The maximum water depth in the Wadden Sea is about NAP-25 m. One of the sand extraction sites in the area reaches a water depth of NAP-45 m. The model base is set at a fixed depth of NAP-50 m.

2.2 Model version

This study uses an unpublished beta-release of the GeoTOP “Oostelijke Wadden” model, dated 9 September 2014. It is important to note that this beta-release has not passed a thorough quality control. Some quality issues of the model are already known and, if relevant to the application at hand, described in the next section. However, the quality control of the model may reveal other issues that are presently unknown.

In general, we would like to emphasize that there will be significant differences between the beta-version used in this study and the final version which will be published by TNO in 2015. General issues concerning GeoTOP for the specific use of the product for the site response study are described in section 3.5.3. Issues identified during the first round of quality control of the GeoTOP model, performed by TNO, are described in section 3.5.4.

2.3 Data

The most important data source of the GeoTOP model is DINO, the national Dutch subsurface database operated by TNO – Geological Survey of the Netherlands. At the moment of model construction, this database contained about 425,000 boreholes situated within the onshore part of the Netherlands, of which 42,722 are within the “Oostelijke Wadden” area (‘onshore’ includes the Wadden Sea). All borehole descriptions are stored in a uniform coding system (SBB5.1; Bosch, 2000). The largest part of borehole data consists of manually drilled auger holes collected by the Geological Survey during the 1:50,000 geological mapping campaigns. Most of the other borehole data was provided by from

external parties like groundwater companies and municipalities. Because of the large share of manually drilled boreholes, borehole density decreases rapidly with depth (Figure D.4 and Figure D.5). This implies that in general, model uncertainty increases with depth. The spatial distributions of boreholes with end depths used for the Oostelijke Wadden GeoTOP model are shown in Figure D.6 to Figure D.9.

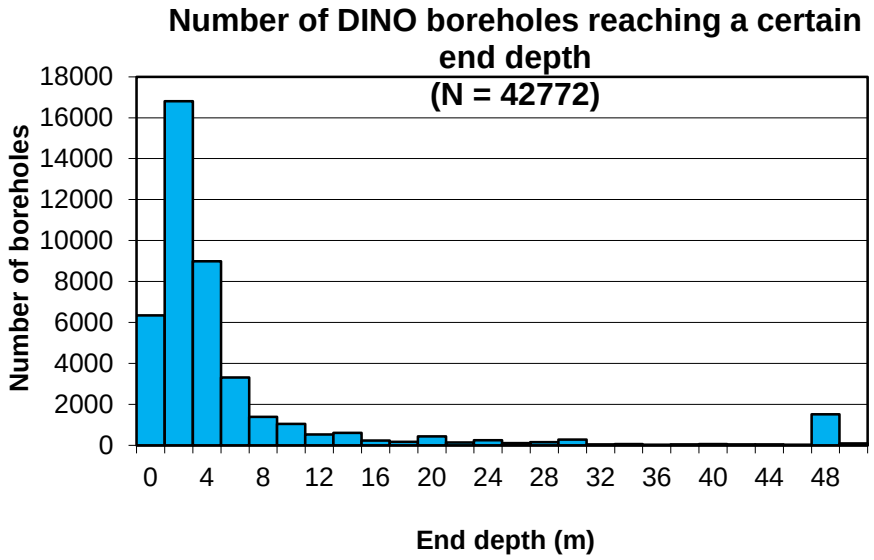

Figure D.4 Number of DINO boreholes reaching a certain end depth. N = 42,772; interval range 2 m.

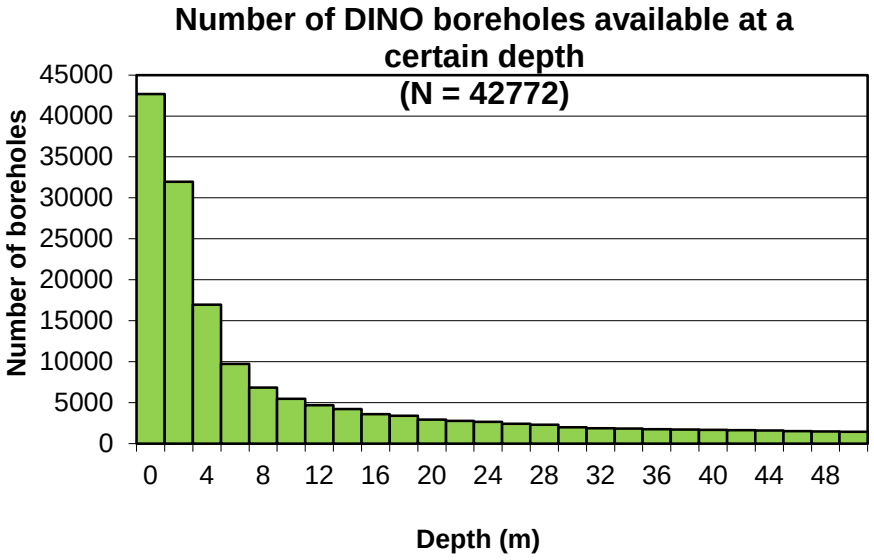

Figure D.5 Number of DINO boreholes available a certain depth. N = 42,772; interval range 2 m. In this figure, the cumulative number of boreholes is shown. For example, all borehole records with maximum depth of e.g. 8 m are also available for all higher situated depth ranges (in this case not only for 6-8 m, but also for 0-2 m, 2-4 m and 4-6 m).

All borehole descriptions within the Oostelijke Wadden area were extracted from the DINO database into the modelling environment and subsequently screened for basic quality criteria. Some 700 borehole descriptions of insufficient quality were excluded from the modelling. A total of 42,722 borehole descriptions were incorporated in the model.

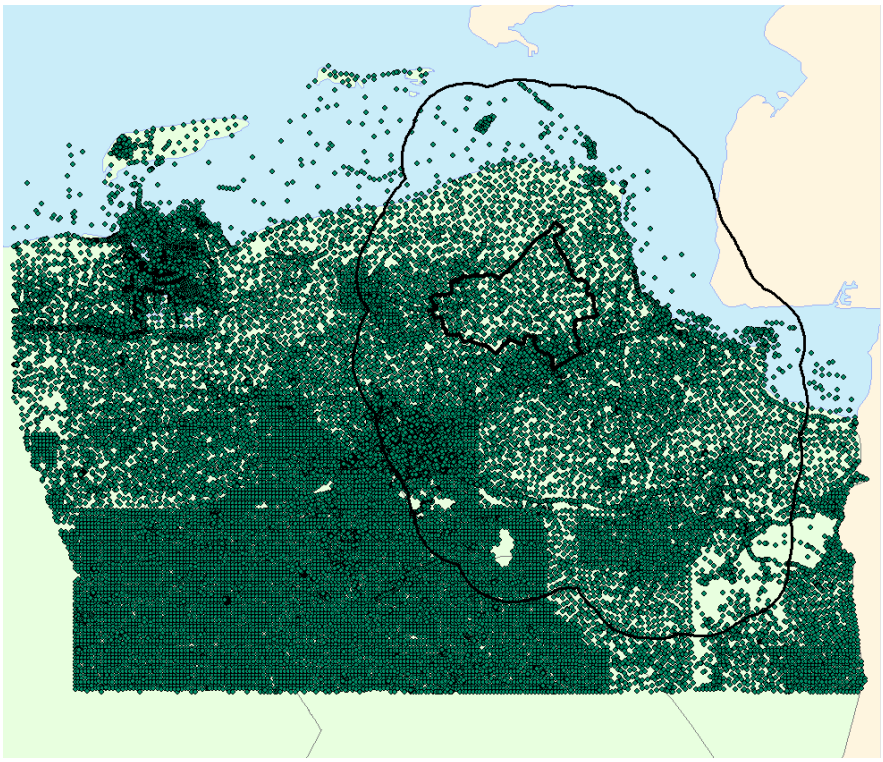

Figure D.6 Location of all DINO boreholes in the Oostelijke Wadden area. The inner black line represents the administrative boundary of the municipality of Loppersum, the outer black line is the outline of the Groningen gas field extended with a buffer of 5 km.

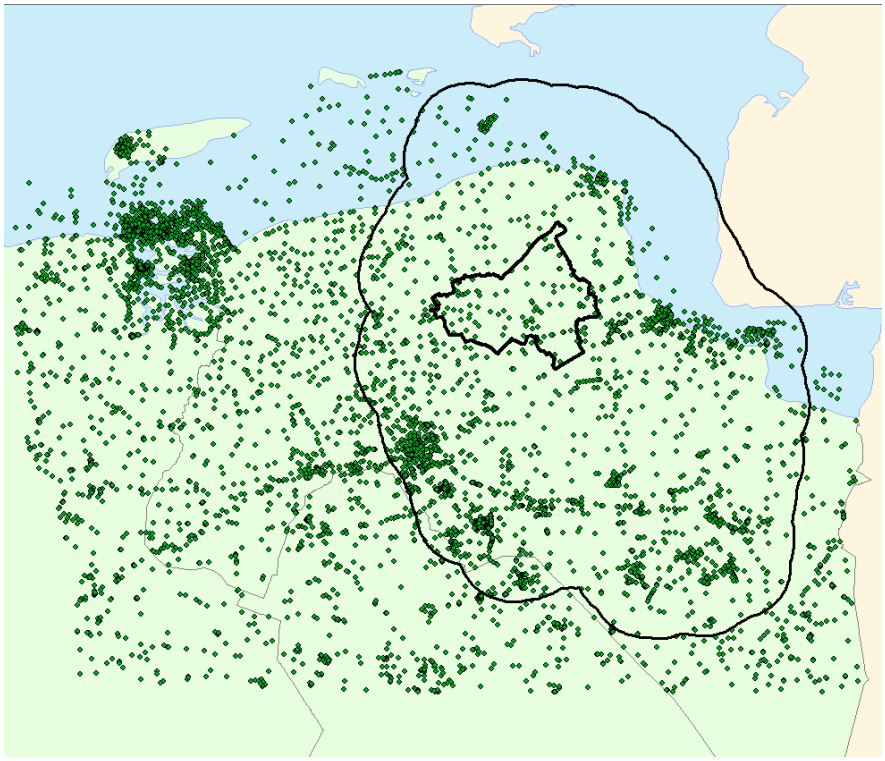

Figure D.7 Same as Figure D.6, with the location of DINO boreholes available at a depth of 10 m below land surface. N = 5843.

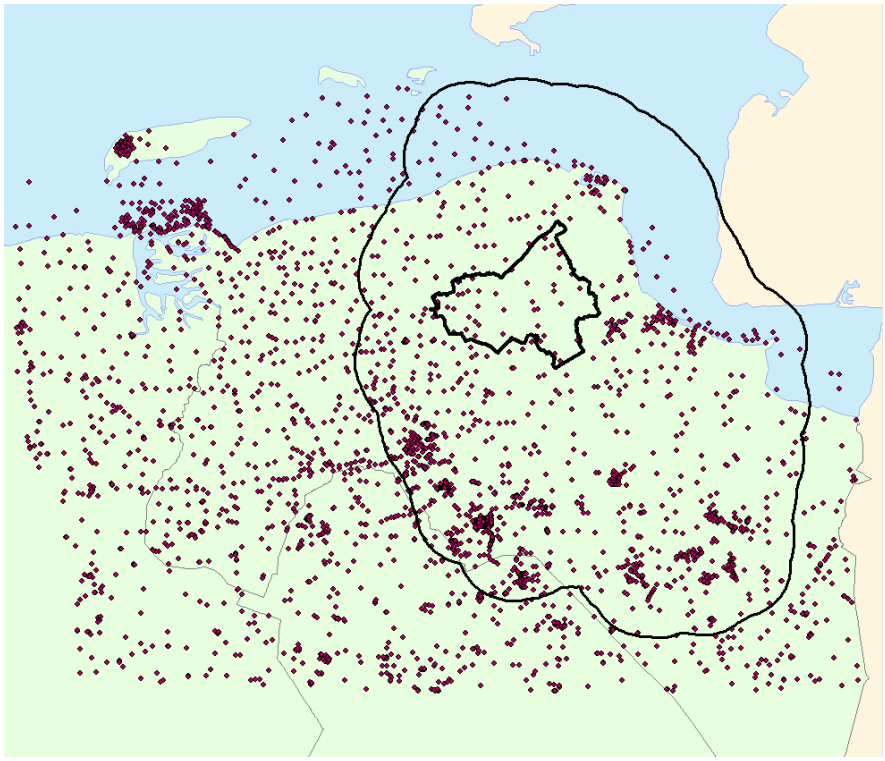

Figure D.8 Same as Figure D.6, with the location of DINO boreholes available at a depth of 20 m below land surface. N = 3251.

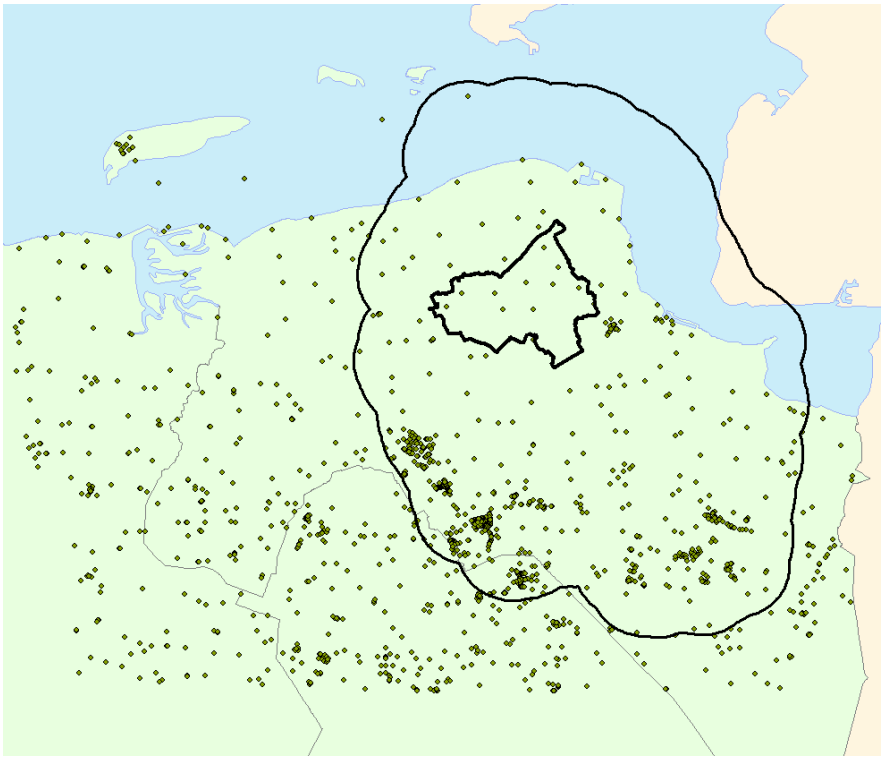

Figure D.9 Same as Figure D.6, with the location of DINO boreholes available at a depth of 50 m below land surface. N = 1480.

The upper boundary of the Oostelijke Wadden model is derived from the 5 by 5 m cell-size national airborne laser altimetry survey dataset (AHN2 – Actueel Hoogtebestand Nederland; www.ahn.nl). We used in-house developed software to mosaic the original 5 by 6.25 km map sheets into a single raster layer covering the entire country and subsequently resampled the data to a 100 by 100 m cell-size. Information on water depths of rivers, canals, Eemshaven and the Wadden Sea was obtained from bathymetric survey data.

Existing digital geological modelling results (raster layers) of the DGM model (version 2.1; Gunnink et al. 2013) were used in order to define the maximum lateral extent of selected lithostratigraphical units. The same raster layers were used as trend surfaces for several units in the 2D modelling procedure.

Other data sources include the soil map 1:50,000 (Steur and Heijlink, 1991; de Vries et al., 2003) and the geomorphological map 1:50,000 (Koomen and Maas, 2004) created by the National Soil Agency Alterra. These maps were used to define the maximum lateral extent of lithostratigraphical units that occur at or close to land surface. The lateral extent of anthropogenic deposits was derived from the national land use map (LGN5 - Landelijk Grondgebruik Nederland; raster resolution 25 by 25 m), developed and maintained by Alterra as well.

In case of the Drenthe Formation, Gieten Member (glacial till) the maximum lateral extent of the unit as well as the procedure to identify the top and the base of the unit in the borehole descriptions was largely based on the results of the so-called MIPWA-study carried out by Vernes et al. (2013).

2.4 Modelling procedure

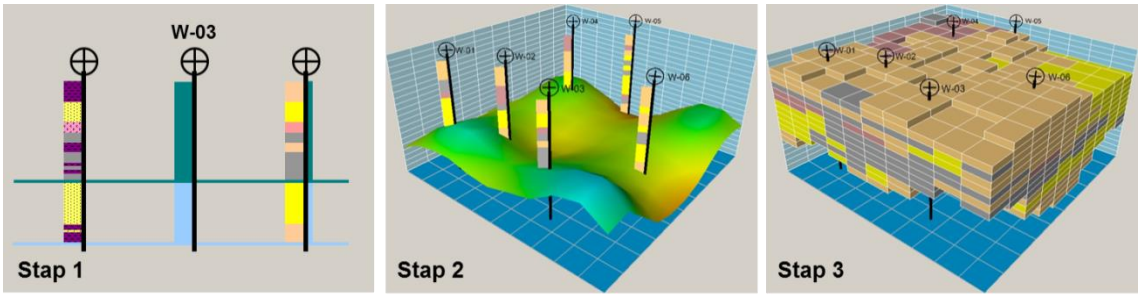

Figure D.10 The most important steps in the modelling procedure of GeoTOP: Step 1 – Interpretation of borehole descriptions in terms of lithostratigraphical units and lithological classes; Step 2 – 2D interpolation of the basal surface of each lithostratigraphical unit; Step 3 – 3D interpolation of lithological class within each lithostratigraphical unit.

The modelling procedure is schematised in Figure D.10. The first step is a geological schematisation of the borehole descriptions into units that have uniform sediment characteristics, using lithostratigraphical and lithological criteria. The lithostratigraphical interpretation of the borehole descriptions is then used in the second modelling step, where 2D bounding surfaces are constructed. These surfaces represent the top and base of the lithostratigraphical units and are subsequently used to place each voxel (100 by 100 by 0.5 m) in the model within the correct lithostratigraphical unit. Finally, the lithological classes in the borehole descriptions are used to perform a 3D stochastic interpolation of lithological class (clay, sand, peat) and if applicable, sand grain-size class within each lithostratigraphical unit. After this step, a 3D geological model is obtained. The use of stochastic techniques such as Sequential Gaussian Simulation and Sequential Indicator Simulation, allows us to compute probabilities for lithostratigraphy and lithology for each voxel, thus providing a measure of model uncertainty.

Details on the modelling procedure are described in the following sections.

2.4.1 Lithostratigraphical interpretation of borehole descriptions

The first step in the lithostratigraphical interpretation of borehole descriptions is the identification of the units to be included in the model. This identification is based on the geological knowledge of the area combined with expert judgement of the feasibility of successfully modelling a unit. For example, in the identification process it was decided not to model the so-called “potklei” (or potclay) as a separate unit, due to the low data density in the Peelo Formation and the occurrence of the “potklei” in different levels that are difficult to distinguish.

Table D.1 shows the lithostratigraphical units that occur in the Oostelijke Wadden model.

Table D.1 Lithostratigraphical units that occur in the GeoTOP "Oostelijke Wadden" model. Units marked with an asterisk (*) are not formally defined in the Lithostratigraphical Nomenclature of the shallow subsurface. "Number" refers to the numerical code for geological unit and lithological class. Fm.= Formation, Mbr. = Member.

Number	Code	Description (stratigraphic unit)	Depositional domain (facies)	Main composition (lithology)
1000	AAOP	Anthropogenic deposits	Man-made	Sand and clay, waste
3000	BXKO	Boxtel Fm, Kootwijk Mbr	Aeolian (drift sands)	Sand
1010	NIGR	Nieuwkoop Fm, Griendtsveen Mbr	Marshes	Peat
1020	NASC	Naaldwijk Fm , Schoorl Mbr	Aeolian (dunes)	Sand
1040	NAZA	Naaldwijk Fm., Zandvoort Mbr	Beach and shoreface	Sand
1045	NINB (*)	Nieuwkoop Fm, Nij Beets Mbr	Marshes	Peat
3011	BXSI1 (*)	Boxtel Fm, Singraven Mbr, unit 1 (uppermost unit)	Marshes	Peat
2000	NA	Naaldwijk Fm, no differentiation between Wormer and Walcheren Members	Tidal, undifferentiated	Sand and clay
1050	NAWA	Naaldwijk Fm, Walcheren Mbr	Tidal, uppermost unit	Sand and clay
1090	NIHO	Nieuwkoop Fm, Hollandveen Mbr	Marshes	Peat
1100	NAWO	Naaldwijk Fm, Wormer Mbr	Tidal, lowermost unit	Clay and sand
1130	NIBA	Nieuwkoop Fm, Basal Peat Bed	Marshes	Peat
3020	BXWI	Boxtel Fm, Wierden Mbr	Aeolian (cover sands)	Sand

Table D.1, continued. Lithostratigraphical units that occur in the GeoTOP "Oostelijke Wadden" model. Units marked with an asterisk (*) are not formally defined in the Lithostratigraphical Nomenclature of the shallow subsurface. "Number" refers to the numerical code for geological unit and lithological class. Fm.= Formation, Mbr. = Member.

Number	Code	Description (stratigraphic unit)	Depositional domain (facies)	Main composition (lithology)
3012	BXSI2 (*)	Boxtel Fm, Singraven Mbr, unit 2 (lowermost unit)	Brooks	Sand and clay
3100	BX	Boxtel Fm undifferentiated	Fluvial (local rivers)	Sand and loam
4110	EE	Eem Fm	Shallow marine / coastal plain	Sand and clay
5000	DR	Drenthe Fm	Glacial	Coarse sand and clay
5010	DRGI	Drenthe Fm, Gieten Mbr	Glacial	Till
5030	DN	Drachten Fm	Aeolian and local rivers / lakes	Sand
5040	URTY	Urk Fm, Tynje Mbr	Fluvial (Rhine)	Sand
5050	PE	Peelo Fm	Subglacial, proglacial and melt water	Sand and clay
5060	UR	Urk Fm	Fluvial (Rhine)	Sand
5080	AP	Appelscha Fm	Fluvial (eastern rivers)	Sand
5120	PZWA	Peize Fm and Waalre Fm (Peize in this area)	Fluvial (Eridanos) and coastal plain	Sand

For each of these units, a map delineating the maximum lateral extent of occurrence was created. Examples of these maps are given in Chapter 2 of the main report (Figure 2.6). A "maximum lateral extent" means that in the final model, a unit will not occur outside the boundaries of the extent. However, it does not necessarily mean that the unit will *always* occur within the boundaries of the extent.

Next, automated procedures (i.e., computer programs written in the programming language Python) were developed to apply a predefined set of criteria to the borehole descriptions that lie within the maximum extent of a certain lithostratigraphical unit. If an interval in the borehole description meets the criteria, this interval is assigned that particular unit. For example, the (relatively simple) criteria for finding Nieuwkoop Formation, Nij Beets Member within its maximum extent are as follows:

- The order in which the borehole interval descriptions are analysed is from top (surface height) to bottom (end depth).

- The base of the interval has to be above the top of any intervals belonging to Drenthe Formation, Gieten Member.
- The base of the interval has to be above NAP-10 m.
- The top of the uppermost interval has to be within 0.75 m from surface height.
- The main lithology code is either “V” (peat), “GY” (gyttja) or “K” (clay).
- Intercalated layers of a different lithology may occur if their cumulative thickness does not exceed 0.2 m.

Note that in this example, the interpretation of the Nij Beets Member partly depends on an earlier interpretation of the Gieten Member. This implies that the different units have to be interpreted in a specific order.

The procedure results in a dataset of borehole locations with top levels and base levels of the Nij Beets Member. This dataset is subsequently plotted on a map along with the maximum lateral extent of the unit after which modifications to the maximum extent and/or the set of criteria may be necessary in order to improve the result. In this way, creating maps of maximum extent and developing automated procedures to assign lithostratigraphical units to borehole intervals is an iterative process that consumes a significant part (~50%) of the total modelling effort.

Similar procedures were developed for all Holocene units in Table D.1 (i.e., anthropogenic deposits through Nieuwkoop Formation, Basal Peat Bed) and three of the Pleistocene units: Boxtel Formation, Wierden and Singraven Members, and Drenthe Formation, Gieten Member. The result is a dataset of borehole locations with top levels and base levels for each of these lithostratigraphical units.

In a separate automated procedure, the borehole descriptions are assigned an alternative lithostratigraphical interpretation which is based on the DGM model. In this relatively simple procedure, the boreholes are intersected with the top and basal raster layers of the units of the DGM model. For each borehole location and depth range it was determined which DGM units were present and which borehole interval top levels were positioned closest to the top raster layer of each of these units. Subsequently, from the sequence of units in the borehole, the base of the unit was derived. This relatively simple way of assigning stratigraphy to the borehole intervals ensures that the stratigraphical interpretation of the boreholes is consistent with the stratigraphical succession in the DGM model.

The results of the DGM interpretation and the datasets with interpreted top levels and base levels of the Holocene units and the three aforementioned Pleistocene units where then combined in a single dataset with the stratigraphical interpretation of the borehole description. In this combination procedure, the latter set of units always overrules the DGM units as illustrated in Figure D.11.

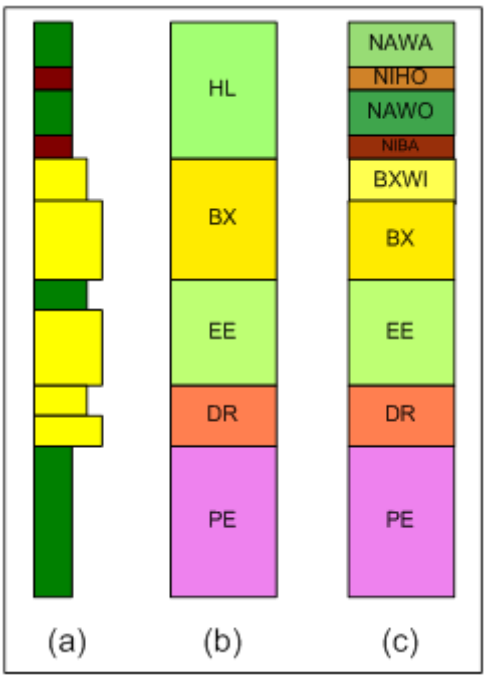

Figure D.11 (a) Borehole description with clay in green, peat in brown and sand in yellow colours; (b) interpretation based on the DGM model; (c) combined interpretation based on the DGM model (units BX, EE, DR, PE) and the datasets with interpreted top and base levels of the Holocene units (NAWA, NIHO, NAWO, NIBA, BXWI) and Pleistocene units (EE, DR, PE). Note that DGM-based unit BX is overruled by the BXWI unit. Example taken from a borehole in Groningen (modified after Stafleu et al. 2012).

2.4.2 Lithological classification of borehole descriptions

The most important attributes of the borehole descriptions that are used in the modelling procedure include top and basal depth of the borehole intervals, main lithology, admixtures of sand, silt and clay, sand median and shell content. Based on these attributes, each borehole interval was assigned a lithological class and each sandy interval was assigned a grain-size class. No lithological classification was applied to the anthropogenic deposits. We used the lithological classification scheme used in the hydrogeological subsurface model REGIS II (Vernes & Van Doorn, 2005) resulting in lithological classes that are suitable for groundwater flow modelling (Table D.2).

Table D.2 Lithological classes in the GeoTOP "Oostelijke Wadden" model.

Lithological class	Grain size
Anthropogenic deposits	N/A
Organic deposits (peat)	N/A
Clay	N/A
Clayey sand and sandy clay	N/A
Fine sand	63 – 150 µm
Medium sand	150 – 300 µm
Coarse sand, gravel and shells	> 300 µm

2.4.3 2D interpolation of lithostratigraphical surfaces

The first step in the 2D interpolation is calculating a trend surface of the base of each lithostratigraphical unit. This trend surface captures regional variations in the depth of the base of the unit. The trend surface has a cell-size of 500 by 500 m and is calculated by linear interpolation of the borehole data using ordinary kriging with a linear variogram. In case of several units that are also present in the DGM model (i.e., Eem Formation, Drenthe Formation and Drachten through Peize Formations; Table D.3), the basal surface of the corresponding unit in the DGM model was used as a trend surface.

In the second step, the depth of the base of each lithostratigraphical unit in each borehole was compared with the depth of the corresponding trend surface. The differences between the depth of the regional surface and the boreholes, the so-called 'residuals', represent a measure of how well the surface fits to the data, and were subsequently interpolated using Sequential Gaussian Simulation (SGS; Goovaerts, 1997; Chilès and Delfiner, 2012). The simple block kriging algorithm was used, in which the model-mean was set to 0. SGS estimates the residual value at a given location based on the values of the data points in a circular search neighbourhood and a variogram model describing the spatial correlation. The variogram model ensures that the data most closely correlated with the target cells are given the greatest weight in the interpolation.

The simulations were carried out using the Isatis® modelling software package (www.geovariances.com) and resulted in 100 different realisations of statistically equally probable residual variations. From these realisations, a mean residual surface with a cell-size of 100 by 100 m was calculated. By adding this surface to the original trend surface, a new basal surface was created for use in the remainder of the modelling process. By using the standard deviation of the 100 Sequential Gaussian Simulation (SGS) we calculated the probability that each voxel in the 3D modelling space is part of the lithostratigraphical unit, giving an indication of model uncertainty. Although we could have used kriging to interpolate the residuals, this would not have given us the opportunity to construct multiple, equally probable 2D lithostratigraphical models, which is possible with the SGS method.

In the third step, an integrated layer model was constructed that incorporated all of the newly created basal surfaces as well as known stratigraphical order and cross-cutting relationships. In the integrated layer model, top surfaces were defined by overlying basal surfaces. After completion of the layer model, the basal and top surfaces were used to assign the correct lithostratigraphical unit to each voxel within the 3D model space. Voxels of which the midpoint falls between the top and base of a lithostratigraphical unit were assigned that particular unit.

Several critical decisions were made during construction of this model. As an example, in situations where a thin occurrence of the Basal Peat Bed would be intersected by an overlying unit, we assigned a minimum thickness of 0.3 meters to the Basal Peat Bed below the base of the overlying units. This was done in order to prevent the Basal Peat Bed, regarded as a key unit in Holocene stratigraphy, to be largely removed during model construction. Other exceptions and deviations from the standard procedure as described above are summarised in Table D.3.

Table D.3 Modelled lithostratigraphical units with an indication of the trend surface used (calculated or using the basal surface of the corresponding DGM unit) and, if applicable, deviations from the standard modelling procedure. Fm.= Formation, Mbr. = Member.

Unit	Trend	Remarks
Anthropogenic deposits	Calculated	Trend and residuals were calculated for the thickness of the unit rather than the depth of the base of the unit. The depth of the base was subsequently calculated by subtracting the interpolated thickness from the height of the land surface. This procedure honours the close relationship of anthropogenic deposits with land surface height; Minimum thickness of 0.5 m applied.
Boxtel Fm, Kootwijk Mbr	Calculated	
Nieuwkoop Fm, Griendtsveen Mbr	Calculated	Modelled as a single surface along with “Nieuwkoop Fm, Hollandveen and Nij Beets Members”.
Naaldwijk Fm , Schoorl Mbr	Calculated	
Naaldwijk Fm., Zandvoort Mbr	Calculated	
Nieuwkoop Fm, Nij Beets Mbr	Calculated	Modelled as a single surface along with “Nieuwkoop Fm, Hollandveen and Griendtsveen Members”.
Boxtel Fm, Singraven Mbr, unit 1 (uppermost unit)	Calculated	

Table D.3, continued Modelled lithostratigraphical units with an indication of the trend surface used (calculated or using the basal surface of the corresponding DGM unit) and, if applicable, deviations from the standard modelling procedure. Fm.= Formation, Mbr. = Member.

Unit	Trend	Remarks
Naaldwijk Fm, no differentiation between Wormer and Walcheren Members	Calculated	Modelled as a single surface along with "Naaldwijk Fm, Wormer Mbr".
Naaldwijk Fm, Walcheren Mbr	Calculated	Minimum thickness of 0.5 m applied.
Nieuwkoop Fm, Hollandveen Mbr	Calculated	Modelled as a single surface along with "Nieuwkoop Fm, Nij Beets and Griendtsveen Members".
Naaldwijk Fm, Wormer Mbr	Calculated	Modelled as a single surface along with "Naaldwijk Fm, no differentiation between Wormer and Walcheren Members".
Nieuwkoop Fm, Basal Peat Bed	Calculated	Minimum thickness of 0.3 m applied.
Boxtel Fm, Wierden Mbr	Calculated	
Boxtel Fm, Singraven Mbr, unit 2 (lowermost unit)	Calculated	Modelled as a single surface along with "Boxtel Fm undifferentiated".
Boxtel Fm undifferentiated	Calculated	Modelled as a single surface along with "Boxtel Fm, Singraven Mbr, unit 2 (lowermost unit)".
Eem Fm	DGM	
Drenthe Fm	DGM	
Drenthe Fm, Gieten Mbr	Calculated	Maximum lateral extent of the unit as well as the procedure to identify the top and the base of the unit in the borehole descriptions was largely based on the results of the so-called MIPWA-study carried out by Vernes et al. (2013).
Drachten Fm	DGM	
Urk Fm, Tynje Mbr	DGM	
Peelo Fm	DGM	No residuals were calculated for this unit; the surface in GeoTOP equals the one in DGM.

Table D.3, continued Modelled lithostratigraphical units with an indication of the trend surface used (calculated or using the basal surface of the corresponding DGM unit) and, if applicable, deviations from the standard modelling procedure. Fm.= Formation, Mbr. = Member.

Unit	Trend	Remarks
Urk Fm	DGM	
Appelscha Fm	DGM	
Peize Fm and Waalre Fm (Peize in this area)	DGM	

2.4.4 3D interpolation of lithological class

The lithological classes in the boreholes were used as input for a 3D stochastic simulation procedure within each lithostratigraphical unit. For this, we used the Sequential Indicator Simulation technique (SIS; Goovaerts, 1997; Chilès & Delfiner, 2012) using the Isatis® modelling software package of Geovariances. SIS, based on the indicator kriging formalism, was used because it is a well-established method to simulate lithological class distributions, it requires modest computation time and is straightforward to implement (Goovaerts, 1997; Chilès and Delfiner, 2012). SIS estimates lithological classes for each voxel within a particular lithostratigraphical unit based on the lithological class of the surrounding borehole intervals and previously simulated nodes of the same lithostratigraphical unit. SIS was applied to all units in the model except for the anthropogenic deposits that were simply assigned a single lithological class.

In SIS, the borehole data are first migrated to the closest voxel and considered as hard data afterwards (marked “D” in Figure D.12). All the remaining voxels are scanned using a random path. A neighbourhood is established, centred on the target voxel (marked “?” in Figure D.12). Within this neighbourhood, the procedure searches for the hard data from the boreholes and for voxels that are already simulated (marked “S” in Figure D.12). The neighbourhood is searched using a variogram model which ensures that the data most closely correlated with the target voxels are given the greatest weight. The data are then coded into a set of indicators (hence the name indicator simulation). For each lithological class, the indicator is set to 1 if the data belongs to the lithological class and to 0 if not. The next step in SIS consists of a co-kriging phase (block kriging) taking into account the previous information, resulting in a probability between 0 and 1 for each lithological class. The values are plotted in a cumulative distribution function (marked “CDF” in Figure D.12). Then a random value between 0 and 1 is drawn and compared to the cumulative distribution function. The simulated lithological class at the target voxel corresponds to the rank of the interval to which the random value belongs.

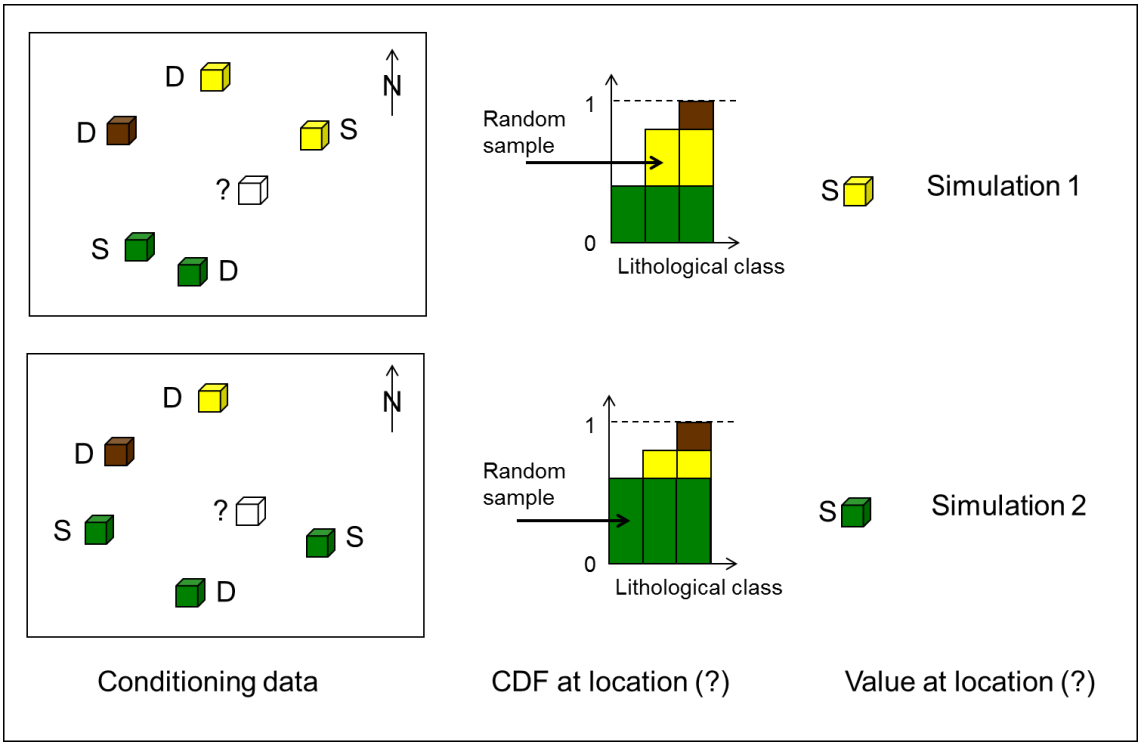

Figure D.12 Two different simulations of lithological class at the same target voxel using Sequential Indicator Simulation. See text for discussion. CDF – Cumulative Distribution Function.

Especially in the deeper parts of the model, the neighbourhood search at a target voxel may end up with no data (neither hard data from boreholes nor already simulated voxels). The result is then drawn from proportions. These are the global proportions of each lithological class observed in the boreholes which are assumed to be constant throughout the lithostratigraphical unit. In case of the Naaldwijk Formation (with no differentiation between Wormer and Walcheren Members) we decided to apply a vertical proportion curve (VPC) rather than a global proportion. A VPC was necessary because the shallow boreholes overestimate the global proportion of the shallow tidal flat clays. The VPC describes the expected proportion as a function of depth. At shallow depths, the VPC shows a high proportion of clay and a low proportion of sand, at greater depths the situation is reversed. A similar VPC was constructed for the Naaldwijk Formation, Schoorl Member.

In case of the sand grain sizes, the borehole data included intervals that have a described lithology “sand” but lack grain-size data. We solved this problem by dividing the interpolation procedure into a number of steps. First, we calculated 10 simulations of the distribution of sand versus non-sand sediment, using all the borehole data available. Then, for each of the 10 resulting realisations, we selected the voxels that were assigned a sand lithology. Next, we calculated another 10 simulations for these selected voxels, using only the borehole data with known grain-size estimates, resulting in 100 realisations of sand grain sizes in total. The same procedure was applied to 10 realisations of non-sand voxels. The 100 realisations of sand voxels were finally combined with the 100 realisations of non-sand voxels, resulting in 100, statistically equally probable realisations of lithological class distributions. From these realisations probabilities of occurrence for each lithological class were calculated resulting in an indication of model uncertainty. In addition, the probabilities were used to compute a “most likely lithological class” using the averaging method for indicator datasets described by Soares (1992). However, the 100 individual realisations remain available for further use in e.g. groundwater modelling but are not used in the current study.

E DGM and REGIS II models

The descriptions of DGM and REGIS II are provided by TNO Geological Survey of the Netherlands.

The models

Modern digital mapping of the Dutch subsurface started in 1999 with the development of the so-called **Digital Geological Model** (DGM; Gunnink et al., 2013). DGM is a 3D lithostratigraphical frame- work model of the onshore part of the Netherlands. DGM consists of a series of raster layers. Each lithostratigraphical unit is represented by rasters for the top, bottom, and thickness of the unit. The lithostratigraphical units are at the formation level; Holocene deposits are represented as a single layer (Figure E.1).

The list of modelled units in DGM with depositional domain, main composition and age is provided in Table E.1.

A second important step in digital mapping was the development of the **Regional Geohydrological Information System** (REGIS II; Vernes and Van Doorn 2005), which further subdivides the lithostratigraphical units of DGM into aquifers and aquitards (Figure E.2). Representative values for hydrological parameters (e.g., hydraulic conductivity and effective porosity) are calculated and assigned to the model, making it suitable for groundwater modelling on a regional scale. Like DGM, REGIS II models the Holocene deposits as a single cover layer. REGIS II is widely used by regional authorities and water supply companies for groundwater flow modelling studies.

Model versions

The current version of DGM is v2.2, published in 2014. GeoTOP “Oostelijke Wadden” uses this version for the modelling of the Boxtel Formation and all other formations at a stratigraphically lower position.

For REGIS II, version v2.1 was used. This version was published in 2008 and made available on DINOloket in 2009. It is based on the lithostratigraphical framework of DGM version v1.1. TNO Geological Survey of the Netherlands currently works on an update which is based on DGM version v2.2. This update will be published by TNO in 2015.

Both models are freely available at the web portal DINOloket:
https://www.dinoloket.nl/ondergrondmodellen

Issues with respect to the application at hand

Aquifers and aquitards versus sand layers and clay layers

The aquifers and aquitards in the REGIS II model are permeable and impermeable layers respectively. They are often misleadingly referred to as “sand layers” and “clay layers”, implying a homogeneous lithological composition. In reality, both the aquifers and aquitards may contain a variety of lithologies.

Versioning

REGIS II v2.1 is based on DGM v1.1 whereas GeoTOP “Oostelijke Wadden” uses DGM v2.2. This implies that mismatches between GeoTOP to REGIS II may occur at the transition at NAP-50 m.

Lithological composition of the Peelo Formation

As mentioned in Appendix D, the Peelo Formation is characterised by a very complex lithological composition. In the REGIS II model, the hydrogeological composition is modelled as five layers:

(a) an upper impermeable layer “pek1”
(b) a lower impermeable layer “pek2”
(c) three permeable layers “pez1”, “pez2” and “pez3” (Figure E.2). In this study, we make the simplified assumption that each of these hydrogeological layers has a uniform shear wave velocity.

Table E.1 List of modelled units in DGM with depositional domain, main composition and age (from Gunnink et al. 2013).

Unit	Abbreviation	Depositional domain	Main composition	Age (approx.)
Holocene (undifferentiated)	HL	Fluvial / coastal plain	Sand, clay and peat	Holocene
Boxtel	BX	Aeolian and local rivers	Sand (very fine to coarse), loam	Middle Pleistocene to Late Pleistocene[1]
Kreftenheye	KR	Fluvial (Rhine)	Sand (medium fine to very coarse)	Saalian to Weichselian
Eem	EE	Shallow marine / coastal plain	Sand (fine to medium coarse) and clay (shells)	Eemian
Kreftenheye-below Eem	KRZU[4]	Fluvial (Rhine)	Coarse sand	Saalian
Beegden	BE	Fluvial (Meuse)	Sand (medium coarse to very coarse)	Late Pliocene to Late Pleistocene[1]
Drente	DR	Glacial	Till, coarse sand and clay	Saalian
Ice-pushed	-	Glacial	Constitutes older sediments (ice-pushed)	Saalian
Drachten	DN	Aeolian and local rivers/lakes	Sand (medium fine to medium coarse)	Middle Pleistocene to Early Saalian
Urk-Tynje	URTY	Fluvial (Rhine)	Sand (medium coarse to very coarse)	Middle Pleistocene
Peelo	PE	Subglacial and meltwater	Sand (very fine to very coarse) and clay	Elsterian
Urk-Veenhuizen	URVE	Fluvial (Rhine)	Sand (medium coarse to very coarse)	Middle Pleistocene
Sterksel	ST	Fluvial (Rhine and Meuse)	Sand (medium coarse to very coarse)	Middle Pleistocene
Stramproy	SY	Fluvial and aeolian	Sand (very fine to very coarse)	Early to Late Pleistocene
Appelscha	AP	Fluvial (eastern rivers)	Sand (medium coarse to very coarse)	Middle Pleistocene
Peize[2]	PZ	Fluvial (Eridanos) and coastal plain	Sand (medium coarse to very coarse)	Pliocene to Early Pleistocene
Waalre[2]	WA	Fluvial (Rhine/Meuse) and estuary	Sand (medium fine to very coarse) and clay	Pliocene to Early Pleistocene
Maassluis	MS	Shallow marine and coastal	Sand and clay	Early Pleistocene
Kiezeloöliet	KI	Fluvial (Rhine and Meuse)	Sand (medium to coarse)	Pliocene
Oosterhout	OO	Shallow marine	Sand	Pliocene
Breda	BR	Shallow marine	Sand (very fine to medium coarse) and clay	Miocene to Early Pliocene
Rupel[3]	RU	Marine	Clay	Early Oligocene
Tongeren[3]	TO	Shallow marine / lagoon	Sand	Early Oligocene
Dongen[3]	DO	Marine	Clay and sand	Early to Middle Eocene
Landen[3]	LA	Shallow marine	(Sandy) clay and (glauconite) sand	Early Eocene
Heyenrath[3]	HT	Solution-residue of limestone	Flint	Pliocene to Quaternary
Houthem[3]	HO	Marine	Chalk	Early Paleocene
Maastricht[3]	MT	Marine	Chalk	Late Cretaceous
Gulpen[3]	GU	Marine	Chalk	Late Cretaceous
Vaals[3]	VA	Near coastal	Sand (fine)	Late Cretaceous
Aken[3]	AK	Near coastal	Sand and clay	Cretaceous

1 The Holocene part of the Formation is modeled in the amalgated unit ‘Holocene’.

2 Peize Formation and Waalre Formation are modelled as a combined unit in DGM.

3 Units are not modelled across the entire country.

4 This unit is erroneously abbreviated to KRZU in the model and on www.dinoloket.nl. This will be corrected in the next version of DGM.

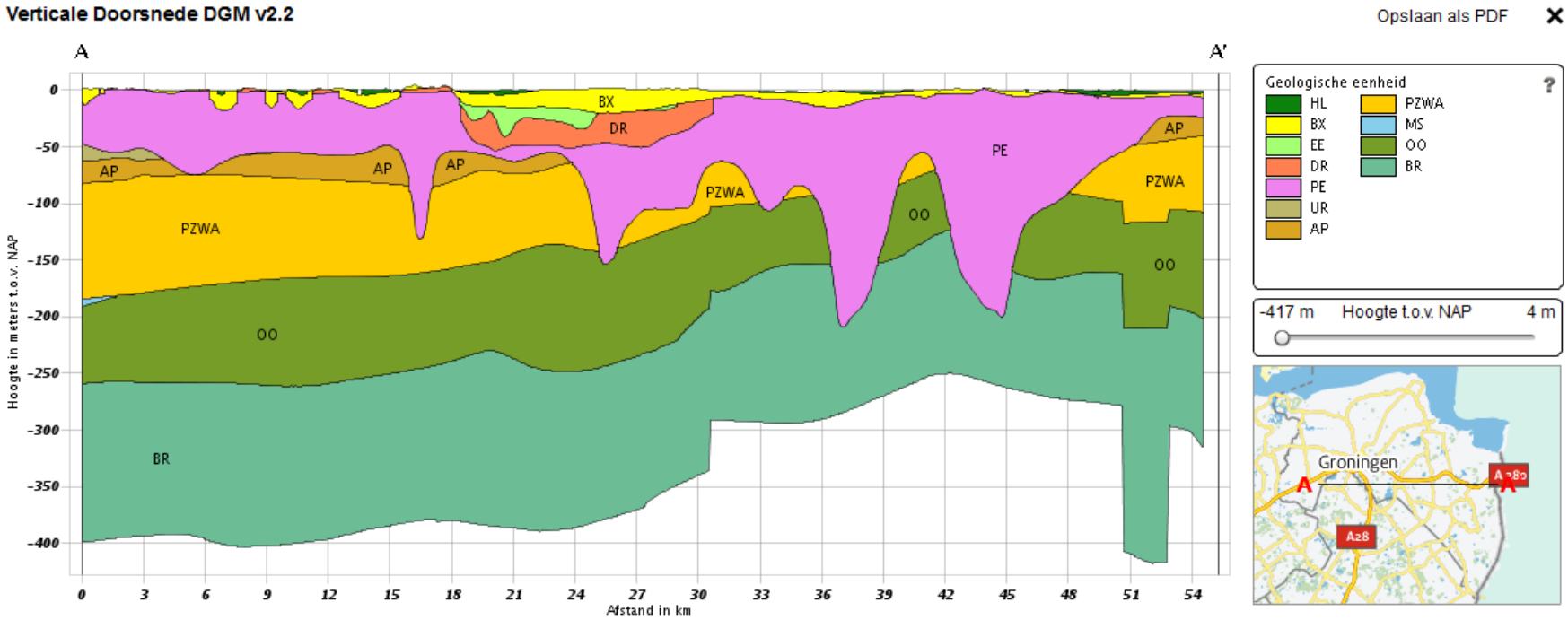

Figure E.1 West – East oriented vertical profile through the DGM model from the town of Leek to the German border. Note the pronounced glacial valleys of the Peelo Formation (pink). The reader is encouraged to create additional cross-sections on the web portal https://www.dinoloket.nl/ondergrondmodellen.

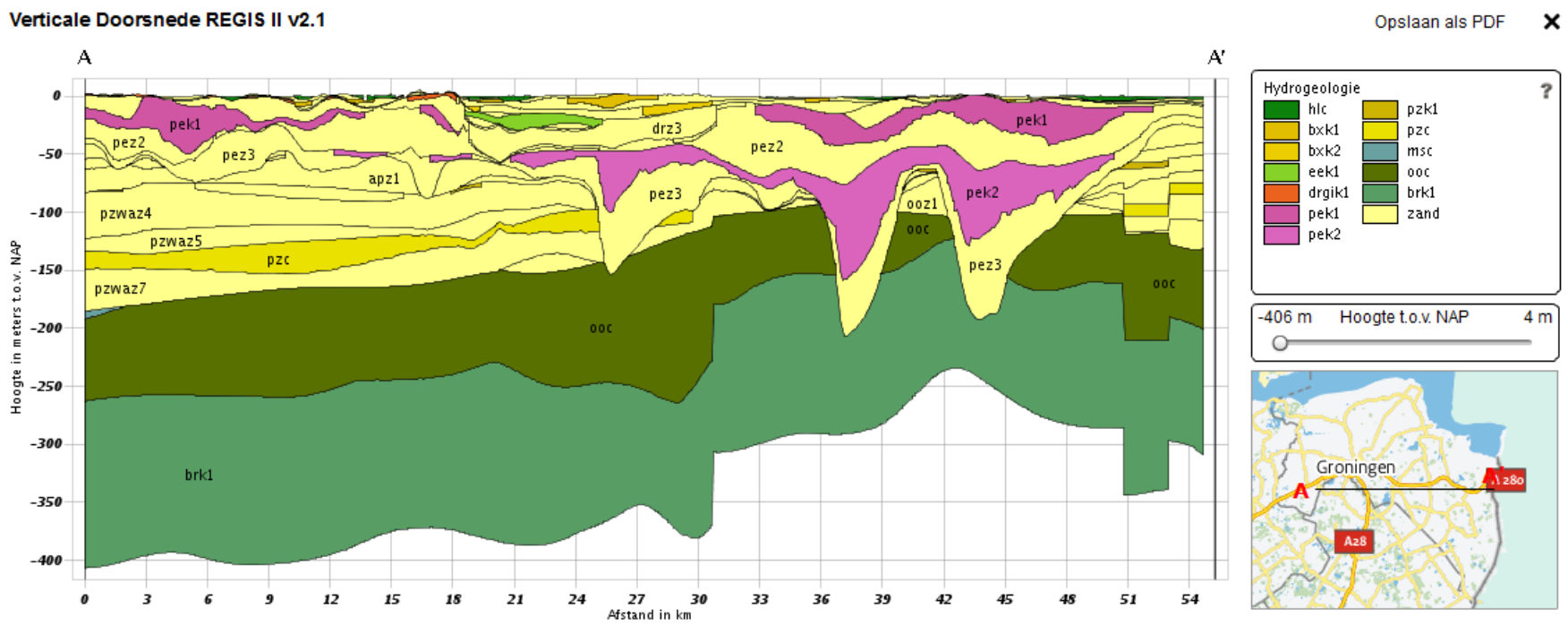

Figure E.2 West – East oriented vertical profile through the REGIS II model from the town of Leek to the German border. Note the two aquitards "pek1" and "pek2" within the Peelo Formation (pink). The reader is encouraged to create additional cross-sections on the web portal https://www.dinoloket.nl/ondergrondmodellen.

F Site response analysis of characteristic profile types

1 Introduction

For the assessment of the site response in Groningen during earthquakes a series of site response calculations is to be made. Inputs for these calculations are the profile types in Groningen. These profile types will be extracted from the Groningen subsurface model based on geology.

Please note that the aim of these calculations is not to calculate the site response at a particular location and/or for a particular acceleration record. The calculations are meant to give a general indication of site responses to be expected in Groningen.

The site response calculations were performed using STRATA (Kottke et al., 2013). STRATA is available from https://nees.org/resources/strata. This software performs one-dimension linear-elastic and equivalent-linear (SHAKE type) site response analyses using time series or random vibration theory ground motions. STRATA allows for stochastic variation of the site properties, including the shear modulus reduction and material damping curves, shear-wave velocity, layering, and depth to baserock. One of the inputs of STRATA is the soil-type profile: a vertical succession of layers with a soil-type and a shear-wave velocity attached to them. STRATA uses the term 'soil' for unconsolidated sediments. The baserock is the elastic half-space that forms the deepest unit in the STRATA vertical succession of layers.

2 Soil profiles

2.1 Profile description 7 typical Groningen profile types

From prior geological knowledge of the geology of Groningen, seven typical soil profiles (profile types) were selected from the DINO database. These profiles were selected for their typical succession of lithologies and formations. Moreover, CPT information at or near the borehole location was required to facilitate lithology classification based on cone resistance values from the CPTs. The 7 selected profiles are visualised in Figure F.1.

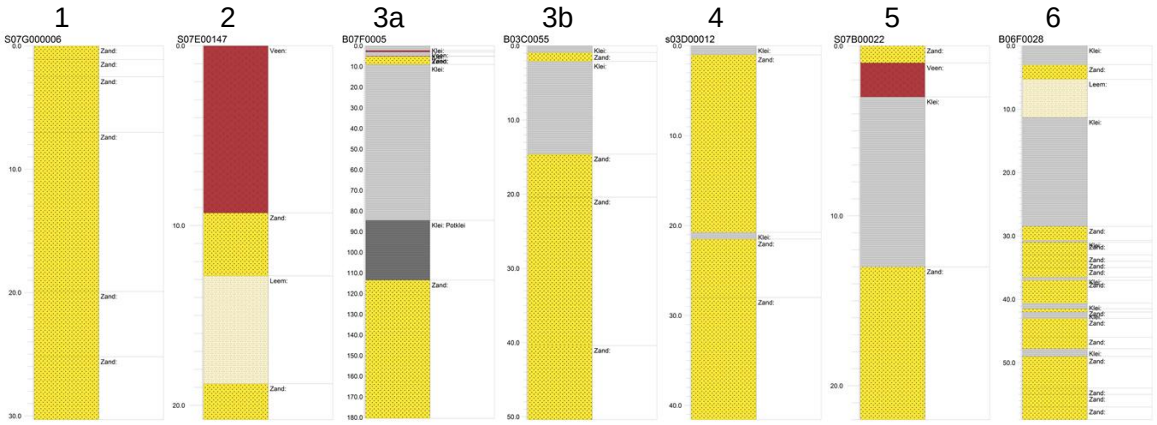

Figure F.1 Preliminary typical profile types used for the sensitivity analysis of site response using STRATA. From left to right: 1) sand only, 2) > 3 m peat on sand, 3a) > 1 m clay on peat on Pleistocene sand containing potclay, 3b) > 1 m clay on Pleistocene sand without potclay, 4) 15 m tidal sand, 5) >>5 m clay with thin peat layer, 6) glacial till on clay.

The borehole or CPT from the DINO database that defined the typical soil profile is stated in Table F.1. The length of the profile types varies between 22 and 180 m. The maximum depth of the profile types is assumed to coincide with the top level of baserock (measured from the surface) where the earthquake signal is applied.

Table F.1 Sources from DINO for seven typical Groningen profile types

Profile number	Profile lithology	Borehole (B) or CPT (S) code	Profile length (m)
1	Sand only	S07G000006	30.3
2	> 3 m peat on sand	S07E00147	28.4
3a	> 1 m clay on peat on Pleistocene sand containing potclay	B07F0005	180.5
3b	> 1 m clay on Pleistocene sand without potclay	B03C0055	50.4
4	15 m tidal sand	s03D00012	31.6
5	>>5 m clay with thin peat layer	S07B00022	22
6	glacial till on clay	B06F0028	33

2.2 General properties

The general properties of the soil profile are the small strain shear modulus(G_{max}) (or shear wave velocity V_s) and the density (ρ). The shear wave velocity is computed from the small strain modulus and the density of soil using the following equation:

$$V_s = \sqrt{G_{max}/\rho}$$

The density of the soil layers is estimated from standard geotechnical values. The small strain shear modulus (G_{max}) of a soil layer is estimated from the cone resistance (q_c) from CPT using preliminary correlations. The correlation between the cone resistance and shear wave velocity is approximate, and based on a quick comparison between measured cone resistance and shear wave velocity at a limited number of locations. In the future, these correlations will be updated. The density and G_{max} correlation is summarised in Table F.2.

Table F.2 Density and G_{max} estimates for different lithologies

Soil type	Density (10^3kg/m^3)	G_{max}
Sand	2	$10*q_c$
Clay	1.6	$40*q_c$
Peat	1 to 1.2	$40*q_c$
Loam	2	$20*q_c$

2.3 Baserock properties

The earthquake signal will be applied at the top of baserock. The baserock has general properties as follows:

- Volume weight: 22 kN/m^3.
- Damping: 1%.

The thickness of the baserock is assumed to be infinite. The top level of the baserock is assumed to be located at the bottom level of the last soil layer of a soil profile. The shear wave velocity (V_s) of the baserock is 400 m/s, unless the V_s value of the layer above exceeds this value. In that case, the V_s value has the same value as the layer above.

Unlike the soil layers above baserock, the baserock is assumed to be elastic and its damping and the shear wave velocity will not degrade with change of shear strain.

2.4 Dynamic soil properties

For the site response calculations, the dynamic soil properties related to damping (D) and shear modulus (G) are defined. Since nonlinear models were used in the calculations, both damping (D) and shear modulus (G) were shear strain (γ) dependent.

No site-specific shear modulus degradation and damping curves are available yet. Therefore, we used the standard curves available in STRATA. For the sensitivity calculations described in this appendix we selected curves that represent approximately the average of the available curves for sand and clay. There are no standard curves for peat included in STRATA. In literature, only a limited number of shear modulus degradation and damping curves for peat are published. These curves show large variations in possible relations (Figure F.2). The curves by Vucetic and Dobry (1991) for clay with a PI = 200 are representative for the behaviour at relative low stresses. Therefore, for the time being, we selected these curves were selected for the peat layers. In Figure F.2 and Figure F.3, the curve we selected is compared to the published curves. We recommend improving the shear degradation and damping curves for peat for Groningen.

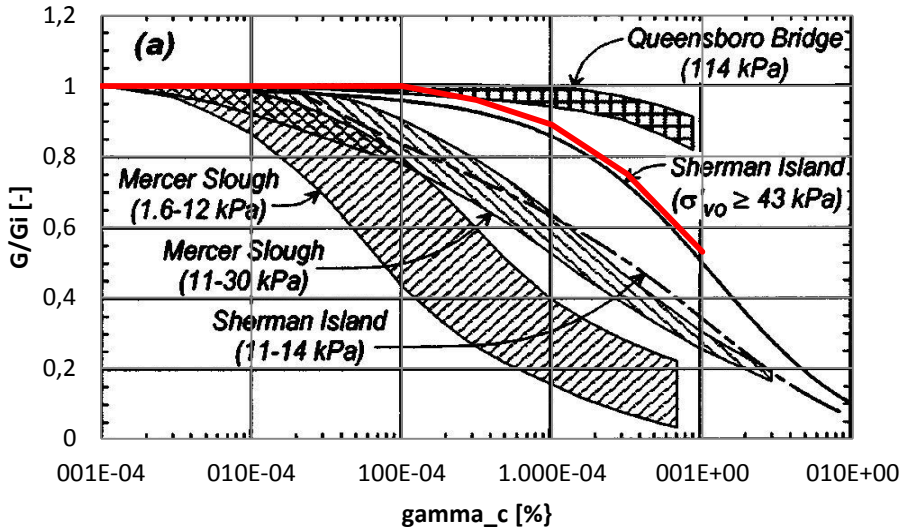

Figure F.2 Comparison selected shear modulus reduction curve for peat (red line) with different published curves (from Wehling et al, 2003).

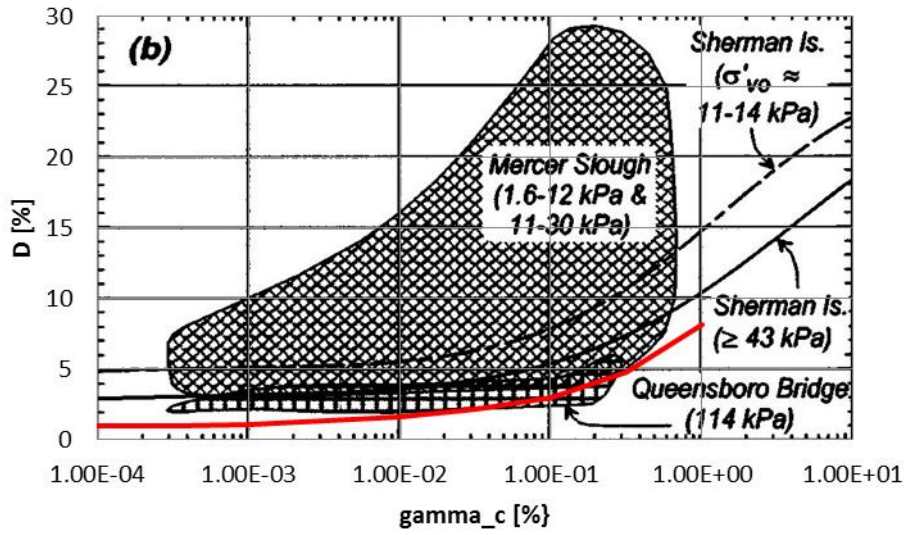

Figure F.3 Comparison selected degradation reduction curve for peat (red line) with different published curves (from Wehling et al, 2003).

The non-linear dynamic soil properties model for shear modulus (G) and damping (D) are soil type specific. The following models (standard curves provided within the STRATA program) were applied for both shear modulus (G) and damping (D):

- Sand : Idriss (1990), sand
- Clay : EPRI (1993), PI=30
- Clay (pek2) : Vucetic and Dobry (1991), PI=15
- Peat : Vucetic and Dobry (1991), PI=200
- Loam : Idriss (1990), sand

Clay (pek2) refers to Peelo clay. The Idriss (1990) model for sand was applied to all variations of sand (very fine, medium fine, medium coarse and coarse).

2.5 Material properties of soil layers

The layer representation and material property assignment for the seven profile types are presented in Table F.3 to Table F.9. The cone resistance for each layer is derived from the CPT graphs and based on local experience.

Table F.3 Profile type 1: sand only.

Depth [m+NAP]		Soil type	q_c [MPa]	G_{max}/q_c [-]	ρ [ton/m^3]	V_s [m/sec]	H [m]
Top	Bottom						
0.61	-0.5	sand	6	10	2	173.2051	1.11
-0.5	-1.9	sand	4	10	2	141.4214	1.4
-1.9	-6.4	sand	6	10	2	173.2051	4.5
-6.4	-19.3	sand	15	10	2	273.8613	12.9
-19.3	-24.6	sand	3	10	2	122.4745	5.3
-24.6	-29.7	sand	35	10	2	418.33	5.1

Table F.4 Profile type 2: peat layer of more than 3m thick underlying a medium sand layer.

Depth [m+NAP]		Soil type	q_c [MPa]	G_{max}/q_c [-]	ρ [ton/m^3]	V_s [m/sec]	H [m]
Top	Bottom						
0.8	-8.5	Peat	0.3	40	1	109.5445	9.3
-8.5	-12	Sand	20	10	2	316.2278	3.5
-12	-18	Loam	6	20	2	244.949	6
-18	-20	Sand	20	10	2	316.2278	2

Table F.5 Profile type 3a: Clay layer of more than 1m thick on a 2m thick peat layer underlying a Pleistocene sand layer with Peelo clay.

Depth [m+NAP]		Soil type	q_c [MPa]	G_{max}/q_c [-]	ρ [ton/m^3]	V_s [m/sec]	H [m]
Top	Bottom						
-0.88	-3.13	clay	0.2	40	1.6	70.71068	2.25
-3.13	-3.88	peat	0.2	40	1	89.44272	0.75
-3.88	-5.88	clay	0.5	40	1.6	111.8034	2
-5.88	-5.98	peat	0.2	40	1	89.44272	0.1
-5.98	-9.88	sand	6	10	2	173.2051	3.9
-9.88	-85.38	clay	3	40	1.6	273.8613	75.5
-85.38	-114.38	clay (pek2)	3	40	1.6	273.8613	29
-114.38	-181.38	sand	50	10	2	500	67

Table F.6 Profile type 3b: Clay layer of more than 1m thick underlying a Pleistocene sand layer without Peelo clay.

Depth [m+NAP]		Soil type	q_c [MPa]	G_{max}/q_c [-]	ρ [ton/m^3]	V_s [m/sec]	H [m]
Top	Bottom						
0.4	-0.5	clay	0.3	40	1.6	86.60254	0.9
-0.5	-1.7	sand	3	10	2	122.4745	1.2
-1.7	-14.2	clay	0.5	40	1.6	111.8034	12.5
-14.2	-20	sand	15	10	2	273.8613	5.8
-20	-40	sand	30	10	2	387.2983	20
-40	-50	sand	50	10	2	500	10

Table F.7 Profile type 4: Inter tidal sand layer of ±15 m thick underlying a coarse-dense sand layer.

Depth [m+NAP]		Soil type	q_c [MPa]	G_{max}/q_c [-]	ρ [ton/m^3]	V_s [m/s]	H [m]
Top	Bottom						
1.6	0.6	clay	0.5	40	1.6	111.8034	1
0.6	-19.15	sand, med. fine	7	10	2	187.0829	19.75
-19.15	-19.9	clay	0.5	40	1.6	111.8034	0.75
-19.9	-26.4	sand, med. coarse	15	10	2	273.8613	6.5
-26.4	-30	sand, coarse	35	10	2	418.33	3.6

Table F.8 Profile type 5: Clay layer of more than 5m thick with ± 1m thick peat layers underlying a loose to medium sand layer.

Depth [m+NAP]		*Soil type*	*q_c [MPa]*	*G_{max}/q_c [-]*	*ρ [ton/m^3]*	*V_s [m/sec]*	*H [m]*
Top	Bottom						
-0.2	-1. 2	sand	1	10	2	70.71068	1
-1.2	-3.2	peat	0.2	40	1.2	81.64966	2
-3.2	-13.2	clay	0.3	40	1.6	86.60254	10
-13.2	-22.2	sand	8	10	2	200	9

Table F.9 Profile type 6: Glacial till on clay layer underlying a dense sand layer.

Depth [m+NAP]		*Soil type*	*q_c [MPa]*	*G_{max}/q_c [-]*	*ρ [ton/m^3]*	*V_s [m/sec]*	*H [m]*
Top	Bottom						
1.3	-1.7	clay	0.1	40	1.6	50	3
-1.7	-4	sand, very fine	4	10	2	141.4214	2.3
-4	-10	loam	1	20	2	100	6
-10	-27.2	clay	0.8	40	1.6	141.4214	17.2
-27.2	-29.4	sand	30	10	2	387.2983	2.2
-29.4	-29.7	clay	3	40	1.6	273.8613	0.3
-29.7	-31.7	sand	30	10	1.6	433.0127	2

The used cone resistance profiles of the seven profile types are shown in Figure F.4. The calculated shear wave velocity profiles (from G_{max} and ρ) for the seven profile types are shown in Figure F.5.

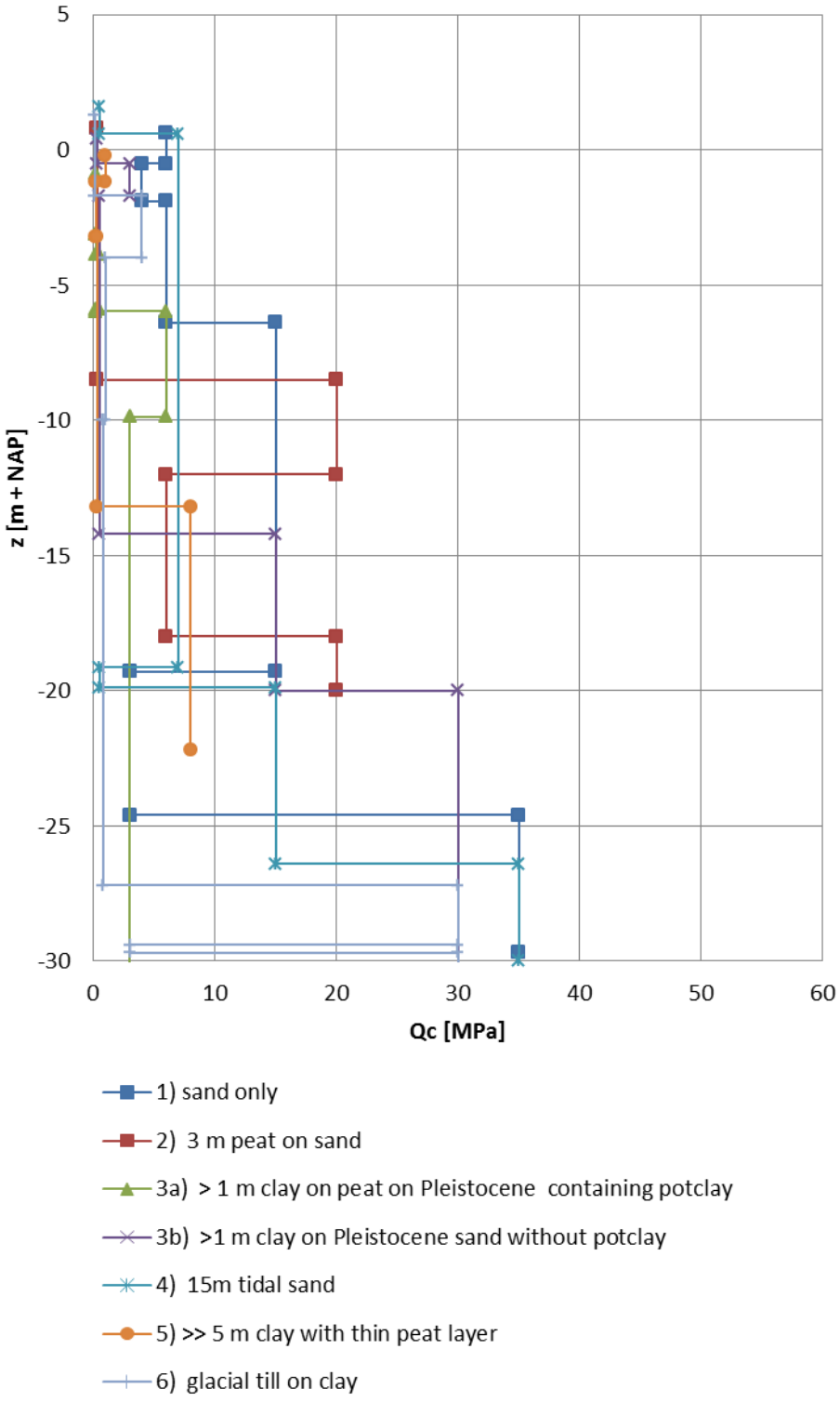

Figure F.4 Used CPT profiles for seven typical Groningen profile types

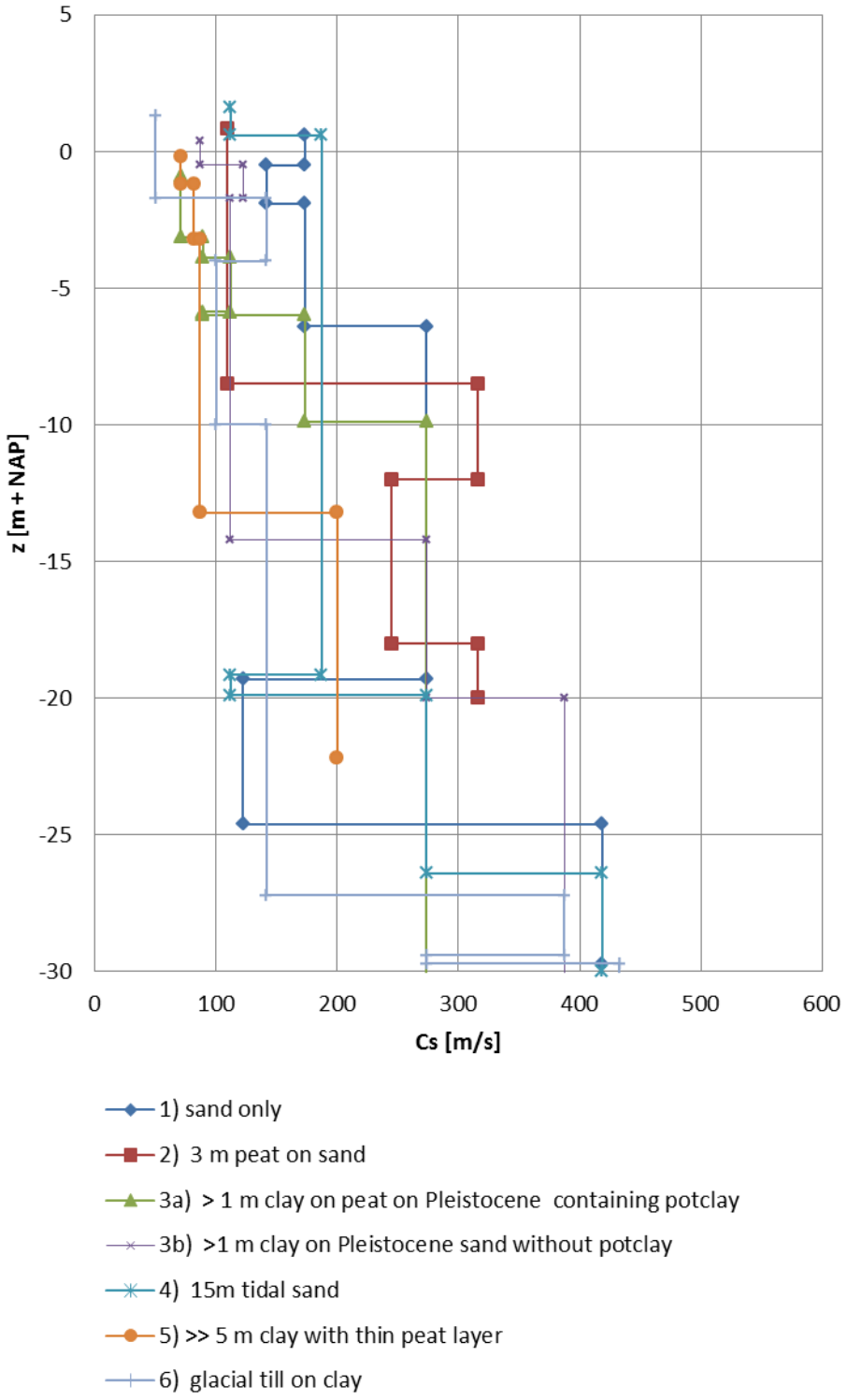

Figure F.5 Calculated shear wave velocity (V_s or C_s) profiles for seven typical Groningen profile types

3 Input signals

At the time of performing the sensitivity study, we selected two signals from Groningen earthquakes that were available at that time. The input signals are based on two records measured at station WSE: the Hoeksmeer earthquake of 27 June 2011 and the Huizinge earthquake of 16 August 2012 (Table F.10).

Table F.10 Input signals for STRATA calculations

Event	Date	Earthquake	Station	Epicentral distance [km]	Magnitude (M_w)
5	2011-06-27	Hoeksmeer	WSE (Westeremden)	7.92	3.4
6	2012-08-16	Huizinge	WSE (Westeremden)	1.25	3.6

The acceleration records at baserock (30 m depth) were determined using deconvolution of the surface signals to 30 m depth. In the deconvolution, the approximate soil profile at the location of the station Westeremden (WSE) was used. The soil profile at location WSE is shown Figure F.6

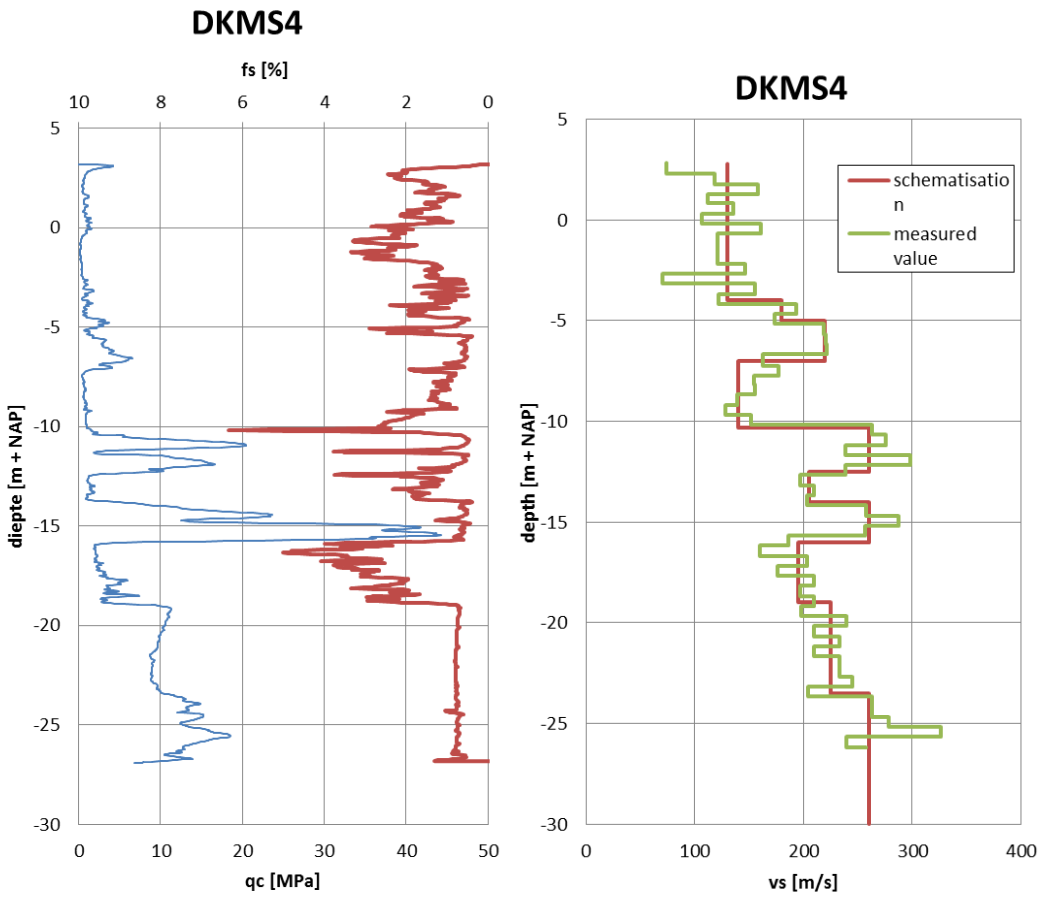

Figure F.6 Left: CPT at location WSE (cone resistance and local friction). Right: shear wave velocity profiles showing the measured shear wave velocity (green) and the simplified profile (red) used in the calculations.

Calculations are made with scaling the peak ground accelerations at baserock to 0.1g, 0.2g, 0.35g and 0.4g. No adjustment of the frequency for higher peak accelerations was applied. The signals were applied at the top level of baserock. Figure F.7 and Figure F.8 show the input signals deconvolved to 30 m depth.

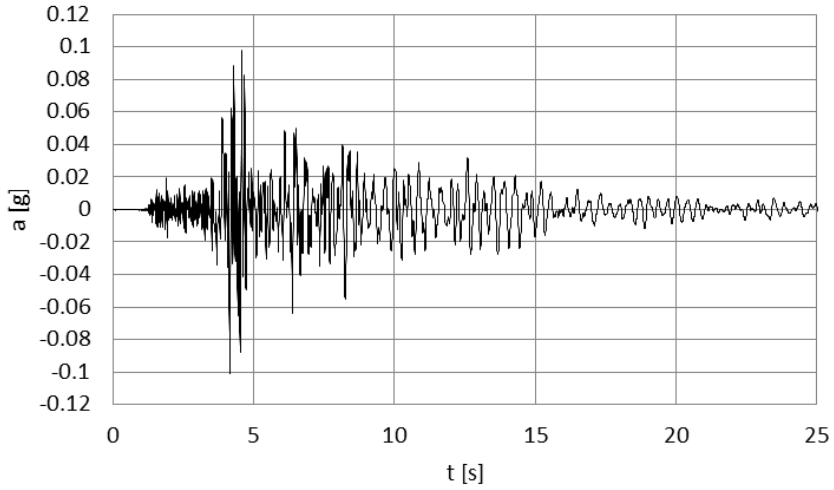

Figure F.7 Acceleration time series of Hoeksmeer, deconvolved to 30 m depth and scaled to peak acceleration of 0.1g.

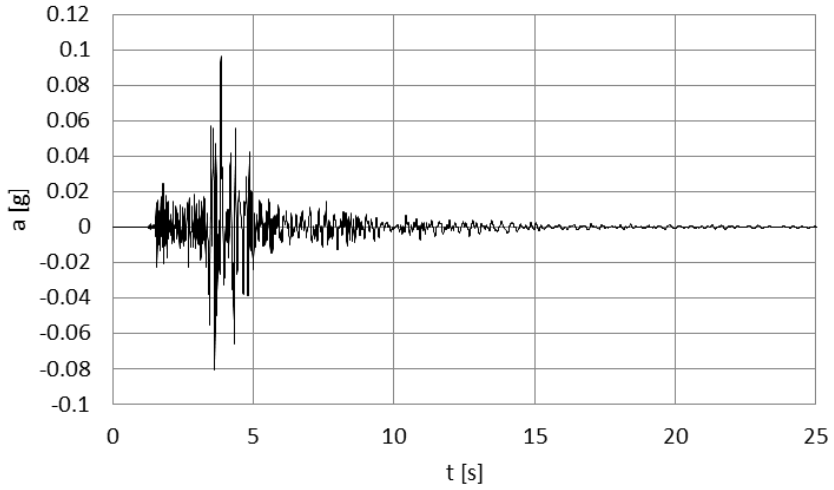

Figure F.8 Acceleration time series of Huizinge, deconvolved to 30 m depth and scaled to peak acceleration of 0.1g.

The frequency content of the signals is presented below in Figure F.9 and Figure F.10. The Hoeksmeer signal (Figure F.9) contains one dominant frequency (at 2 Hz) that produces the highest amplitude and two frequencies that produces lower amplitudes (at 5 Hz and 10 Hz). The signal of Huizinge (Figure F.10) has three dominant frequencies producing the same amplitudes (at 2 Hz, 5Hz and 11 Hz). The highest peak amplitude is observed at Hoeksmeer signal. However, both signals have similar range of dominant frequencies content.

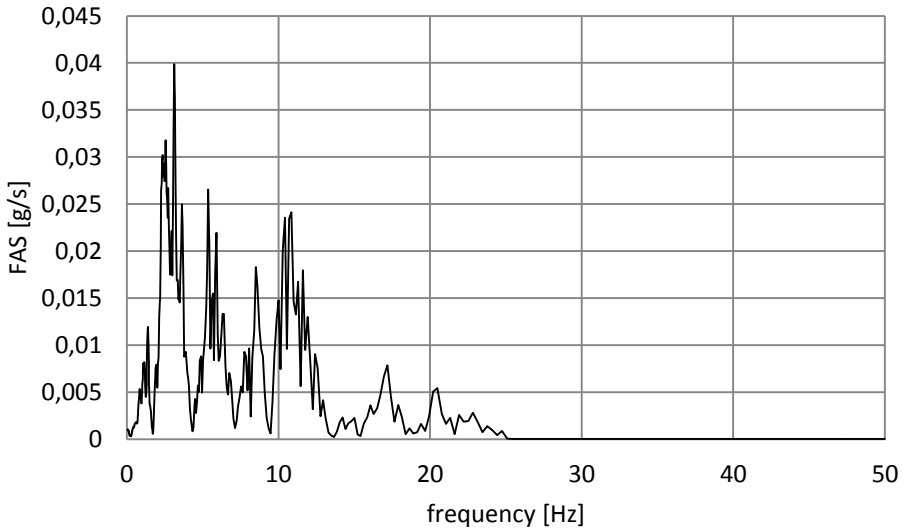

Figure F.9 Fourier amplitude spectrum of Hoeksmeer, deconvolved to 30 m depth and scaled to peak acceleration of 0.1g.

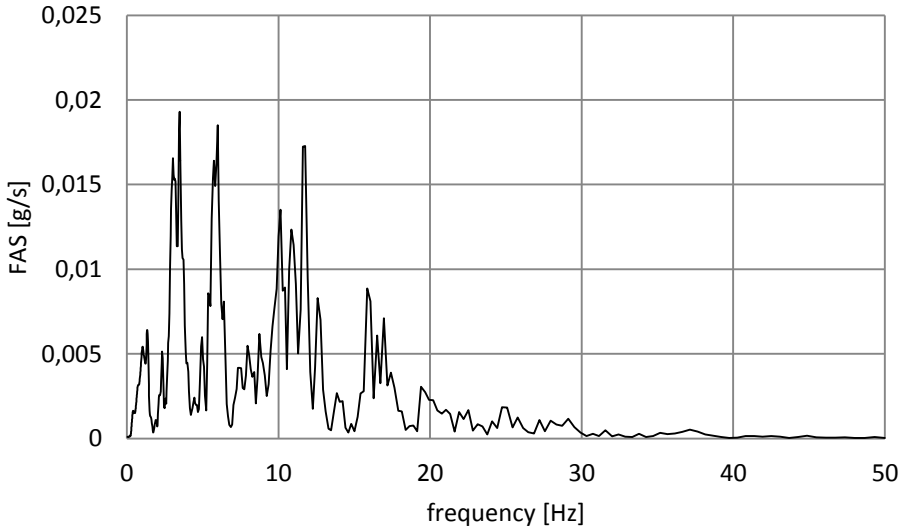

Figure F.10 Fourier amplitude spectrum of Huizinge, deconvolved to 30 m depth and scaled to peak acceleration of 0.1g.

4 Calculation result

4.1 PGA at surface for seven typical Groningen profile types

The peak ground acceleration (PGA) at the surface for the seven typical Groningen profile types is plotted versus peak acceleration (PA) at the top of baserock in Figure F.11 to Figure F.14.

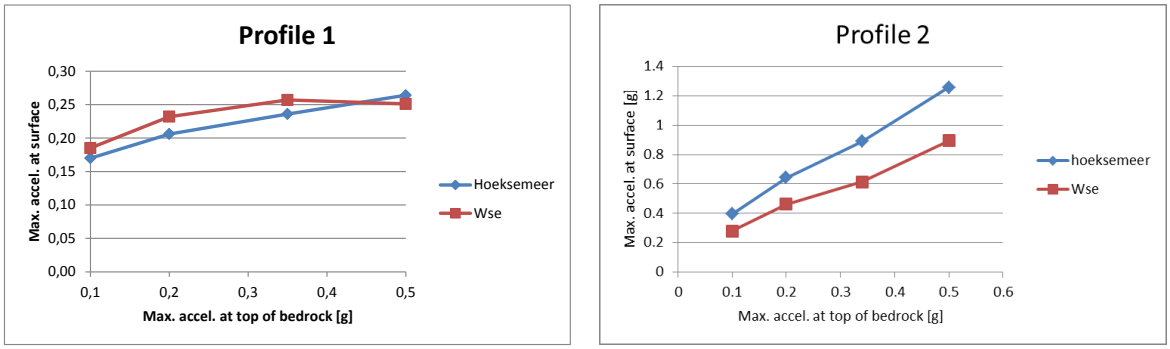

Figure F.11 PGA at surface vs. peak acceleration at top of baserock for profile type 1 (left) and profile type 2 (right).

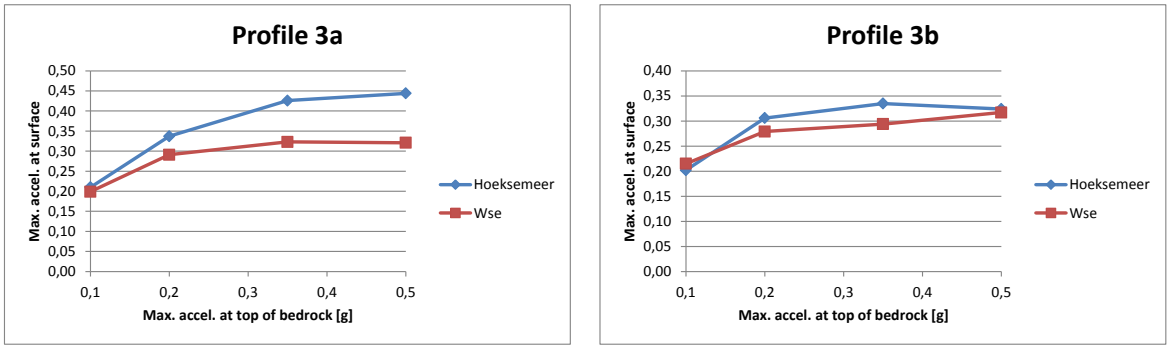

Figure F.12 PGA at surface vs. peak acceleration at top of baserock for profile type 3a (left) and profile type 3b (right).

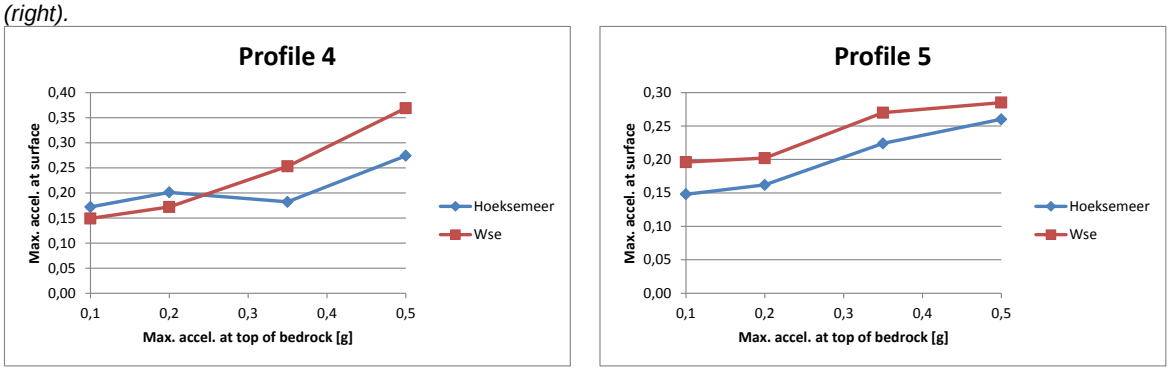

Figure F.13 PGA at surface vs. peak acceleration at top of baserock for profile type 4 (left) and profile type 5 (right).

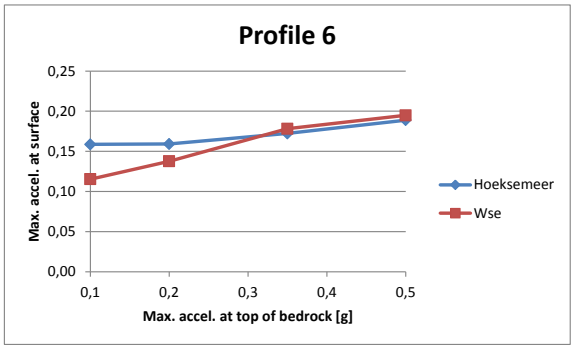

Figure F.14 PGA at surface vs. peak acceleration at top of baserock for profile type 6.

4.2 Amplification factor

The amplification factor refers to the amplification factor which is derived from $PGA_{surface}/PA_{baserock}$. For the seven typical Groningen profile types, the amplification factor is plotted versus PA at the top of baserock in Figure F.15 to Figure F.18.

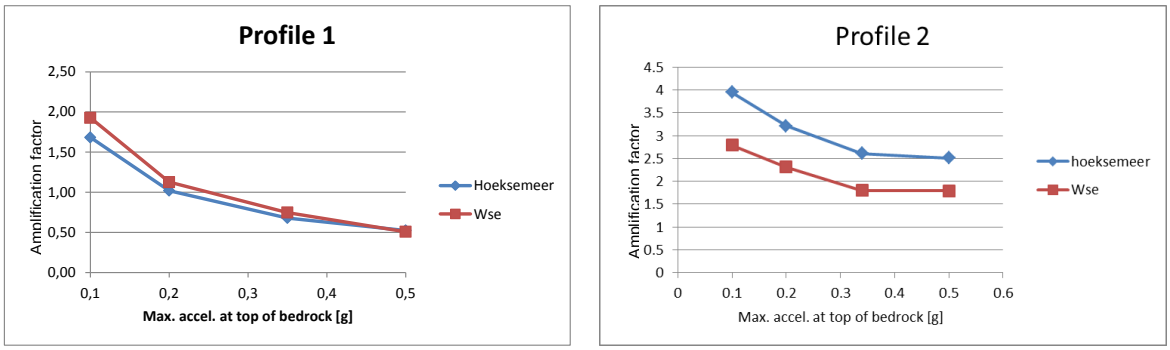

Figure F.15 Amplification factor vs. peak acceleration at top of baserock for profile type 1 (left) and profile type 2 (right).

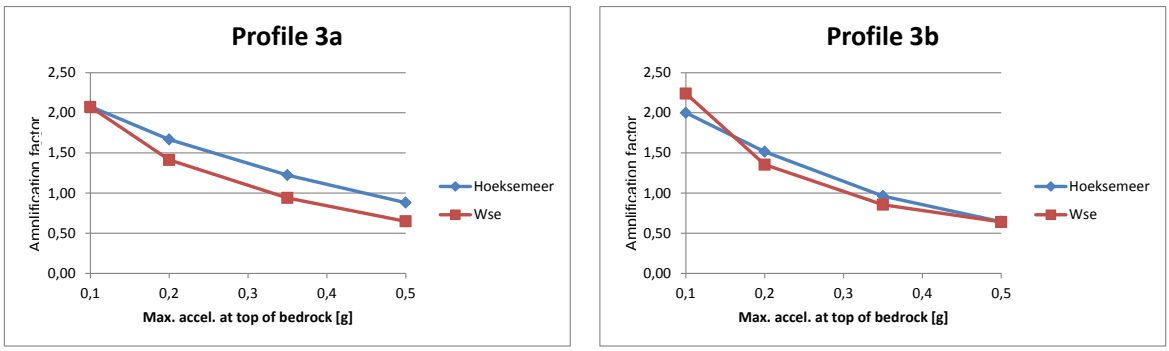

Figure F.16 Amplification factor vs. peak acceleration at top of baserock for profile type 3a (left) and profile type 3b (right).

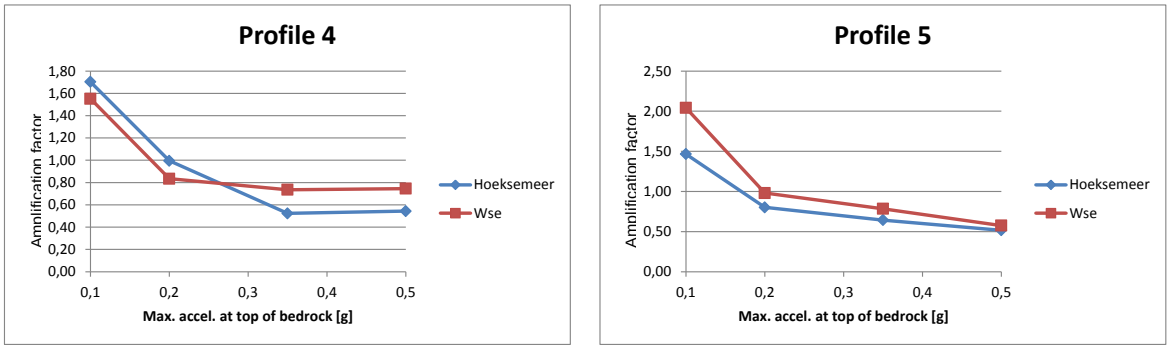

Figure F.17 Amplification factor vs. peak acceleration at top of baserock for profile type 4 (left) and profile type 5 (right).

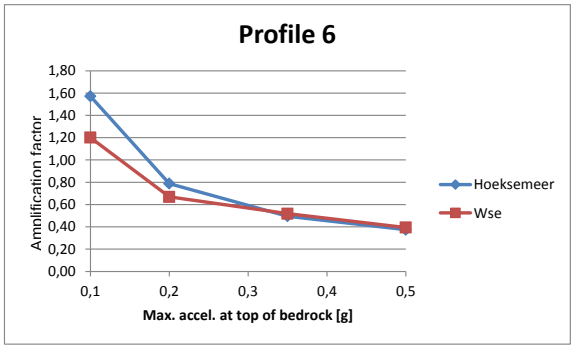

Figure F.18 Amplification factor vs. peak acceleration at top of baserock for profile type 6.

5 Discussion and conclusion

All considered profile types show an increase in PGA at the surface for increasing peak acceleration at baserock. Profile type 4 is an exception that shows locally for one record a more or less constant PGA at surface for base accelerations up to 0.4g.

Concerning the amplification factor, all cases show a decrease in amplification factor for increasing peak acceleration at baserock. This is to be expected, because with increasing acceleration at base level the shear strain amplitude increases and therefore the effect of soil non-linearity increases as well.

For low accelerations at base level, the variation in PGA at the surface is limited. For increasing peak accelerations at baserock, the differences in site response increase. Nearly all profiles suggest that there is a limit to the maximum PGA at surface. Depending on the soil layering this limit is between 0.2g and 0.5g (for input signals ranging from 0.1g to 0.5g).

Profile 2 is an exception in this respect. Profile 2 shows the highest PGA at the surface and the highest amplification factor, about twice the value obtained for the other considered profiles. Profile 2 has a thick peat layer of 9 m at the top with a wet unit weight of 10 kN/m^3. For the peat layer the used shear modulus reduction and the damping curve show less reduction and damping (energy dissipation) for higher shear strain amplitudes as the used curves for clay (see Figure F.19 and Figure F.20). This implies that the behaviour of peat in the calculation is nearly linear-elastic over a wider range of shear strain amplitudes. This conclusion holds for the assumed dynamic characteristics assigned to peat.

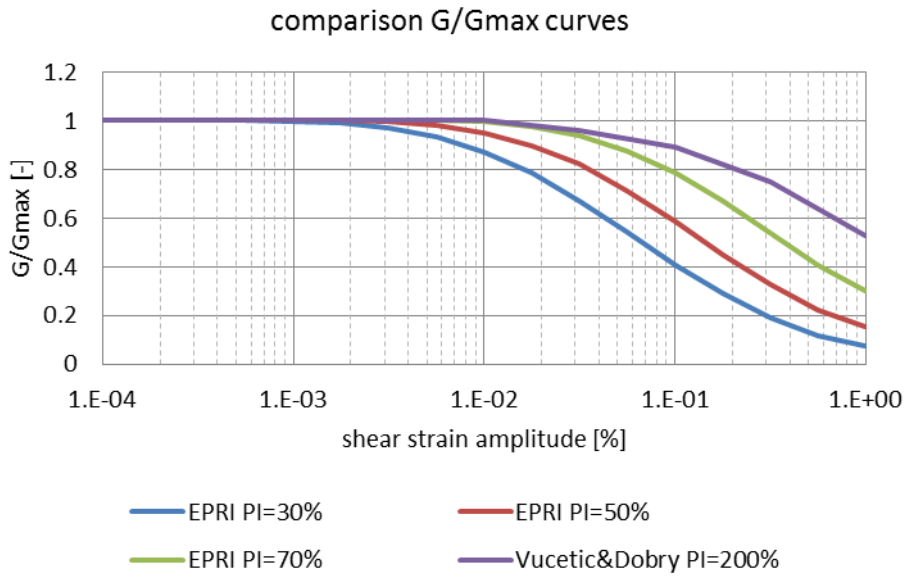

Figure F.19 Comparison of shear modulus reduction curves for different lithologies. EPRI PI=30% is used for clay, Vucetic&Dobry PI=200% is used for peat.

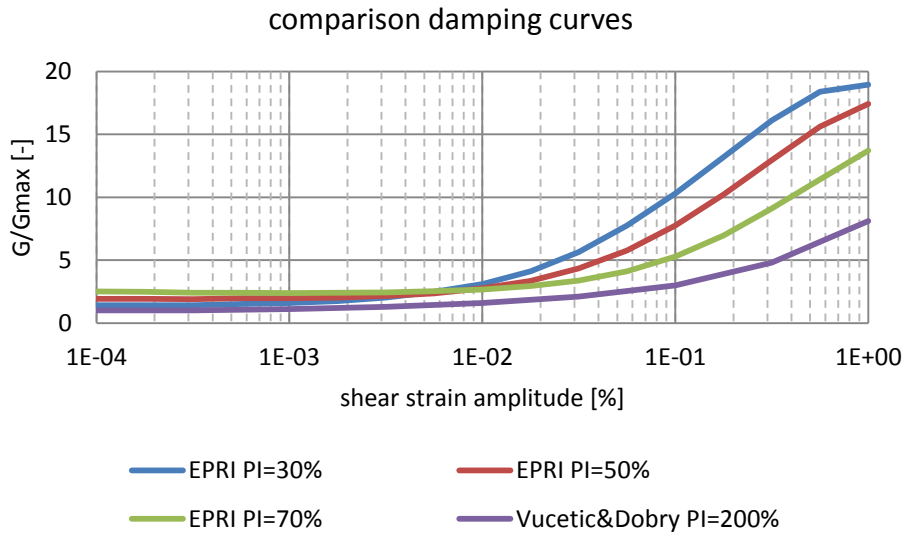

Figure F.20 Comparison damping curves for different lithologies. EPRI PI=30% is used for clay, Vucetic&Dobry PI=200% is used for peat.

In this analysis, no check has been made whether the maximum shear stress in the different soil layers does not exceed the yield strength of that layer. If the yield strength is exceeded, the transfer of energy (accelerations) is limited by the yield strength. This effect may lead to a decrease in peak acceleration at the surface for higher peak accelerations at baserock.

In future sensitivity analyses, not only PGA, but also spectral accelerations need to be considered.

G Site response analysis – a sensitivity analysis for variations in depth and thickness

1 Introduction

For assessing the site response during an earthquake the subsoil of Groningen is mapped. For an optimal mapping knowledge on the sensitivity of the site response for the thickness of different soil layers is most welcomed. This gives guidance on the required degree of detail in the mapping.

In order to get guidance on this aspect a series of calculations with the program STRATA is made. Please note that the aim of these calculations is not to calculate the site response at a particular location and/or for a particular acceleration record.

The site response calculations were performed using STRATA. The site response calculations were performed using STRATA (Kottke et al., 2013). STRATA is available from https://nees.org/resources/strata. This software performs one-dimension linear-elastic and equivalent-linear (SHAKE type) site response analyses using time series or random vibration theory ground motions. STRATA allows for stochastic variation of the site properties, including the shear modulus reduction and material damping curves, shear-wave velocity, layering, and depth to baserock. One of the inputs of STRATA is the soil-type profile: a vertical succession of layers with a soil-type and a shear-wave velocity attached to them. STRATA uses the term 'soil' for unconsolidated sediments. The baserock is the elastic half-space that forms the deepest unit in the STRATA vertical succession of layers.

2 Soil profiles

2.1 Soil parameters

For the sensitivity calculations described in this appendix, the parameters, degradation and damping curves are listed in Table G.1.

Table G.1 Overview material properties used in the site response calculations

Name	γ [kN/m^3]	Degradation curve	Damping curve	Shear wave velocity V_s [m/s]
Zand (sand)	20	Idriss (1990), sand	Idriss (1990), sand	175 /250
Klei (clay)	15	EPRI (1993), PI=30%	EPRI (1993), PI=30%	70 / 100
Veen (peat)	12	Vucetic and Dobry (1991), PI=200%	Vucetic and Dobry (1991), PI=200%	30
Eem clay	16	EPRI (1993), PI=30%	EPRI (1993), PI=30%	70

2.2 Soil layering

Based on previous experience and knowledge of the soil layering in Groningen a suite of possible soil profiles are selected that are expected to cover the variation in soil profiles. The following variations are implemented:

- Varying clay thickness for clay with V_s of 70 m/s.
- Varying clay thickness for clay with V_s of 100 m/s.
- Varying thickness of the top peat layer.
- Varying the thickness of a peat layer below clay (clay stiffness varying with depth).
- Varying the thickness of a peat layer below clay (clay stiffness constant).
- Varying the thickness of peat which is interbedded in clay.
- Varying the thickness of Eem clay.
- Varying the thickness of sand between two clay layers (bottom clay is stiff).
- Varying the thickness of sand between two clay layers (bottom clay is stiff) for a larger total depth of the soil column.
- Varying the depth of the Eem clay, top clay layer of 8 m.
- Varying the depth of the Eem clay, top clay layer of 6 m.
- Varying the shear wave velocity of peat for fixed thickness and depth.
- Varying the shear wave velocity of Eem clay for fixed thickness and depth.
- Varying frequency of the input signal.

3 Input signals

For the calculations, two acceleration records at baserock are used. Basis for the signals are two records measured at station Wse, the Hoeksmeer earthquake of 27 June 2011 and the Huizinge earthquake of 16 August 2012 (Table G.2).

Table G.2 Input signals for STRATA calculations

Event	Date	Earthquake	Station	Epicentral distance [km]	Magnitude (M_w)
5	2011-06-27	Hoeksmeer	WSE (Westeremden)	7.92	3.4
6	2012-08-16	Huizinge	WSE (Westeremden)	1.25	3.6

The acceleration records at baserock (30 m depth) were determined using deconvolution of the surface signals to 30 m depth. In the deconvolution, the approximate soil profile at the location of the station was used.

Calculations are made with scaling the peak ground accelerations at baserock to 0.14g. No adjustment of the frequency for higher peak accelerations was applied. The signals were applied at the top level of baserock. Figure G.1 shows the input signals deconvolved to 30 m depth.

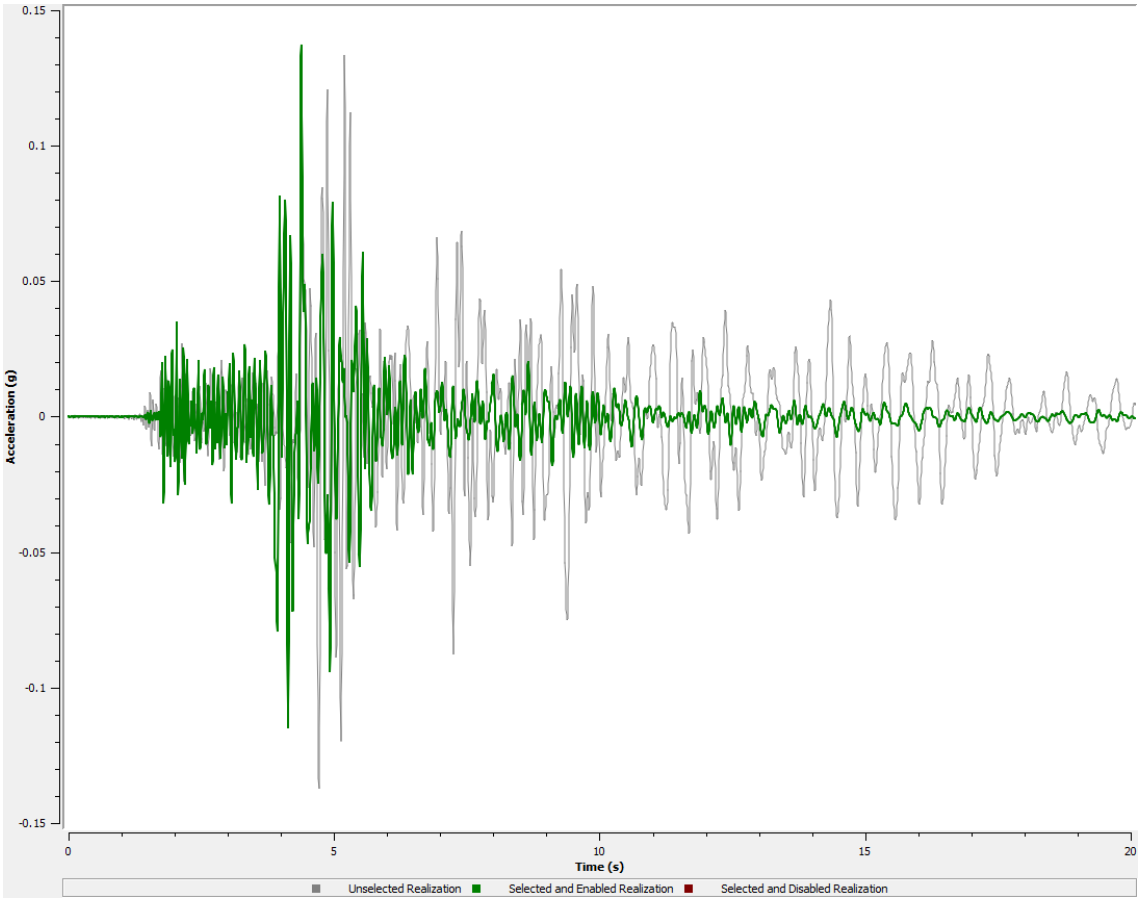

Figure G.1 Acceleration time series of Hoeksmeer (grey line) and Huizinge (green line), deconvolved to 30 m depth and scaled to peak acceleration of 0.14g.

4 Calculation results

4.1 General

In each series of the performed calculations a reference soil profile is defined. In each series the properties of one of the layers of the soil profile is varied and the effect on the site response is calculated. The site response is characterised by the calculated Peak Ground Acceleration (PGA). Other options would be plotting peak accelerations or shear strain with depth, or the response spectrum. As two input signals are used also two results are obtained. The obtained results are plotted as function of the thickness of the varied parameter. This gives the effect of varying that parameter on the calculated response.

In the next sections the performed calculations are presented. For each series of calculations the following is given:

- Purpose of the series of calculations
- Name of the STRATA file (added for Deltares checking purposes)
- Varied parameter
- Table with input parameters of soil profiles.
- Graph with calculated response, red line for the response for Huizinge input signal, blue line for Hoeksmeer input signal.

4.2 *Clay with shear wave velocity V_s = 70 m/s*

- Purpose: effect thickness clay top layer
- Calculation name:prof3akru.strata
- Varied thickness: clay

Table G.3 Soil profile Clay with shear wave velocity Vs = 70 m/s

Layer	Shear wave velocity V_s [m/s]	Thickness [m]	Remark
Clay	70	0 – 5.5	Varied thickness
Sand	175	9.5 – 4	Adjusted to obtain total height of peat and sand of 9.5 m
Clay	275	20.9	

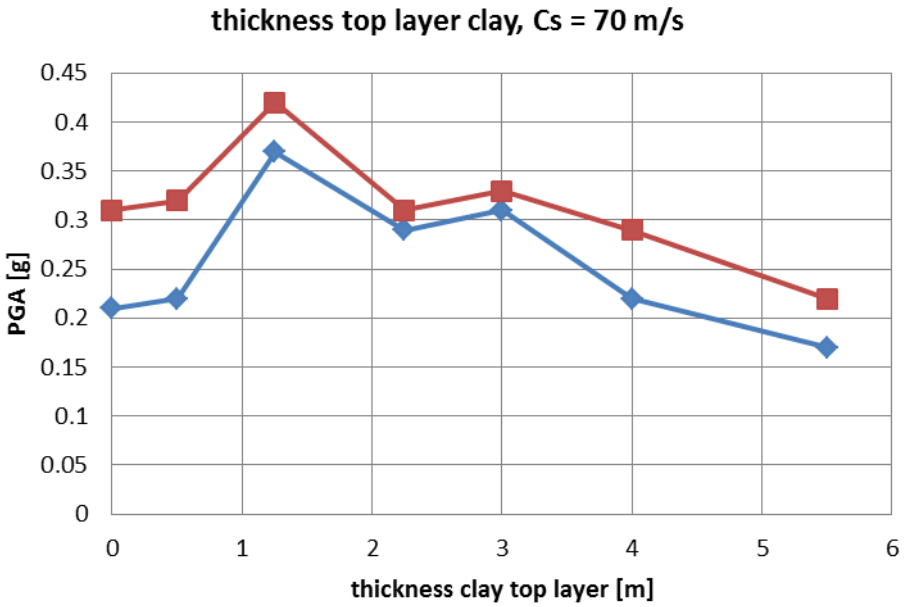

Figure G.2 Site response of varying thickness of clay with shear wave velocity V_s = 70 m/s. Red = response for Huizinge input signal, blue for Hoeksmeer input signal.

4.3 Clay with shear wave velocity V_s = 100 m/s

- Purpose: effect thickness clay top layer, with increased stiffness
- Calculation name:prof3akru.strata
- Varied thickness: clay

Table G.4 Soil profile Clay with shear wave velocity V_s = 100 m/s

Layer	Shear wave velocity V_s [m/s]	Thickness [m]	Remark
Clay	100	0 – 5.5	Varied thickness
Sand	175	9.5 - 4	Adjusted to obtain total height of peat and sand of 9.5 m
Clay	275	20.9	

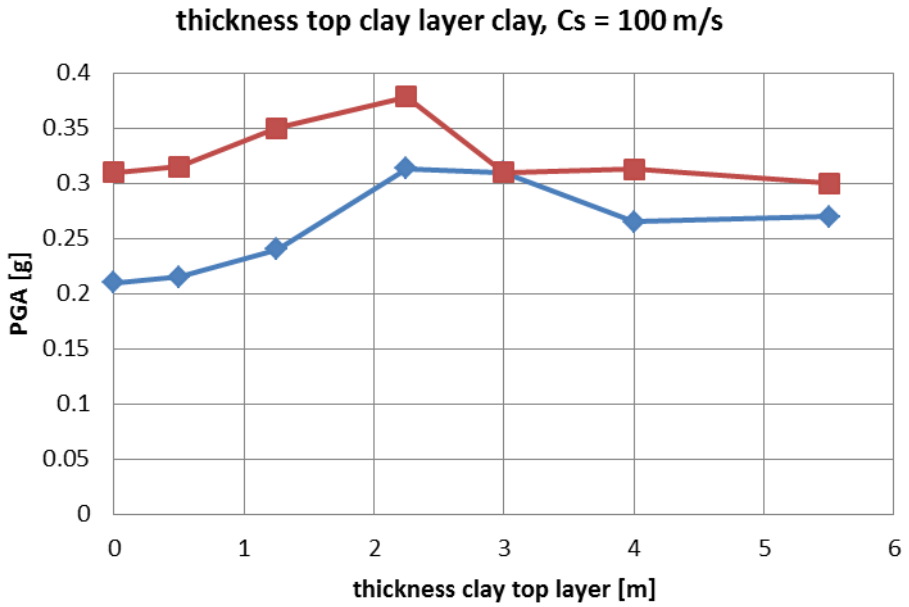

Figure G.3 Site response of varying thickness of clay with shear wave velocity V_s = 100 m/s. Red = response for Huizinge input signal, blue for Hoeksmeer input signal.

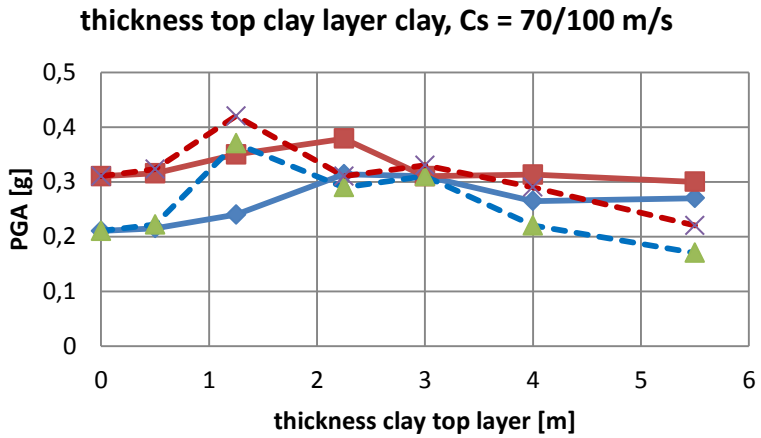

Figure G.4 Comparison results of site response for clay with shear wave velocity V_s = 70 m/s (dashed line) and V_s = 100 m/s (solid line). Red = response for Huizinge input signal, blue for Hoeksmeer input signal.

4.4 Thickness peat1 (top layer)

- Purpose: effect thickness peat top layer
- Calculation name:prof3akru2.strata
- Varied thickness: peat

Table G.5 Soil profile Thickness peat1 (top layer)

Layer	Shear wave velocity V_s [m/s]	Thickness [m]	Remark
Peat	30	0 – 5.5	Varied thickness
Sand	175	5.5 – 0	Adjusted to obtain total height of peat and sand of 5.5 m
Clay	275	20.9	

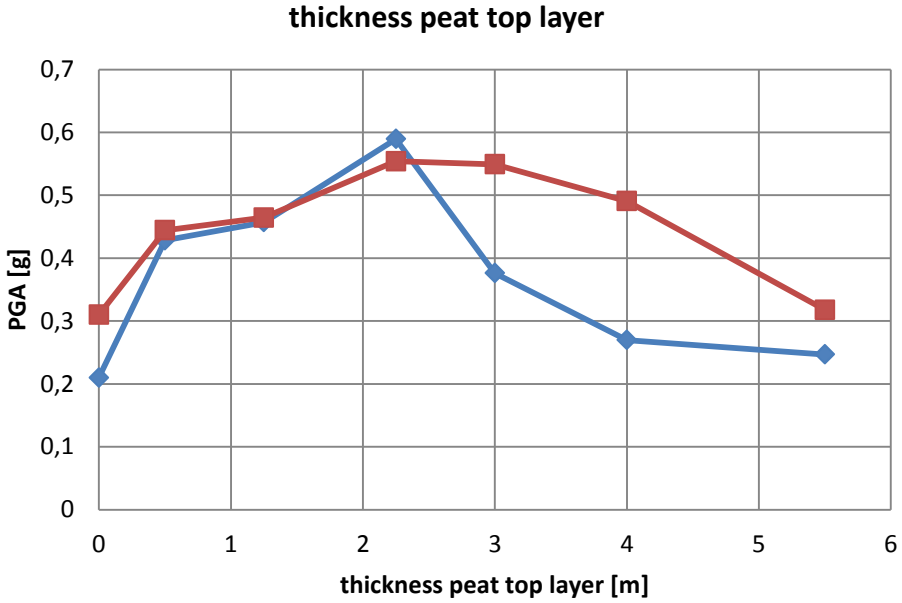

Figure G.5 Site response of varying thickness of peat1 (top layer). Red = response for Huizinge input signal, blue for Hoeksmeer input signal.

4.5 Thickness peat2 (thickness peat below clay)

- Purpose: effect thickness peat below clay, stiffness clay increases with depth
- Calculation name:prof3akru3.strata
- Varied thickness: peat

Table G.6 Soil profile Thickness peat2 (thickness peat below clay)

Layer	Shear wave velocity V_s [m/s]	Thickness [m]	Remark
Clay	70	0.5	
Clay	100	2.5	
Peat	30	0 – 7	Varied thickness
Sand	175	27 - 20	Adjusted to obtain total height of 30 m

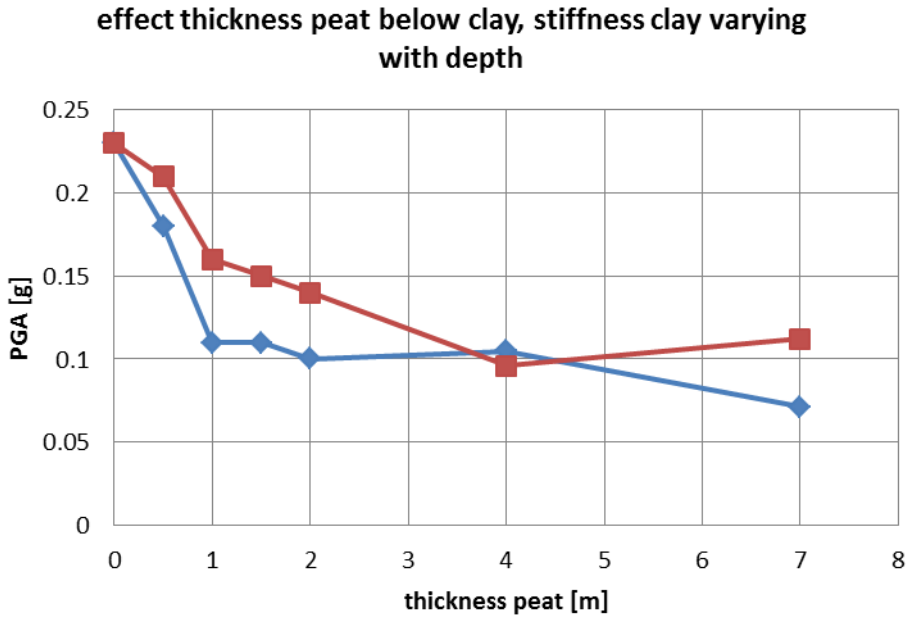

Figure G.6 Site response of varying thickness of peat2 (thickness peat below clay). Red = response for Huizinge input signal, blue for Hoeksmeer input signal.

4.6 Thickness peat3 (thickness peat below clay)

- Purpose: effect thickness peat below clay
- Calculation name:prof3kru.strata
- Varied thickness: peat

Table G.7 Soil profile Thickness peat3 (thickness peat below clay)

Layer	Shear wave velocity V_s [m/s]	Thickness [m]	Remark
Clay	70	3	
Peat	30	0 – 7	Varied thickness
Sand	175	27 - 20	Adjusted to obtain total height of 30 m

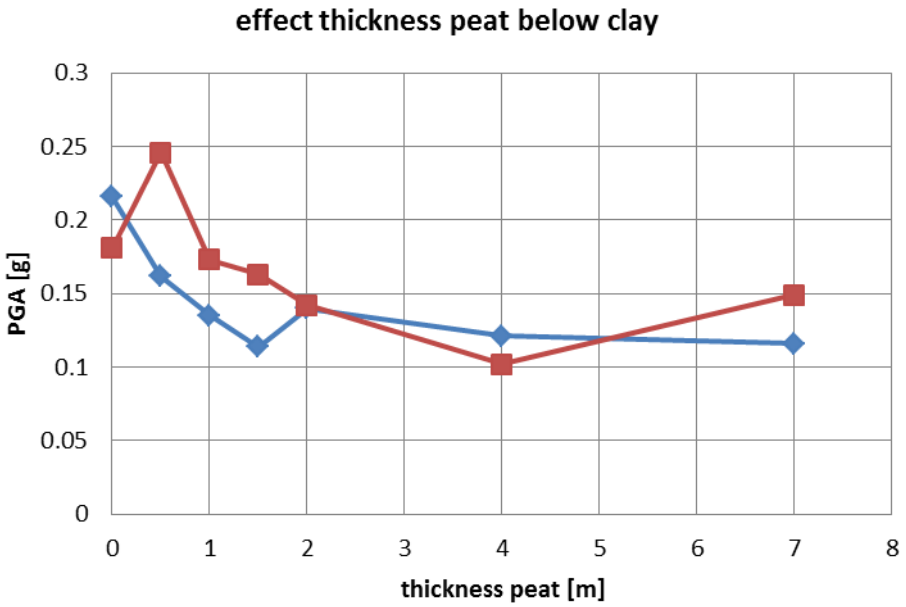

Figure G.7 Site response of varying thickness of peat3 (thickness peat below clay). Red = response for Huizinge input signal, blue for Hoeksmeer input signal.

4.7 Thickness peat4 (peat interbedded in clay)

- Purpose: effect thickness peat below clay
- Calculation name:prof4kru.strata
- Varied thickness: peat

Table G.8 Soil profile Thickness peat4 (peat interbedded in clay)

Layer	Shear wave velocity V_s [m/s]	Thickness [m]	Remark
clay	70	3	
Peat	30	0 – 4	Varied thickness
Clay	70	1	Depth moves downward with increasing thickness peat layer
Sand	175	26 - 23	Adjusted to obtain total height of 30 m

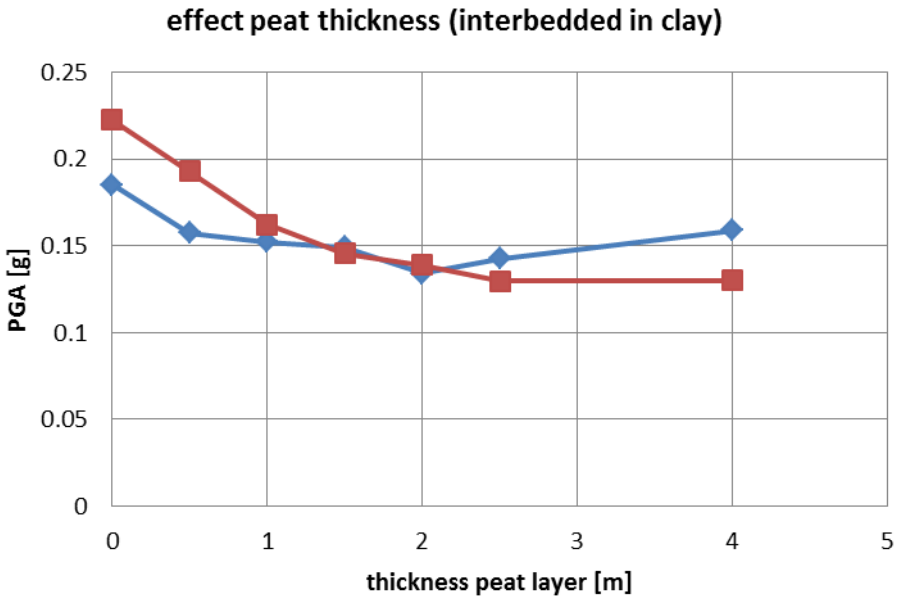

Figure G.8 Site response of varying thickness of peat4 (peat interbedded in clay). Red = response for Huizinge input signal, blue for Hoeksmeer input signal.

4.8 Thickness Eem clay

- Purpose: effect thickness Eem clay
- Calculation name:prof5eem.strata
- Varied thickness: Eem clay

Table G.9 Soil profile Thickness Eem clay

Layer	Shear wave velocity V_s [m/s]	Thickness [m]	Remark
Clay	70	8	
Sand	175	2	
Eem clay	70	0 – 7	Varied thickness
Sand	250	20 - 13	Adjusted to obtain total height of 30 m

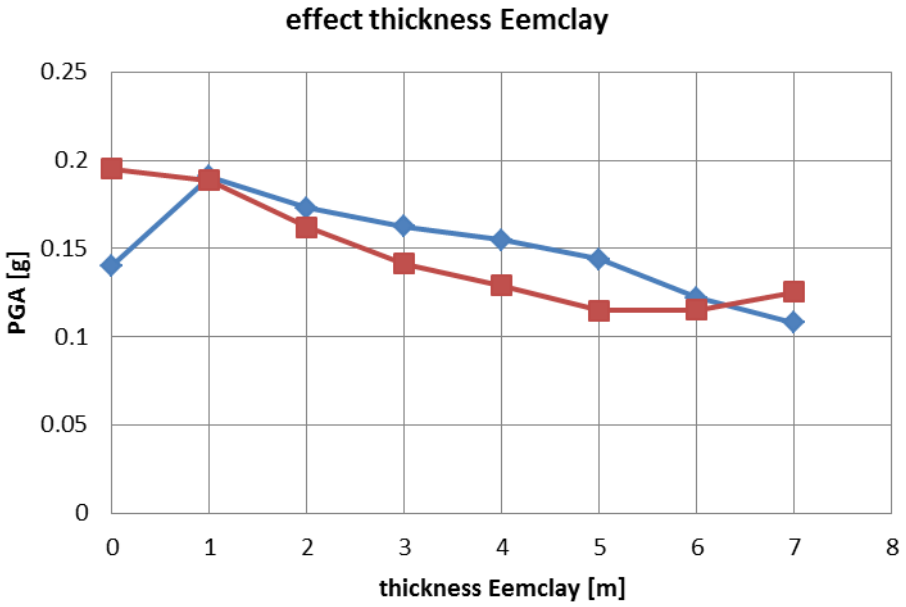

Figure G.9 Site response of varying thickness of Eem clay. Red = response for Huizinge input signal, blue for Hoeksmeer input signal.

4.9 Thickness sand between top clay and stiff clay

- Purpose: effect thickness sand below top clay/top of stiff clay
- Calculation name:sens8.strata
- Varied thickness: sand

Table G.10 Soil profile Thickness sand between top clay and stiff clay

Layer	Shear wave velocity V_s [m/s]	Thickness [m]	Remark
Clay	100	5.0	
Sand	200	5 – 15	Varied sand thickness
Clay (stiff clay)	275 gamma=17.5	20 – 10	Varied top of layer, sum of thickness sand and stiff clay is 25 m

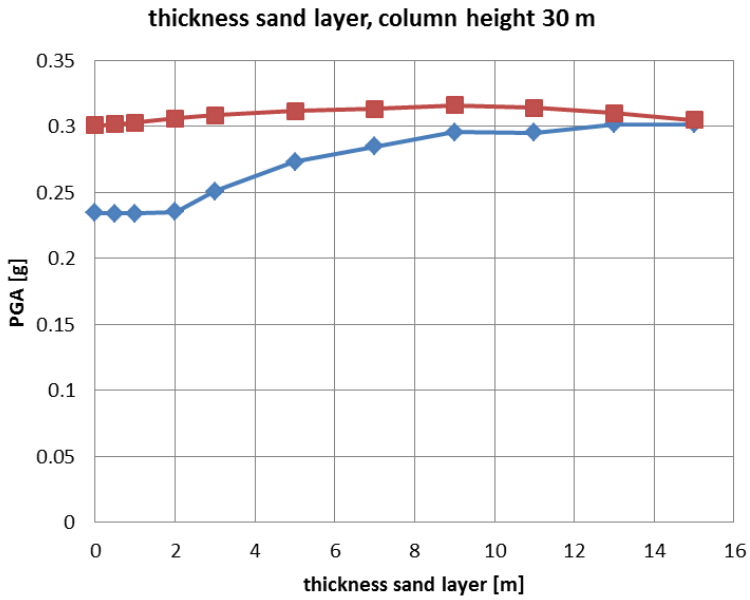

Figure G.10Site response of varying thickness of sand between top clay and stiff clay. Red = response for Huizinge input signal, blue for Hoeksmeer input signal.

4.10 Thickness sand between top clay and stiff clay for column of 50 m

The calculation of section 4.9 is repeated with a total column height of 50 m.

- Purpose: effect thickness sand below top clay and height soil column
- Calculation name:sens8b.strata
- Varied thickness: sand

Table G.11 Soil profile Thickness sand between top clay and stiff clay for column of 50 m

Layer	Shear wave velocity V_s [m/s]	Thickness [m]	Remark
Clay	100	5.0	
Sand	200	5 – 15	Varied sand thickness
Clay	275 gamma=17.5 kN/m^3	40 – 30	Varied top of layer

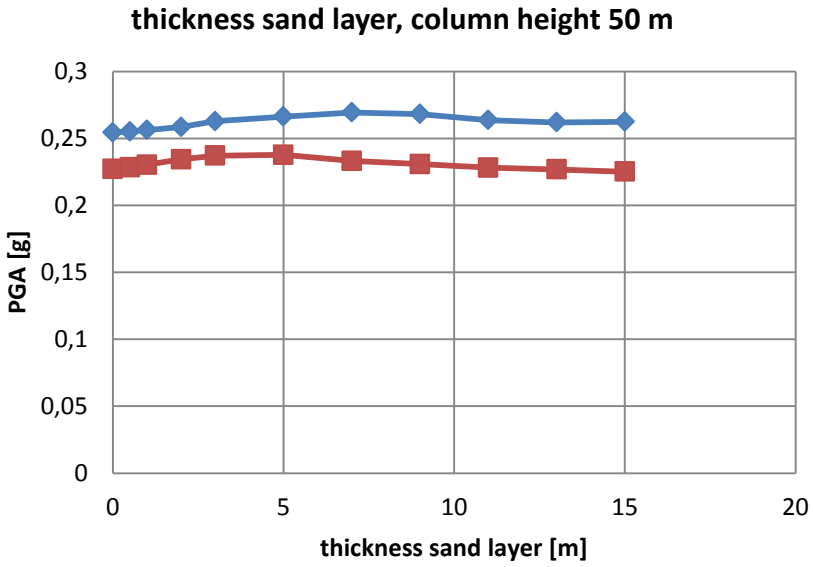

Figure G.11 Site response of varying thickness of sand between top clay and stiff clay for column of 50 m. Red = response for Huizinge input signal, blue for Hoeksmeer input signal.

4.11 Depth Eem clay, 8 m thickness

- Purpose: effect depth Eem clay
- Calculation name:sens9.strata
- Varied thickness: sand layer above and below Eem clay

Table G.12 Soil profile Depth Eem clay, 8 m thickness

Layer	Shear wave velocity V_s [m/s]	Thickness [m]	Remark
Clay	70	8	
Sand	175	0 – 7	Varied thickness layer
Eem clay	100	7	Fixed thickness Eem clay
Sand	250	15 - 8	Adjusted to obtain total height of 30 m

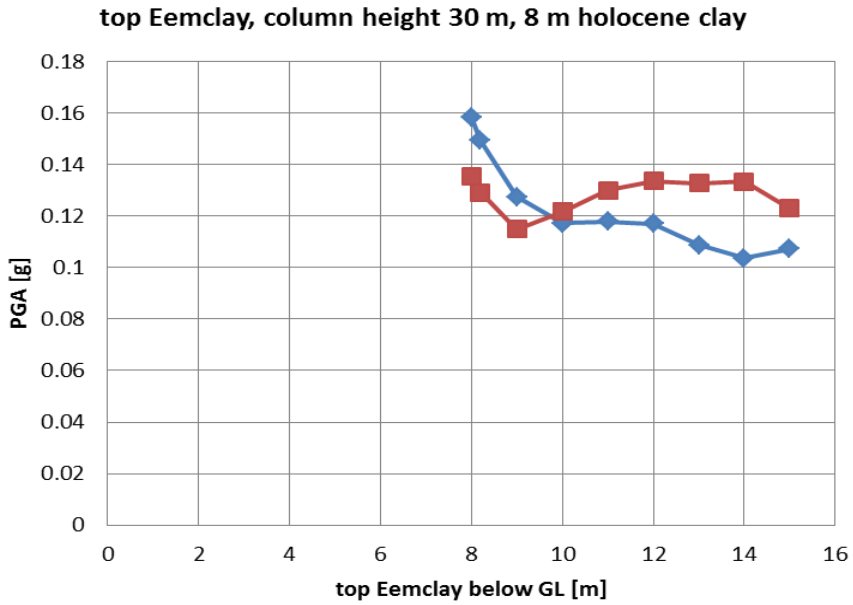

Figure G.12Site response of varying depth of Eem clay, 8 m thickness. Red = response for Huizinge input signal, blue for Hoeksmeer input signal.

4.12 *Depth Eem clay, 6m thickness*

The calculation of section 4.11 is repeated with a 6 m Holocene clay layer instead of an 8 m clay layer.

- Purpose: effect depth Eem clay
- Calculation name:sens9b.strata
- Varied thickness: sand layer above and below Eem clay

Table G.13 Soil profile Depth Eem clay, 6m thickness

Layer	**Shear wave velocity V_s [m/s]**	**Thickness [m]**	**Remark**
Clay	70	6	
Sand	175	0 – 9	Varied thickness layer
Eem clay	100	7	Fixed thickness Eem clay
Sand	250	17 - 8	Adjusted to obtain total height of 30 m

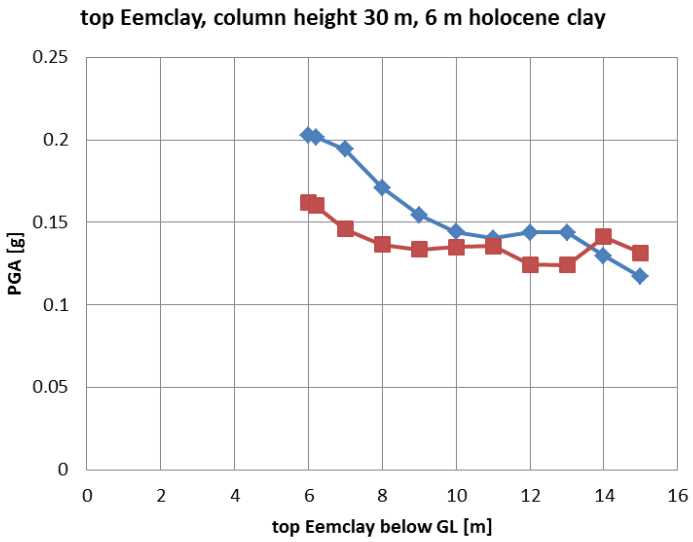

Figure G.13Site response of varying depth of Eem clay, 6m thickness. Red = response for Huizinge input signal, blue for Hoeksmeer input signal.

4.13 Effect shear wave velocity peat

- Purpose: effect shear wave velocity peat layer
- Calculation name:sens10.strata
- Varied parameter: shear wave velocity peat layer

Table G.14 Soil profile Effect shear wave velocity peat

Layer	Shear wave velocity V_s [m/s]	Thickness [m]	Remark
Clay	100	4	
Peat	20 – 100	1	Varied shear wave velocity
Sand	200	25	

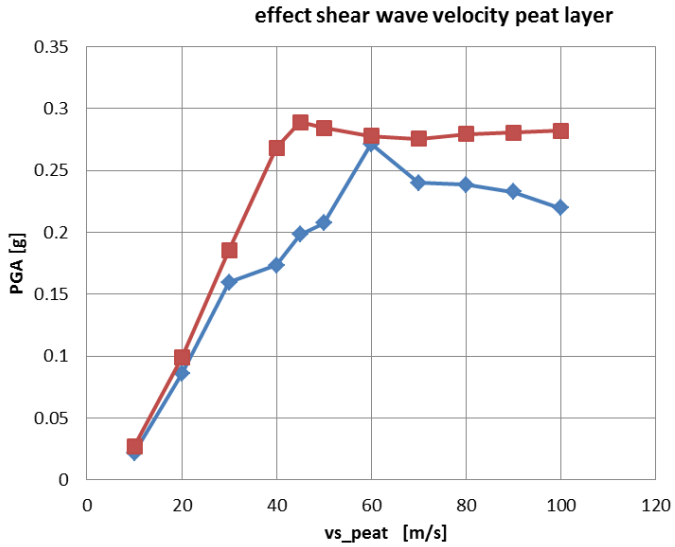

Figure G.14Site response of varying shear wave velocity of peat. Red = response for Huizinge input signal, blue for Hoeksmeer input signal.

4.14 Effect shear wave velocity Eem clay

- Purpose: effect shear wave velocity Eem clay
- Calculation name:sens11.strata
- Varied parameter: shear wave velocity Eem clay

Table G.15 Soil profile Effect shear wave velocity Eem clay

Layer	Shear wave velocity V_s [m/s]	Thickness [m]	Remark
Clay	70	8	
Sand	175	5	
Eem clay	70 - 235	7	Varied shear wave velocity
Sand	250	15	

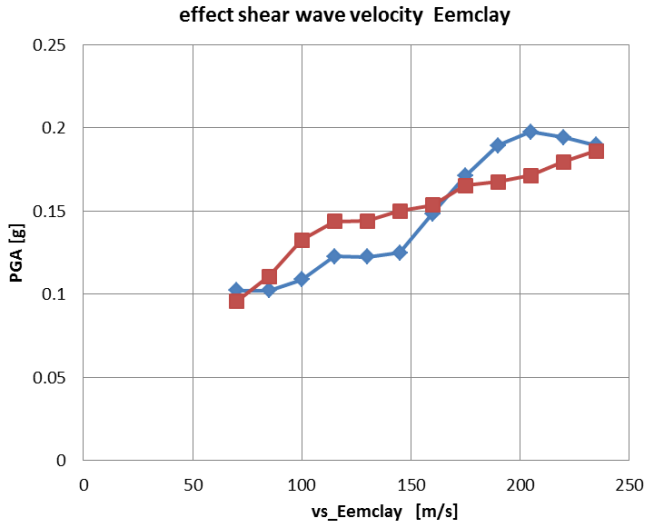

Figure G.15 Site response of varying shear wave velocity of Eem clay. Red = response for Huizinge input signal, blue for Hoeksmeer input signal.

4.15 Effect frequency of clay

- Purpose: effect frequency on site response
- Calculation name:sens12.strata
- Varied parameter: frequency acceleration record

In the previous calculations the frequency of the earthquake signal has not been varied (apart from the fact that two records are used). In order to investigate the effect of the frequency a series of calculations is repeated with varying frequency. The frequency is varied by changing the value of the time step from 0.005 s to 0.01s in steps of 0.001s. Increasing the time step implies that lower frequencies enter the signal, but higher frequencies are lost. This is a crude approach and generally not recommended for adjusting time records for different magnitudes. In this sensitivity study, it is solely used to investigate the effect of the frequency content on the soil response. For this purpose, it is considered to be acceptable for these calculations.

As input record file, the Huizinge earthquake (Table F.10, file = 6.wse 120816-ra-sc) is used. The peak acceleration is scaled to 0.14g. Figure G.16 and Figure G.17 show the 6 used records. Figure G.18 and Figure G.19 show the corresponding Fourier spectra.

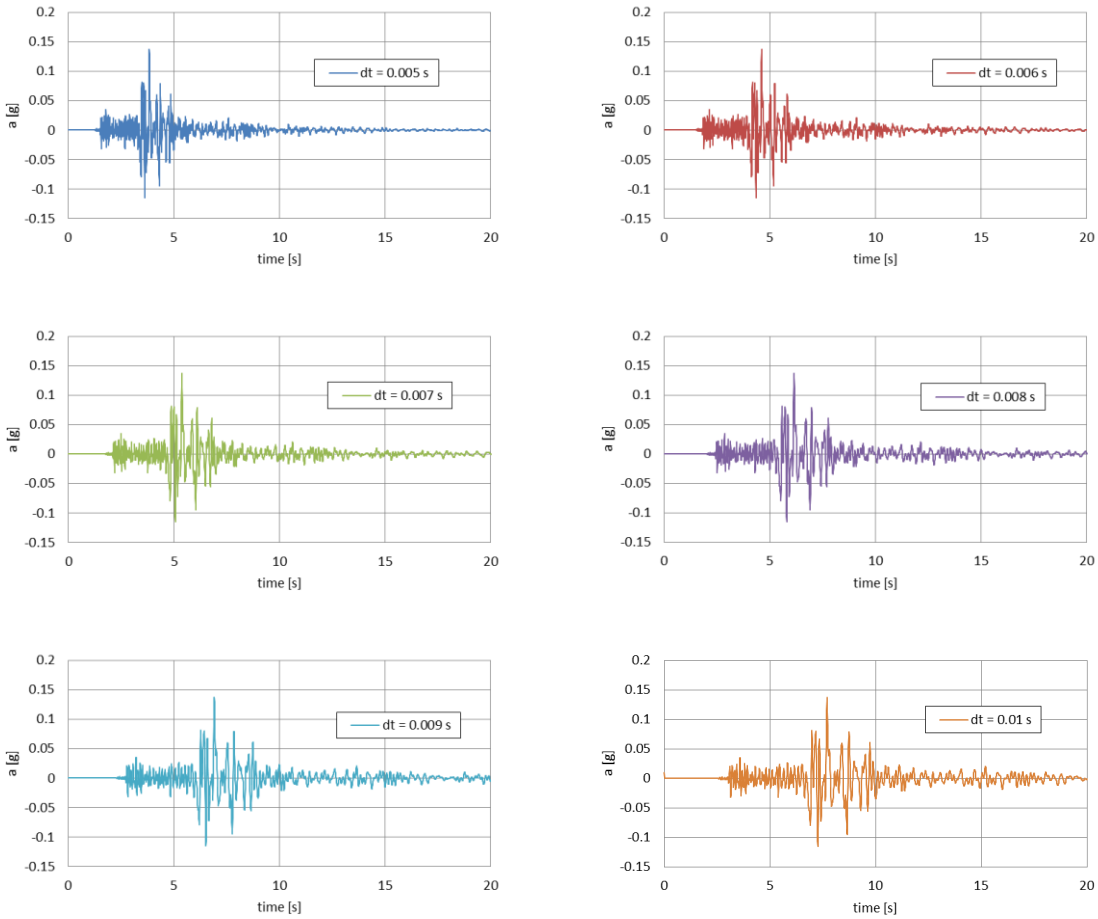

Figure G.16 Used time records with different time steps to investigate the effect of varying frequency.

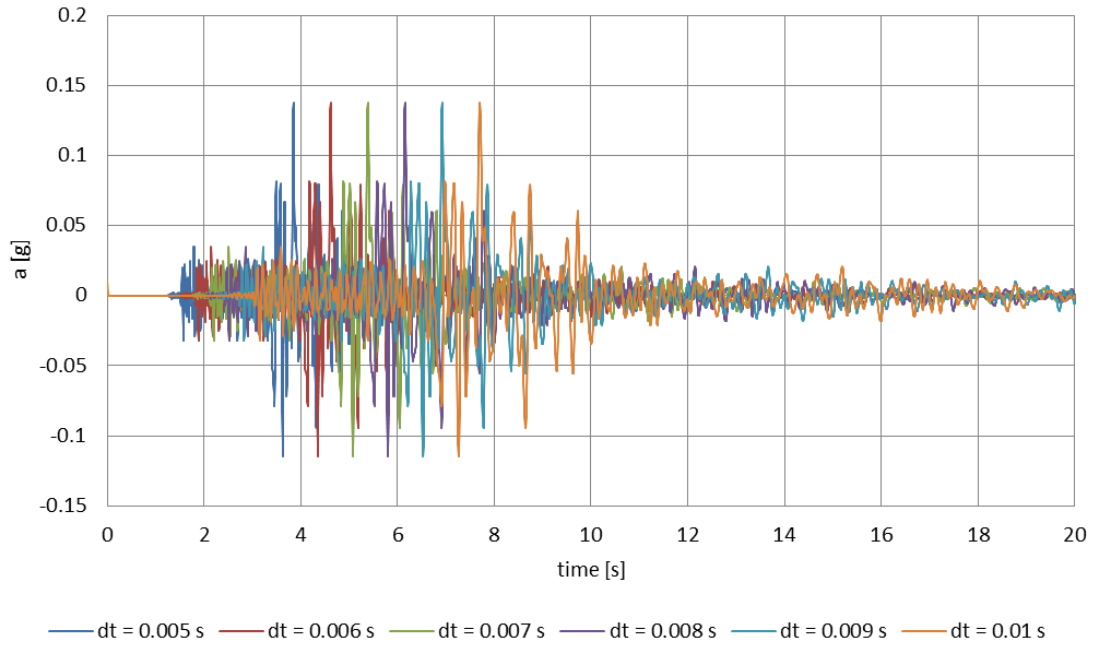

Figure G.17Used time records with different time steps all in one figure, to show the shift in peaks corresponding to changes in frequency.

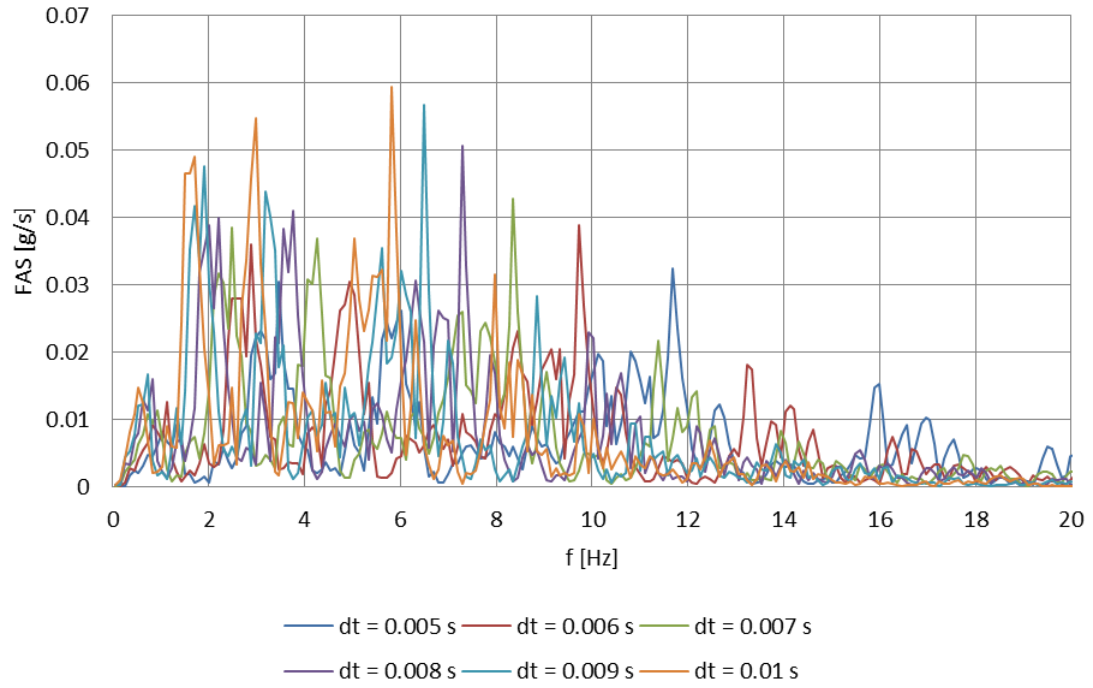

Figure G.18Fourier spectra of input signals of Figure G.16 at base (= deconvolved .to 30 m depth). All frequency spectra in one figure.

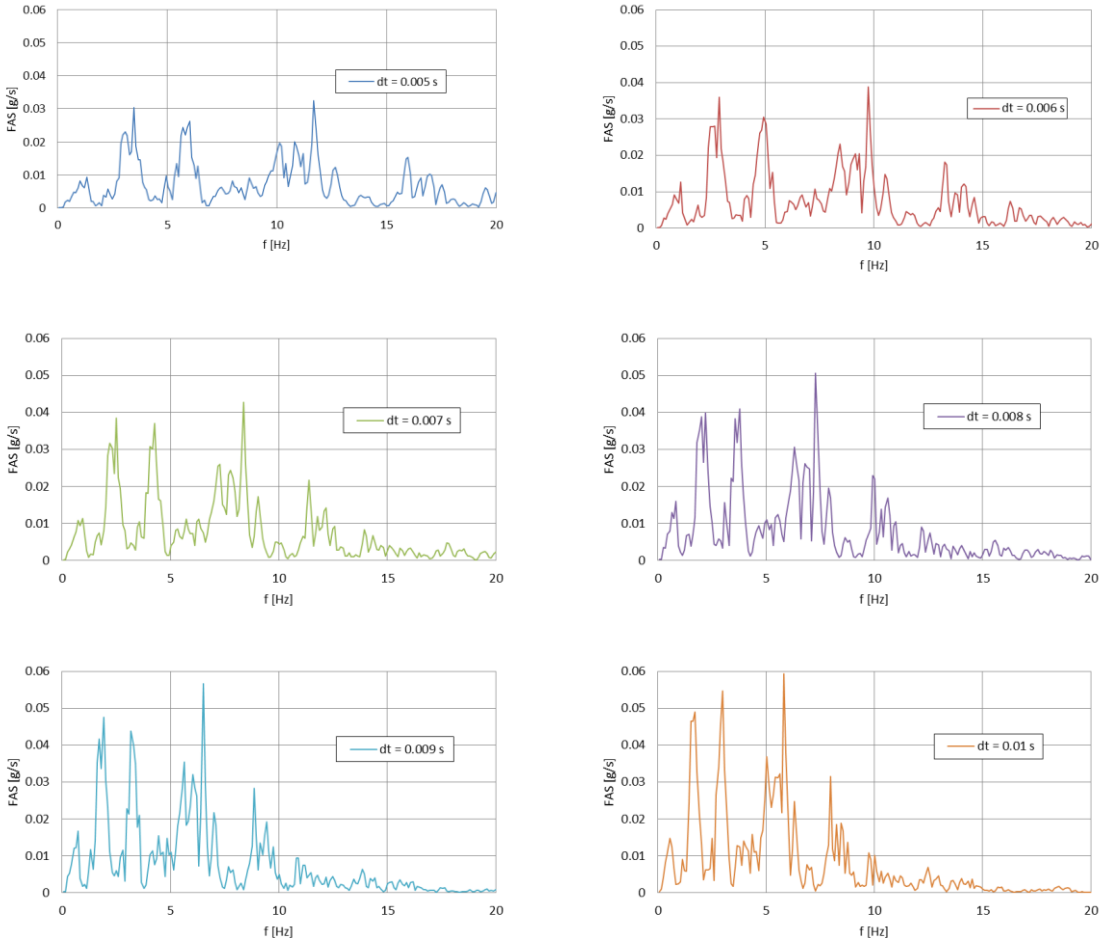

Figure G.19Fourier spectra of input signals of Figure G.16 at base (= deconvolved .to 30 m depth).

Table G.16 Soil profile Effect frequency on clay (comparable to section 4.3)

Layer	Shear wave velocity V_s [m/s]	Thickness [m]	Remark
Clay	100	0 – 7	Varied thickness
Sand	175	9.5 – 2.5	Adjusted to obtain total height of peat and sand of 9 m
Clay	275	20.5	

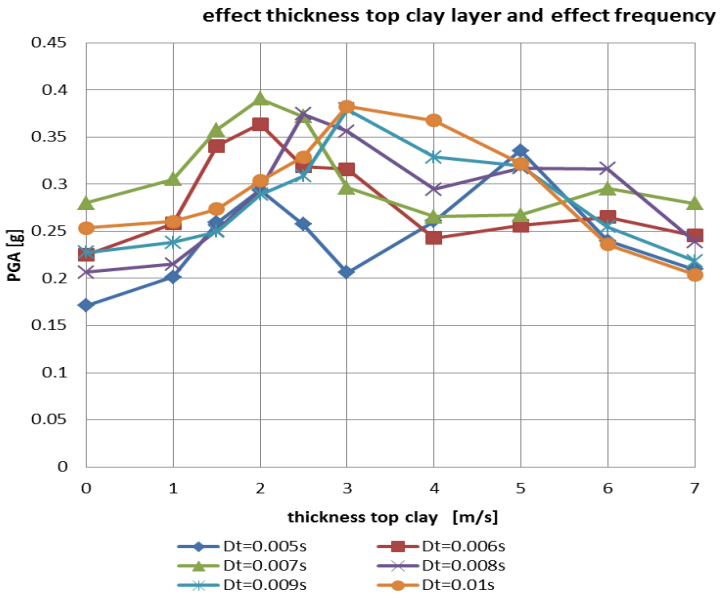

Figure G.20 Site response of varying frequency and thickness of clay.

4.16 Effect frequency for peat embedded in clay

For the second variation the situation of a peat layer embedded in clay is used.

- Purpose: effect frequency on site response
- Calculation name:sens13.strata
- Varied parameter: frequency acceleration record

Table G.17 Soil profile Effect frequency for peat embedded in clay

Layer	Shear wave velocity V_s [m/s]	Thickness [m]	Remark
Clay	70	3	
Peat	30	0 – 4	Varied thickness
Clay	70	1	Depth moves downward with increasing thickness peat layer
Sand	175	8 - 4	Adjusted to obtain total height of 30 m
Clay	275	18	Fixed thickness

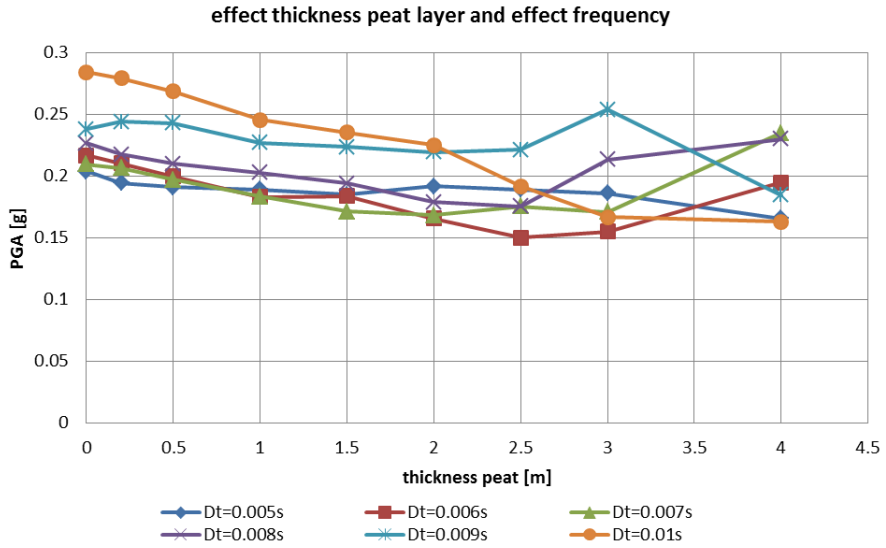

Figure G.21 Site response of varying frequency and thickness of peat embedded in clay

5 Interpretation of results

The sensitivity study resulted in the following observations:

- In general, the effect of variation decreases with depth.
- The effect of a larger contrast in soil properties varies, in general, monotonic with thickness of the layers involved.
- These effects, in general, decrease with increase in thickness of the layers with lower stiffness.
- A notable effect of the thickness of surface layers is found with high amplification (3 x) for thin softer surface layers decreasing with depth to below 5 m thickness.
- These conclusions hold for PGA. Future sensitivity studies will include spectral accelerations as well.

From these observations, general rules for the level of detail were defined (section 4.2).